THE ROLE OF ICE SURFACES IN AFFECTING NIGHTTIME REMOVAL OF NITROGEN OXIDES IN HIGH LATITUDE PLUMES

A

THESIS

Presented to the Faculty

Of the University of Alaska Fairbanks

in Partial Fulfillment of the Requirements

for the Degree of

DOCTOR OF PHILOSOPHY

By

Deanna M. Huff, B.S.

Fairbanks, Alaska

December 2010

THE ROLE OF ICE SURFACES IN AFFECTING NIGHTTIME REMOVAL OF NITROGEN OXIDES IN HIGH LATITUDE PLUMES

By

Deanna M. Huff, B.S.

RECOMMENDED:

Advisory Committee Chair

Chair, Department of Chemistry and Biochemistry

APPROVED:

Dean, College of Natural Science and Mathematics

Dean of the Graduate School

Dec 6, 2010

Date

Abstract

Nitrogen oxides play an important role in the atmosphere by affecting ozone-mediated oxidation pathways. Nitrogen oxide removal from the atmosphere occurs via nitric acid formation. This nitric acid deposits to Earth's surface, leading to acidification and nitrogen fertilization. Under dark and cold conditions that commonly exist in the winter at high latitudes, nighttime reactions oxidize NO_2 to the nitrate radical, NO_3, and these molecules react to form N_2O_5. The heterogeneous hydrolysis of N_2O_5, which is catalyzed by surfaces, forms nitric acid. Modeling studies indicate that a majority of the NO_x removal at high latitudes results from nighttime N_2O_5 chemistry. The N_2O_5 intermediate molecules may react on snowpack surfaces or on atmospheric particles. Past field studies demonstrated that aerosol surfaces are not solely responsible for the removal of N_2O_5 near Earth's surface at high latitudes. In this work, we have used aerodynamic gradient micrometeorological methods to measure the deposition velocity of N_2O_5 to snowpack. This measurement is the first time that snowpack deposition has been quantified directly. We have found that snowpack deposition near Earth's surface at high latitudes is a significant chemical loss process for N_2O_5. Further studies demonstrated higher mixing ratios and longer lifetimes of N_2O_5 aloft. Increasing N_2O_5 abundance and longevity with altitude implicates different loss mechanisms contribute at various altitudes in the atmosphere. Near Earth's surface, N_2O_5 is very reactive, while aloft it acts more as a reservoir species that can transport further. Understanding the controlling mechanisms for

NO_x removal under high latitude conditions will lead to better characterization of the NO_x transport in pollution plumes and nitric acid deposition patterns.

Table of Contents

List of Figures

Page

List of Tables

Page

Acknowledgements

I would like to thank NSF for the funding of my project under grant ATM-0926220 and ATM-0624448. Also, the University of Alaska Fairbanks Department of Chemistry and Biochemistry for providing me with Teaching Assistantships and the University of Alaska Fairbanks Graduate School for awarding me a Thesis Completion Fellowship. I would like to thank Bill Simpson for the opportunity to work on this project and all of his mentoring and advice. I would like to thank Randy Apodaca for his CRDS expertise. I would also like to thank Patrick Joyce and Deanna Donohoue for helping with my field studies. I would like to thank my committee members Tom Trainor, Cathy Cahill and Alex Laskin (PNNL) for their support and the Environmental Chemistry Group. I would also like to thank Alex Laskin for lending me equipment for my aerosol work. The field studies would not have been possible without the help of Tom Douglas and Art Galvin at CRREL who gave me an equipment hut and meteorological instruments. I thank Javier Fochosatto for his knowledge of micrometeorology.

I would also like to thank my husband Ben, my family, friends and especially Trevor White for their support.

Chapter 1 Introduction

1.1 Motivation

High temperature combustion processes produce nitric oxide, NO, which reacts with atmospheric ozone to form nitrogen dioxide, NO_2, resulting in pollution of the atmosphere and changes to the atmosphere's chemical reactivity. Because of their rapid interconversion, we refer to the sum of NO and NO_2 as the chemical family NO_x. At high latitudes, the main source of NO_x is combustion of fuels for transportation (e.g. automobiles, aircraft), power, heat, and industrial applications (e.g. oil and gas production). In the Arctic and sub-Arctic, these sources are concentrated in small geographic areas surrounded by large regions with little to no NO_x sources. Nitrogen oxides are centrally involved in controlling the tropospheric ozone budget. Photolysis and oxidation in the atmospheric processing of NO_x can destroy or produce ozone and produces nitric acid. In polluted lower latitude conditions, an overabundance of tropospheric ozone, resulting from NO_x chemistry, has documented harmful effects on humans (Finlayson-Pitts and Pitts, 2000). The final fate of nitrogen oxides in the atmosphere is further oxidation to form nitric acid. Nitric acid deposits to the Earth's surface and can lead to harmful nitrification of ecosystems. High latitude NO_x pollution will continue to increase with population growth, further oil production and new Arctic shipping pathways. As NO_x pollution increases, nitric acid input to the Earth's surface will increase affecting the Arctic ecosystem by increasing nitrification as has already been observed in mid-latitudes (Bytnerowicz et al., 1998; Fenn et al., 2003; Galloway et

al., 2003; Sanderson et al., 2006; Driscoll et al., 2009).

The production mechanism and rate of nitric acid formation are not well understood at high latitudes. Nitric acid is formed by a variety of competing mechanisms, each of which has differing dependence on atmospheric conditions. Only by understanding those mechanisms can we make meaningful predictions regarding the impacts of NO_x pollution on the arctic ecosystem. Additionally, as the climate changes, there will be changes to how and where the NO_x is oxidized and nitric acid is deposited to the Earth's surface.

1.2 Background

In the Arctic, the cold and dark winter conditions favor the following nighttime pathway (R1-R3) for forming nitric acid. At night, NO_2 further reacts with ozone to form NO_3, the nitrate radical. In the absence of sunlight, the nitrate radical builds up and forms N_2O_5 via Reaction (R2).

$$NO_2 + O_3 \rightarrow NO_3 + O_2 \qquad \text{(R1)}$$

$$NO_2 + NO_3 \leftrightarrows N_2O_5 \qquad \text{(R2)}$$

$$N_2O_5 + H_2O \xrightarrow{\text{Surface}} 2HNO_3 \qquad \text{(R3)}$$

During the day, NO_3 does not build up. The abundance of the NO_3 is controlled by daytime processes, such as reaction with NO (R4) or photolysis (R5). Reaction (R4) is also a nighttime reaction near local NO emission sources before that NO has time to react with ozone (typically a few minutes). Once directly emitted NO has converted to NO_2 at

night, Reaction (R4) ceases. In contrast, during the day, photolysis of NO_2 (R6) can produce a regional source of NO, once again suppressing NO_3 abundance via reaction (R4).

$$NO + NO_3 \rightarrow 2NO_2 \qquad \text{(R4)}$$

$$NO_3 + h\nu \rightarrow NO_2 + O^{\cdot} \qquad \text{(R5)}$$

$$NO_2 + h\nu \rightarrow NO + O^{\cdot} \qquad \text{(R6)}$$

The production of nitric acid during the day is controlled by reaction of NO_2 with the hydroxyl radical, reaction (R7).

$$NO_2 + OH \rightarrow HNO_3 \qquad \text{(R7)}$$

The oxygen radicals ($O^{\cdot}$) formed in Reaction (R5-6) react with O_2 to form ozone during the day. Daytime processes produce excess ozone through photolysis, as opposed to nighttime processes that consume ozone (R1).

Reaction (R3) is the heterogeneous hydrolysis of N_2O_5, where heterogeneous means the gas reacts on a surface. This reaction proceeds on a surface because the surface acts as a catalyst that stabilizes the intermediates and lowers the energy barriers along the pathway to nitric acid formation. Which surfaces act catalytically in the Arctic is not known. The speed of Reaction (R3) depends upon the catalytic surface area available for this reaction and the uptake probability per gas-surface collision, γ. Measuring the efficiency of the reactive uptake of N_2O_5 (γ), a ratio between 0 and 1, is important for

determining the speed of Reaction (R3). If γ is 1, then every N_2O_5 gas molecule collision with a reactive surface would result in the production of two molecules of nitric acid and the rate limiting step would actually be the production of NO_3 (R1). If γ is close to zero, then the majority of N_2O_5 gas -- surface collisions result in no reaction, decreasing the efficiency of nitric acid formation at night. In this situation, N_2O_5 would then be considered a reservoir of NO_x (rather than an intermediate species) and would lead to the long-range transport of the pollutant.

1.3 Reactive uptake coefficient of N_2O_5 - Laboratory studies

In laboratory studies, the reactive uptake coefficient of N_2O_5, γ is determined using aqueous aerosol particles as the catalytic surface for the gas molecules of N_2O_5 to react on. Most of the earlier work characterizing γ on aqueous aerosol particles was done on sulfate- containing aerosol particles. Sulfate aerosol particles make up a large fraction of tropospheric aerosol particles. They are formed from the oxidation of SO_2 which results in sulfuric acid aerosol particles (Finlayson-Pitts and Pitts, 2000). Early laboratory measurements indicated that γ was around 0.1, for N_2O_5 reacting with aerosol particles containing sulfate and ammonium bisulfate (Mozurkewich and Calvert, 1988; Kirchner et al., 1990; Van Doren et al., 1991; Hanson and Ravishankara, 1991a). Mozurkewich and Calvert (1988) used a flow tube reactor system on sulfuric acid, water and ammonium bisulfate micron-size aerosol particles. Mozurkewich and Calvert (1988) found a γ value of 0.12 for micron-sized aerosol particles containing sulfuric acid. Van Doren et al.

(1991) measured a slightly lower value of γ for pure water, 0.04-0.06. Similar values of γ in these earlier studies were also confirmed by Hanson and Lovejoy (1994) using a flow tube reactor system. Zhang et al. (1995) and Mentel et al. (1999) investigated the effect of nitric acid in addition to sulfate in aerosol particles and found that the reactive uptake coefficients were in the range of 0.02 – 0.04 for sulfate aerosol particles and an order of magnitude lower with the addition of nitric acid. This was then called the "nitrate effect" by Mentel et al. (1999). Subsequent laboratory studies were performed by Hu and Abbat (1997) and Hallquist et al. (2000) suggested that sulfuric acid aerosol γ ranges were 0.03 to 0.05 on sub-micron aqueous aerosol particles. However, Hu and Abbat (1997) also mention good agreement with γ obtained in earlier lab studies by Mozurkewich and Calvert (1988) for ammonium bisulfate containing aerosol particles (NH_4HSO_4).

Multiple studies have indicated that the addition of organic compounds to aerosol particles can decrease the reactive uptake coefficient, γ. Badger et al. (2006) showed that γ was smaller for organic aerosol particles as compared to more acidic sulfate aerosol particles. Thornton and Abbatt (2005) and McNeill et al. (2006) showed that the gas-aqueous aerosol interface is influenced by salts and organics in the aerosol composition. Their results showed a γ in the range of 0.016-0.03 for sea salt aerosol particles and an order of magnitude lower values for aqueous aerosol particles containing organic coatings of sodium dodecyl sulfate (McNeill et al., 2006) and hexanoic acid (Thornton and Abbatt, 2005). The reactive uptake coefficient for sea salt aerosol particles is similar

to a previous study by Behnke et al. (1997) on NaCl aerosol particles. Thornton et al. (2003) showed that γ depended on relative humidity and aerosol composition for malonic and azelaic organic aerosol particles with and without sulfate. In addition to the laboratory organic film aerosol studies, a recent study on water-soluble organics showed little to no effect of organic compounds in a sulfate aerosol on the uptake of N_2O_5 (Griffiths et al., 2009). Bertram and Thornton (2009) demonstrated a stronger dependence on water content than previous authors have seen (Thornton et al., 2003; Hallquist et al., 2000) and that Cl^- can increase the uptake of N_2O_5 by lowering the nitrate effect.

Aerosol particles are involved in the fate of NO_x chemistry by serving as the reactive surface on which N_2O_5 reacts to form nitric acid; they also contain chloride ions that can lead ozone production in the following laboratory studies. Roberts et al. (2008) performed laboratory studies showing that N_2O_5 reacting with aerosol chloride forms nitryl chloride. They also found that during the day, photolysis forms NO_x and chlorine radicals in atmospheric aerosol particles with low to moderate Cl^- concentrations. They further confirmed that N_2O_5 reacted with chloride over a wide range of aerosol substrates and pH levels and was in agreement with γ values of earlier studies for a narrow range of NaCl aerosol particles (Behnke et al.,1997).

There are several laboratory studies investigating N_2O_5 reactive uptake coefficients on ice. All of the studies were done at very cold temperatures (180 K - 220 K) similar to the polar stratospheric cloud reactions that are involved in the depletion of stratospheric ozone (Hanson and Ravishankara, 1991b; Leu, 1988; Quinlan et al., 1990). Leu (1988)

and Quinlan et al. (1990) found that the N_2O_5 reactive uptake coefficient on ice was 0.028 and 0.03. Hanson and Ravishankara (1991b) used an ion flow tube reactor and showed a similar reactive uptake coefficient on pure ice of 0.024 and a sulfuric acid ice aerosol value of 0.008. In addition, Hanson and Ravishankara (1991b) found that adding nitric acid trihydrate (NAT) reduced the reactive uptake coefficient by over an order of magnitude to 0.0006. All of the laboratory studies on the reactive uptake coefficient of N_2O_5 and ice are at temperatures that are not representative of tropospheric ice temperatures closer to freezing. Since it is still difficult to examine the surface of an ambient ice aerosol, more laboratory and field studies at relevant tropospheric temperatures are needed to better quantify γ on ice.

1.4 Reactive uptake coefficient of N_2O_5 - Field studies

Field measurements of N_2O_5 (Brown et al., 2001; Matsumoto et al., 2005; Wood et al., 2005; Brown et al., 2006; Osthoff et al., 2008; Bertram and Thornton, 2009) have been conducted recently at mid latitudes. Brown et al. (2006) conducted a major flight campaign field experiment in the mid latitudes to measure γ for East Coast sub-micron aqueous aerosol particles. Brown et al. (2006) sampled three different regions for gases, N_2O_5, NO_2, O_3 and aerosol particles.

As described above, the surface reactivity of N_2O_5 (γ) represents the number of reactive collisions per gas-molecule collision with an aerosol surface. To measure the reactive uptake coefficient of N_2O_5 on submicron aqueous aerosol particles in the field

Brown et al. (2006) used the following formula

$$\gamma = \frac{4k_{N_2O_5}}{c * SA}. \qquad (1.1)$$

The uptake coefficient, γ, is calculated using the first order loss rate coefficient ($k_{N_2O_5}$), reactive surface area density (SA) in $\mu m^2/cm^3$ of submicron aerosol particles and the molecular speed of N_2O_5 (c) in m/s. Brown et al. (2006) found that sulfate-rich aerosol particles had greater reactive uptake coefficients than organic-rich particles. Using Eq. (1.1), Brown et al. (2006) reported γ values of 0.017 for region I which had high sulfate aerosol content and an order magnitude lower, 0.0016, for region III near the coast and aerosol particles with low sulfate. The aerosol surface area does decrease from region I (SA= 1000 $\mu m^2/cm^3$) to region III (SA= 300 $\mu m^2/cm^3$), but does not control the γ value decrease. Brown et al. (2006) found that the aerosol chemical composition varied the surface reactivity of N_2O_5. Region I was dominated by sulfate aerosol particles and region III had aerosol particles with low sulfate and high organic content. Brown et al. (2006) results confirmed laboratory studies that showed γ variability is due to different aerosol compositions. The variability in reactive uptake coefficient led to different lifetimes of N_2O_5 due to the varying aerosol composition.

The molecule N_2O_5 reacts with water, as in Reaction (R3), and N_2O_5 reacts with Cl^- and has been documented in the field by Osthoff et al. (2008) to be an important halogen activation pathway. Halogen activation arises from formation of nitryl chloride, a nighttime reservoir, photolyzes to form the chlorine radical and NO_2 during the day.

Recently, Thornton et al. (2009) showed that this halogen activation pathway is not only important in coastal areas, but also important inland as shown in this mid-continental field study performed in Colorado.

1.5 Arctic field studies of determining N_2O_5 lifetimes

Past work has characterized γ and its dependence upon aerosol particle composition in laboratory and field studies. The great majority of the work was done at mid-latitudes (above freezing). In the past, our group has conducted two high latitude field studies. In addition to measuring the lifetime of N_2O_5, which was completed in a field study in 2006 (Ayers and Simpson, 2006), we completed a field study measuring N_2O_5 and aerosol surface density using a DRUM sampler (Cahill et al., 1997; Perry et al., 1999). We deployed a field portable N_2O_5 instrument that used cavity ring down spectroscopy (CRDS) technique to measure N_2O_5 in the field (Simpson, 2003; Ayers et al., 2005).

During our field campaign in 2007, we measured the mixing ratios of N_2O_5, NO_x and O_3 as well as aerosol particles, wind speed and temperature (Apodaca et al., 2008). We calculated a chemical loss of N_2O_5 or $k_{N_2O_5}$ and a dry aerosol surface area density. In the field, the steady state lifetime of N_2O_5 ($\tau_{N_2O_5ss}$) is quantified by the following:

$$1/k_{N_2O_5} = \tau_{N_2O_5ss} = \frac{[N_2O_5]}{k_1[NO_2][O_3]}. \qquad (1.2)$$

In Eq. (1.2), the source rate of N_2O_5 is the rate coefficient for Reaction (R1), k_1, multiplied by the concentrations of NO_2 and ozone. The nighttime intermediate

compound, N_2O_5, can revert back to NO_2 and NO_3 at higher temperatures. The calculation of the steady- state lifetimes of N_2O_5 using Eq. (1.2) requires that chemical loss is from N_2O_5 and not reactive losses of NO_3. Because Reaction (R2) is temperature dependant equilibrium, we can use the following ratio as a factor in determining the direction of the reaction,

$$\frac{[N_2O_5]}{[NO_3]} = K_{eq} * [NO_2]. \qquad (1.3)$$

In Reaction (R2) concentration of N_2O_5, is divided by the concentration of NO_3 and is equal to the concentration of NO_2 multiplied by the equilibrium constant, K_{eq}. Under warmer temperatures commonly found in mid latitudes, the ratio shifts to the right and the steady state of NO_3 needs to be addressed. At cold temperatures commonly found in the Arctic, the formation of N_2O_5 is favored and Reaction (R2) proceeds to the right. We assume that we are at steady state of N_2O_5 due to the low temperatures and fast conversion from NO_3 to N_2O_5 via the forward Reaction (R2). In addition to the fast loss conditions of N_2O_5 from near-surface field measurements ($\approx$ 6 minutes) we achieve steady state rapidly in the dark and cold high latitude conditions (Apodaca et al., 2008). Using the steady state approximation (Eq. 1.2), we calculated the lifetimes of N_2O_5. We compared these lifetimes to the relative humidity and found a steady state lifetime for N_2O_5 of 20 minutes for unsaturated airmasses (less than 100% relative humidity with respect to ice) and 6 minutes for saturated airmasses (greater than 100% relative humidity with respect to ice).

We measured the steady state lifetime of N_2O_5 and the aerosol surface area density. As stated earlier, Reaction (R3) proceeds on a reactive surface; in laboratory studies and field studies this reactive surface is considered to be atmospheric aerosol particles. Aerosol particles act as catalysts that increase the speed of Reaction (R3). To estimate the reaction speed of R1, we used Eq. (1.1). The dry aerosol surface area was measured to be on the order of 50 $\mu m^2/cm^3$. This value is quite low compared to that of Brown et al. (2006) who measured aerosol surface areas of 1000 $\mu m^2/cm^3$ in the polluted Ohio River Valley. For our field study, even assuming unreasonably high values of γ (~1), the observed surface area is insufficient to explain the N_2O_5 chemical loss rate we observed. The correlation of the lifetimes of N_2O_5 and saturation with respect to ice, coupled with the fact that we found low dry aerosol surface area to explain the chemical loss of N_2O_5, led us to start to investigate other possible reactive surfaces for N_2O_5 heterogeneous hydrolysis. From these data, we started to implicate ice as a possible reactive surface for catalyzing N_2O_5 heterogeneous hydrolysis.

During the dark and cold conditions that exist in the Arctic, the formation of ice occurs. At night in the Arctic, the atmosphere near the Earth's surface is almost always saturated with respect to ice (Andreas et al., 2002). There are two main possibilities for how N_2O_5 is removed by ice surfaces: snowpack deposition and reaction on atmospheric ice particles. Snowpack deposition due to saturated air masses is a dynamic process that is characterized by micrometeorological observations in addition to N_2O_5. Atmospheric ice particle nucleation is also a possibility, since ice nucleates near the threshold of 100% relative humidity (Curry et al., 1990).

1.6 Sub-processes of heterogeneous hydrolysis of N_2O_5

From our previous field studies, ice surfaces are implicated in the catalysis of the heterogeneous hydrolysis of N_2O_5 (R3) (Apodaca et al., 2008). We can consider how these high latitude reactive surfaces catalyze the heterogeneous hydrolysis of N_2O_5 by dividing catalyst processes into two sub-processes; depositional and atmospheric processes.

First, we consider depositional processes. The nighttime compound, N_2O_5, can be lost near the surface through a dynamic process that depends on meteorological conditions and turbulent contact with the ground. In Fig. 1.1 this process is represented as Reaction (R3a), depositional processes. At high latitudes, snowpack covers the Earth's surface for most of the year. Understanding N_2O_5 deposition to the snowpack will help quantify the chemical loss of N_2O_5 and the effect snowpack deposition has on the steady state lifetime of N_2O_5 (Eq. 1.2) near the surface.

To quantify the effect of snowpack deposition, we measured the deposition velocity of N_2O_5. Deposition velocity is the effective speed (cm/s) at which a gas or particle deposits to the Earth's surface. Often we call this the "dry" deposition velocity as opposed to "wet" deposition, which means reaction in the atmosphere followed by rain scavenging of the aerosol-particle bound products (Finlayson-Pitts and Pitts, 2000).

Deposition velocities for the gases O_3, NO, NO_2 and HNO_3 have been studied in the past and are involved the chemistry of N_2O_5 (R1-R3). There have been many

measurements of the deposition velocity for O_3 during the summer, spring and winter on varying terrain (Wesely and Hicks, 2000; Bocquet, 2007; Helmig et al., 2007). In a review article by Wesely and Hicks (2000), several of the ozone deposition velocities are summarized. For ozone over snow covered ground, the deposition velocity ranges from 0.0 to 0.2 cm/s. More recently, Arctic studies of the deposition velocities above a snow pack have been measured for ozone and found to be 0.01 cm/s (Helmig et al., 2007). Wesely and Hicks (2000) summarized NO and NO_2 deposition velocities. NO deposition velocities are difficult to report because of the rapid conversion of NO to NO_2. These velocities are generally considered negligible and are typically studied as emission velocities from the snowpack (Wesely and Hicks, 2000). There are several studies quantifying the emission of NO_x from the snowpack and, though NO_x emission from the snowpack can be significant, it is said to be driven by photochemistry (Honrath et al., 1999; Jones et al., 2001). Jones et al. (2001) studied NO_x emission form the Arctic snowpack by measuring NO_2 at two different heights and found a diurnal cycling of NO_x with deposition velocities near zero at night.

Lovett (1994) has reported deposition velocities in the range of 1 to 4 cm/s for nitric acid over a canopy. The reported deposition velocity of nitric acid over snow is 0.5- 1.4 cm/s Cadle et al., 1985). There are no past deposition velocities reported, to our knowledge, for N_2O_5.

Besides direct deposition of N_2O_5 to the Earth's surface, we want to address possible atmospheric processes. Reaction (R3), the heterogonous hydrolysis of N_2O_5 primarily

occurs on submicron aqueous aerosol particles at mid latitudes. The reactive uptake coefficient of N_2O_5 has been measured in the field using Eq. (1.1) for specific surface area densities. We know from Arctic field studies that in addition to submicron aqueous aerosol particles we also have high relative humidity and cold temperatures. The reactive urface area can increase by the additional formation of ice particles, super cooled water droplets and the swelling of aerosol particles due to ice formation on the particle. All of these possible conditions are considered together as the atmospheric processes represented in Fig. 1.1 as Reaction (R3b).

Ice particle formation as an atmospheric process (R3b) is a strong possibility in the Arctic, because at night the temperature drops and the relative humidity rises. The relative humidity is often near 100% with respect to ice at night when the temperatures are low. Ice particles around 100 microns in diameter are often seen as ice pillars in the atmosphere due to light from city sources reflecting off the ice crystals. Classifying ice particles and their sizes and shapes is difficult. Most ice particle characteristics come from upper-atmosphere, daytime ice particles observations. Several authors have noted the difficulty of quantifying ice particle formation at night, from satellite and surface observations (Curry et al., 1996; Zwally et al., 2002; Curry et al., 1990). Ice particle concentrations have been measured to exceed 1000 L^{-1} in the Arctic (Ohtake et al., 1982; Curry et al., 1990; Girard et al., 2005). In polluted air masses ice particle size distribution measurements are scarce. Benson (1965) measured ice particles in the Arctic in a polluted area to be between 5 and 10 microns in diameter based cooling rates. Ohtake (1969)

measured ice fog ice particles between 4 and 6 microns in radius. Using ice crystal concentration and size distribution, Witte (1968) infers a radius of 10 microns in low flying aircraft measurements at Barrow Alaska. Curry et al. (1990) also measured the average radius for low level clouds in the Arctic to be 7.5 microns in diameter. Gotaas and Benson (1965) cite 25 microns in diameter for spherical particles for a radiative cooling study in the Fairbanks, Alaska area. In addition to the formation of ice particles, Curry et al. (1990) noted that some of the particles formed under ice saturation conditions in the temperature range -7 to -40°C failed to freeze and remained as super-cooled water droplets. In addition to the lack of freezing, the size and shape of the ice particles is needed to quantify the reactive surface area available and size of potential of mass transfer limitation of larger ice particles and number densities are needed to obtain a reasonable reactive uptake coefficient of N_2O_5.

Combining the sub-processes, atmospheric and depositional and correlating these to lifetimes of N_2O_5 aloft and at the surface, we gain knowledge of the controlling mechanisms of N_2O_5 at high latitudes (R3a and R3b) and the vertical profiles of N_2O_5.

1.7 Modeling studies for the heterogeneous hydrolysis of N_2O_5

Laboratory and field studies of N_2O_5 chemistry are used to provide input parameters or validate models designed to examine different atmospheric conditions on a local and global scale. Two of the parameterizations of N_2O_5 reactivity in models are the reactive uptake coefficient (γ) used in global and regional scale models, and the deposition velocity of N_2O_5, used in regional and local models.

An important global modeling study by Dentener and Crutzen (1993) found that during winter 80% of NO_x was removed by the heterogeneous reaction (R3) at high latitudes. Including the reactive uptake coefficient in the model corrected the NO_x budget and proved the importance of including Reaction (R3) in NO_x chemical mechanisms. Dentener and Crutzen's (1993) modeling study led to laboratory studies to parameterize the reactive uptake coefficient of N_2O_5 (γ). Since then, other modeling studies have included the parameter γ in their models. Riemer et al. (2003) included two lower values of γ based more recent laboratory studies, 0.02 for sulfate aerosol particles and 0.002 for nitrate aerosol particles in their model. Evans and Jacob (2005) not only varied the composition of the aerosol, but also included relative humidity and temperature dependences in their model. This model showed a range of increasing uptake coefficients the farther north in latitude as the temperature decreased. Davis et al.'s (2008) parameterization model for N_2O_5 used all the previous laboratory results on the effects of different aerosol compositions in the atmosphere on N_2O_5 chemistry. Davis et al. (2008) is the first modeling study to include the reactive uptake coefficient of N_2O_5 on ice in the model. They used the N_2O_5 uptake value of pure ice from a previous laboratory study, γ = 0.024 (Hanson and Ravishankara, 1991b). Including ice in the modeling of N_2O_5 chemistry proved to be an important element for mid-latitude winters and even longer cold, dark, winters at high-latitudes. Davis et al. (2008) also mentions that no winter field campaign data measuring γ is available and that winter is the most important time for Reaction (R3) because it is a nighttime atmospheric chemistry reaction. The Davis et al. (2008) model study reveals the uncertainty in the parameterization of γ and the

importance of including the nighttime chemical Reaction (R3) into the NO_x budget.

In addition to the modeling parameter for the reactive uptake coefficient of N_2O_5, there is another important parameter we want to consider in models near the surface at high latitudes, the deposition velocity. Deposition velocity is an important modeling parameter that determines the removal of a trace gas near the surface. A value of 1 cm/s is considered a high deposition velocity (Wesely and Hicks, 2000). Sommariva et al. (2009) modeling study parameterized NO_x species in a regional model based on the MCM (Master Chemical Mechanism) and includes N_2O_5 with a deposition velocity of 1 cm/s. They estimated this value based on the deposition velocity of nitric acid (HNO_3), 1 cm/s. Their model found that fog is an important sink for N_2O_5 in a coastal marine environment. The surface area of the fog exceeded $5x10^5$ $\mu m^2/cm^3$ (measured in a field study that provided the comparison data for model runs (Baynard et al., 2007). Though these temperatures are much warmer than at high latitudes, the sizes of the droplets were estimated to be 7.5 microns, similar to the Arctic ice fog measurements discussed above. The modeled N_2O_5 chemical losses were consistent with the heterogeneous uptake coefficient from their previous field studies, γ values of 0.01. Sommariva et al. (2009) found that the model overestimated the mixing ratio of N_2O_5 by 30-50% on average; they believe that the vertical stratification of the marine boundary layer could be one reason for the discrepancy.

The chemistry models MOZART and IMAGES are specifically designed for snow covered areas (Helmig et al., 2007). The most common value applied in large scale

atmospheric chemistry models for the deposition velocity of ozone over a snowpack is 0.05 cm/s (Helmig et al., 2007). Helmig et al. (2007) also states that deposition velocity models do not deal accurately with ozone budgets during wintertime over snowpack because of the large variability in current ozone deposition velocities measurements, -3 to +2 cm/s.

1.8 Dissertation structure

First, it is necessary to determine the number density and surface area of ice particles in the atmosphere. Determining these variables helps to understand the atmospheric processes that control the chemical loss of N_2O_5. The details of the investigation into ice particles as a potential reactive surface for the chemical loss of N_2O_5 are in Chapter 2.

Second, we can measure the snowpack deposition of N_2O_5 by measuring the deposition velocity of N_2O_5 from micrometeorological observations, chemical gas mixing ratios (N_2O_5, NO_x and ozone). The experimental design of our field study to measure the deposition of N_2O_5 to the snowpack can be found in Chapter 3. This chapter includes data on wind speed and direction from an experimental field site used during fall 2009. From the gas measurements alone we can calculate the steady state lifetime of N_2O_5 from Eq. (1.2) and total chemical loss of N_2O_5 (R 3). These calculations and the method for the steady state analysis are in Chapter 4. The details of the aerodynamic gradient flux analysis method are given in Chapter 5. This method of measuring a flux is used to determine the deposition velocity of N_2O_5. The results of the snowpack deposition field study, including deposition velocities and lifetimes of N_2O_5 are presented in Chapter 6.

Chapter 7 presents the sonic anemometer data and the eddy covariance method and used to validate the aerodynamic gradient flux method discussed in Chapter 5.

Thirdly we want to compare our depositional process field results from fall 2009 to field measurements of N_2O_5 mixing ratio and steady- state lifetimes aloft. Chapter 8 contains the results from our spring 2010 study measuring N_2O_5 decoupled from the ground. We also measured the visibility of the atmosphere at the field site and used these measurements to estimate the atmospheric particle surface area. We used meteorological instruments to measure temperature, wind speed and relative humidity to understand the potential for ice particle formation.

Chapter 9 presents the conclusions and future work related to this thesis project. Future work gives ideas for the further role of ice surfaces in the nighttime removal of nitrogen oxides in high latitude plumes.

References

Apodaca, R. L., Huff, D. M., and Simpson, W. R.: The role of ice in N_2O_5 heterogeneous hydrolysis at high latitudes, Atmos. Chem. Phys., 8, 7451-7463, 2008.

Andreas, E. L., Guest, P. S., Persson, P. O. G., Fairall, C. W., Horst, T. W., Moritz, R. E., and Semmer, S. R.: Near-surface water vapor over polar sea ice is always near ice saturation, J. Geophys. Res., 107, SHE 8-1, doi: 10.1029/2000JC000411, 2002.

Arya, S. P.: Introduction to micrometeorology, second ed., Academic press, 420 pp., 2001.

Ayers, J. D., Apodaca, R. L., Simpson, W. R., and Baer, D. S.: Off-axis cavity ringdown spectroscopy: Application to atmospheric nitrate radical detection, Appl. Optics., 44, 7239-7242, 2005.

Ayers, J. D., and Simpson, W. R.: Measurements of N_2O_5 near Fairbanks, Alaska, J. Geophys. Res., 111, D14309, doi:10.1029/2006JD007070, 2006.

Baynard, T., Lovejoy, E. R., Pettersson, A., Brown, S. S., Lack,D., Osthoff, H., Massoli, P., Ciciora, S., Dubé, W. P., and Ravishankara,A. R.: Design and application of a pulsed cavity ringdown aerosol extinction spectrometer for field measurements, Aerosol Sci. Technol., 41, 447–462, 2007.

Badger, C. L., Griffiths, P. T., George, I., Abbatt, J. P. D., and Cox, R. A.: Reactive uptake of N_2O_5 by aerosol particles containing mixtures of humic acid and ammonium sulfate, The Journal of Physical Chemistry A, 110, 6986, 2006.

Behnke, W., George, C., Scheer, V., and Zetzsch, C.: Production and decay of $ClNO_2$ from the reaction of gaseous N_2O_5 with NaCl solution: Bulk and aerosol experiments, J. Geophys. Res., 102, 3795-3804, 10.1029/96jd03057, 1997.

Benson, C.S.: Ice Fog: Low temperature air pollution. Geophys. Inst. Rept. UAG R-173, Univ. of Alaska, 14-17 (DDC No. AD631553), 1965.

Bertram, T. H., and Thornton, J. A.: Toward a general parameterization of N_2O_5 reactivity on aqueous particles: The competing effects of particle liquid water, nitrate and chloride, Atmospheric Chemistry and Physics, 9, 8351-8363, 2009.

Bocquet, F.: Surface layer ozone dynamics and air-snow interactions at summit, Greenland spring and summer ozone exchange velocity and snowpack ozone:The complex interactions, Ph.D., Department of Atmospheric and Oceanic Sciences, University of Colorado, 197 pp., 2007.

Brown, S. S., Stark, H., Ciciora, S. J., and Ravishankara, A. R.: In-situ measurement of atmospheric NO_3 and N_2O_5 via cavity ring-down spectroscopy, Geophys. Res. Lett., 28, 3227, 2001.

Brown, S. S., Dubé, W. P., Osthoff, H. D., Stutz, J., Ryerson, T. B., Wollny, A. G., Brock, C. A., Warneke, C., de Gouw, J. A., Atlas, E., Neuman, J. A., Holloway, J. S., Lerner, B. M., Williams, E. J., Kuster, W. C., Goldan, P. D., Angevine, W. M., Trainer, M., Fehsenfeld, F. C., and Ravishankara, A. R.: Vertical profiles in NO_3 and N_2O_5 measured from an aircraft: Results from the NOAA P-3 and surface platforms during the New England air quality study 2004, J. Geophys. Res., 112, D22304, 10.1029/2007jd008883, 2007.

Brown, S. S., Ryerson, T. B., Wollny, A. G., Brock, C. A., Peltier, R., Sullivan, A. P., Weber, R. J., Dubé, W. P., Trainer, M., Meagher, J. F., Fehsenfeld, F. C., and Ravishankara, A. R.: Variability in nocturnal nitrogen oxide processing and its role in regional air quality, Science, 5757, 67-70, doi: 10.1126/science.1120120, 2006.

Brown, S. S., Stark, H., Ryerson, T. B., Williams, E. J., Nicks, D. K., Jr., Trainer, M., Fehsenfeld, F. C., and Ravishankara, A. R.: Nitrogen oxides in the nocturnal boundary layer: Simultaneous in situ measurements of NO_3, N_2O_5, NO_2, NO, and O_3, J. Geophys. Res., 108, 4299, doi:10.1029/2002jd002917, 2003.

Businger, J. A., Wyngaard, J. C., Izumi, Y., and Bradley, E. F.: Flux-profile relationships in the atmospheric surface layer, Journal of the Atmospheric Sciences, 28, 181-189, 1971.

Bytnerowicz, A., Percy, K., Riechers, G., Padgett, P., and Krywult, M.: Nitric acid vapor effects on forest trees -- deposition and cuticular changes, Chemosphere, 36, 697-702, 1998.

Cadle, S. H., Dasch, J. M., and Mulawa, P. A.: Atmospheric concentrations and the deposition velocity to snow of nitric acid, sulfur dioxide and various particulate species, Atmospheric Environment, 19, 1819-1827, 1985.

Cahill, C. F., Seifert, M. A., Farrell, D., and Jennings, S. G.: Peat smoke: A significant contributor to aerosol optical absorption in ireland, in: A&WMA Spec. Conf., Visual Air Quality, Aerosol particles, & Global Radiation Balance, Attitash Bear Peak Summit, Bartlett, NH., 1997,

Colbeck, I., and Harrison, R. M.: Dry deposition of ozone: Some measurements of deposition velocity and of vertical profiles to 100 metres, Atmospheric Environment (1967), 19, 1807-1818, 1985.

Curry, J. A., Meyer , F. G., Radke, L. F., Brock, C. A., and Ebert , E. E.: Occurrence and characteristics of lower tropospheric ice crystals in the arctic, International Journal of Climatology, 10, 749-764, 1990.

Curry, J. A., Randall, D., and Rossow, W. B.: Overview of arctic cloud and radiation characteristics, J. Climate, 9, 1731-1764, 1996.

Curry, J. A., Hobbs, P., King, M., Randall, D., Minnis, P.: FIRE arctic clouds experiment., Bull. Amer. Meteorol. Soc., 81, 5-30, 2000.

Davis, J.M.,Bhave,P.V. and Foley, K.M.: Parameterization of N_2O_5 reaction probabilities on the surface of particles containing ammonium, sulfate and nitrate., Atmos. Chem. Phys., Atmos. Chem. Phys., 8, 5295-5311, 2008.

Dentener, F. J., and Crutzen, P. J.: Reaction of N_2O_5 on tropospheric aerosol particles: Impacts on the global distributions of NOx, O_3, and OH., J. Geophys. Res., 98, 7149-7163, 1993.

Driscoll, C. T., Lawrence, G. B., Bulger, A. J., Butler, T. J., Cronan, C. S., Eagar, C., Lambert, K. F., Likens, G. E., Stoddard, J. L., and Weathers, K. C.: Acidic deposition in the northeastern united states: Sources and inputs, ecosystem effects, and management strategies, BioScience, 51, 180-198, 10.1641/0006-3568(2001)051[0180:aditnu]2.0.co;2, 2009.

Evans, M. J., and Jacob, D. J.: Impact of new laboratory studies of N_2O_5 hydrolysis on global model budgets of tropospheric nitrogen oxides, ozone and OH, Geophys. Res. Lett., 32, L09813, doi:10.1029/2005GL022469, 2005.

Fenn, M. E., Baron, J. S., Allen, E. B., Rueth, H. M., Nydick, K. R., Geiser, L., Bowman, W. D., Sickman, J. O., Meixner, T., Johnson, D. W., and Neitlich, P.: Ecological effects of nitrogen deposition in the western united states, BioScience, 53, 404-420, doi:10.1641/0006-3568(2003)053[0404:EEONDI]2.0.CO;2, 2003.

Finlayson-Pitts, B. J., and Pitts, J. N.: Chemistry of the upper and lower atmosphere., 2000.

Galloway, J. N., Aber, J. D., Erisman, J. W., Seitzinger, S. P., Howarth, R. W., Cowling, E. B., and Cosby, B. J.: The nitrogen cascade, BioScience, 53, 341-356, doi:10.1641/0006-3568(2003)053[0341:TNC]2.0.CO;2, 2003.

Garrett, T. J., Zhao, C., Dong, X., Mace, G. G., and Hobbs, P. V.: Effects of varying aerosol regimes on low-level arctic stratus, Geophys. Res. Lett., 31, doi:10.1029/2004gl019928, 2004.

Geyer, A., and Stutz, J.: Vertical profiles of NO_3, N_2O_5, O_3, and NO_x in the nocturnal boundary layer: 2. Model studies on the altitude dependence of composition and chemistry, J.Geophys. Res.,109, D12307, 10.1029/2003jd004211, 2004.

Girard, E., and Blanchet, J.-P.: Simulation of arctic diamond dust, ice fog, and thin stratus using an explicit aerosol; cloud & radiation model, Journal of the Atmospheric Sciences, 58, 1199-1221, 2001.

Girard, E., Blanchet, J.-P., and Dubois, Y.: Effects of arctic sulphuric acid aerosol particles on wintertime low-level atmospheric ice crystals, humidity and temperature at alert, Atmospheric Research, 73, 131-148, 2005.

Gotaas, Y., & Benson, C. S.: The effect of Suspended Ice Crystals on Radiative Cooling. Journal of Applied Meteorology , 446-453, 1965.

Griffiths, P. T., Badger, C. L., Cox, R. A., Folkers, M., Henk, H. H., and Mentel, T. F.: Reactive uptake of N_2O_5 by aerosol particles containing dicarboxylic acids. Effect of particle phase, composition, and nitrate content, The Journal of Physical Chemistry A, 113, 5082, 2009.

Hallquist, M., Stewart, D. J., Baker, J., and Cox, R. A.: Hydrolysis of N_2O_5 on submicron sulfuric acid aerosol particles, The Journal of Physical Chemistry A, 104, 3984-3990, doi:10.1021/jp9939625, 2000.

Hanson, D. R., and Ravishankara, A. R.: The reaction probabilities of $ClONO_2$ and N_2O_5 on 40 to 75% sulfuric acid solutions, J. Geophys. Res., 96, 10.1029/91jd01750, 1991a.

Hanson, D. R. and Ravishankara, A.R.: The Reaction Probabilities of $ClONO_2$ and N_2O_5 on Polar Stratospheric Cloud Materials, J. Geophys. Res. 96, 1991b.

Hanson, D. R., and Lovejoy, E.R.: The uptake of N_2O_5 onto small sulfuric acid particles, Geophys. Res. Lett., 21(22), 2401–2404, doi:10.1029/94GL02288, 1994.

Hanson, D. R.: Reaction of N_2O_5 with H_2O on bulk liquids and on particles and the effect of dissolved HNO_3, Geophys. Res. Lett., 24, 10.1029/97gl00917, 1997.

Helmig, D., Ganzeveld, L., Butler, T., and Oltmans, S.: The role of ozone atmosphere-snow gas exchange on polar, boundary-layer tropospheric ozone- a review and sensitivity analysis, Atmos. Chem. Phys., 7, 15-30, 10.5194/acp-7-15-200, 2007.

Heymsfield, A. J., Bansemer, A., Schmitt, C. G., Twohy, C., and Poellet, M. R.: Effective ice particle densities derived from aircraft data, J. Atmos. Sci., 61, 982-1003, 2004.

Honrath, R. E., Peterson, M. C., Guo, S., Dibb, J. E., Shepson, P. B., and Campbell, B.: Evidence of NO_x production within or upon ice particles in the Greenland snowpack, Geophys. Res. Lett., 26, 695-698, 10.1029/1999gl900077, 1999.

Horst, T. W.: The footprint for estimation of atmosphere-surface exchange fluxes by profile techniques, Boundary-Layer Meteorology, 90, 171-188, 1999.

Horst, T. W., and Weil, J. C.: How far is far enough: The fetch requirements for micrometeorological measurement of surface fluxes, Journal of Atmospheric and Oceanic Technology, 11, 1018-1025, 1994.

Hu, J. H., and Abbatt, J. P. D.: Reaction probabilities for N_2O_5 hydrolysis on sulfuric acid and ammonium sulfate aerosol particles at room temperature, The Journal of Physical Chemistry A, 101, 871-878, doi:10.1021/jp9627436, 1997.

Ivanova, D., Mitchell, D. L., Arnott, W. P., and Poellot, M.: A GCM parameterization for bimodal size spectra and ice mass removal rates in mid-latitude cirrus clouds, Atmospheric Research, 59-60, 89-113, 2001.

Jones, A. E., Weller, R., Anderson, P. S., Jacobi, H., W, Wolff, E. W., Schrems, O., and Miller, H.: Measurements of NOx emissions from the Antarctic snowpack, Geophys. Res. Lett., 28, 1499-1502, 10.1029/2000gl011956, 2001.

Kirchner, W., Welter, F., Bongartz, A., Kames, J., Schweighoefer, S., and Schurath, U.: Trace gas exchange at the air/water interface: Measurements of mass accommodation coefficients, Journal of Atmospheric Chemistry, 10, 427-449, doi:10.1007/bf00115784, 1990.

Leu, M.T.: Heterogeneous reactions of N_2O_5 with H_2O and HCl on ice surfaces: Implications for Antarctic ozone depletion, Geophys. Res. Lett., 15, 10.1029/GL015i008p00851, 1988.

Lovett, G. M.: Atmospheric deposition of nutrients and pollutants in North America: An ecological perspective, Ecological Applications, 4, 630-650, doi:10.2307/1941997, 1994.

Matsumoto, J., Imai, H., Kosugi, N., and Kajii, Y.: In situ measurement of N_2O_5 in the urban atmosphere by thermal decomposition/laser-induced fluorescence technique,

Atmospheric Environment, 39, 6802-6811, doi:10.1016/j.atmosenv.2005.07.055, 2005.

McNeill, V. F., Patterson, J., Wolfe, G. M., and Thornton, J. A.: The effect of varying levels of surfactant on the reactive uptake of N_2O_5 to aqueous aerosol, Atmos. Chem. Phys., 6, 1635–1644, 2006.

Mentel, T. F., Sohn, M., and Wahner, A.: Nitrate effect in the heterogeneous hydrolysis of dinitrogen pentoxide on aqueous aerosol particles, Phys. Chem. Chem. Phys., 1, 5451-5457,1999.

Mogili, P. K., Kleiber, P. D., Young, M. A., and Grassian, V. H.: N_2O_5 hydrolysis on the components of mineral dust and sea salt aerosol: Comparison study in an environmental aerosol reaction chamber, Atmospheric Environment, 40, 7401-7408, 2006.

Monteith, J. L., and Unsworth, M. H.: Principles of environmental physics, second ed., 291pp., Edward Arnold, 1990.

Mozurkewich, M., and Calvert, J. G.: Reaction probability of N_2O_5 on aqueous aerosol particles, J. Geophys. Res., 93, doi:10.1029/JD093iD12p15889, 1988.

Munro, D. S., and Oke, T. R.: Aerodynamic boundary-layer adjustment over a crop in neutral stability, Boundary-Layer Meteorology, 9, 53-61, 1975.

Ohtake, T.,and P.J. Huffman: Visual Range in Ice Fog. J. Appl. Meteor.,8, 499-501,1969.

Ohtake, T., Jayaweera, K., and Sakurai, K. I.: Observation of ice crystal-formation in lower arctic atmosphere, Journal of the Atmospheric Sciences, 39, 2898-2904, 1982.

Oke, T. R.: Boundary layer climates, 2nd ed., Methuen, London, 435 pp., 1987.

Osthoff, H. D., Roberts, J. M., Ravishankara, A. R., Williams, E. J., Lerner, B. M., Sommariva, R., Bates, T. S., Coffman, D., Quinn, P. K., Dibb, J. E., Stark, H., Burkholder, J. B., Talukdar, R. K., Meagher, J., Fehsenfeld, F. C., and Brown, S. S.: High levels of nitryl chloride in the polluted subtropical marine boundary layer, Nature Geosci, 1, 324-328, 2008.

Pardyjak, E. R., Monti, P., and Fernando, H. J. S.: Flux richardson number measurements in stable atmospheric shear flows, Journal of Fluid Mechanics, 459, 307-316, doi:10.1017/S0022112002008406, 2002.

Perry, K. D., Cahill, T. A., Schell, R. C., and Harris, J. M.: Long-range transport of anthropogenic aerosol particles to the national oceanic and atmospheric administration baseline station at mauna loa observatory, hawaii
Journal of Geophysical Research, 104, 18,251-218,533, 1999.

Quinlan, M. A., Reihs, C.M.,Gomen, D.M. and Tolbert M.A.: Heterogeneous reactions on model Polar Stratospheric Cloud Surfaces: Reaction of N_2O_5 on ice and nitric acid trihydrate,J. Phys. Chem.,9,pp, 3255-3260, 1990.

Riemer, N., Vogel, H., Vogel, B., Schell, B., Ackermann, I., Kessler, C., and Hass, H.: Impact of the heterogeneous hydrolysis of N_2O_5 on chemistry and nitrate aerosol formation in the lower troposphere under photosmog conditions, J. Geophys. Res., 108,doi: 10.1029/2002jd002436, 2003.

Roberts, J. M., Osthoff, H. D., Brown, S. S., and Ravishankara, A. R.: N_2O_5 oxidizes chloride to Cl_2 in acidic atmospheric aerosol, Science, 321, 1059, 10.1126/science.1158777, 2008.

Sanderson, M. G., Collins, W. J., Johnson, C. E., and Derwent, R. G.: Present and future acid deposition to ecosystems: The effect of climate change, Atmospheric Environment, 40, 1275-1283, 2006.

Simpson, W. R.: Continuous wave cavity ring-down spectroscopy applied to in-situ detection of dinitrogen pentoxide (N_2O_5). Rev. Sci. Inst, 74, 3442-3452, 2003.

Sommariva, R., Osthoff, H. D., Brown, S. S., Bates, T. S., Baynard, T., Coffman, D., de Gouw, J. A., Goldan, P. D., Kuster, W. C., Lerner, B. M., Stark, H., Warneke, C., Williams, E. J., Fehsenfeld, F. C., Ravishankara, A. R., and Trainer, M.: Radicals in the marine boundary layer during NEAQS 2004: a model study of day-time and night-time sources and sinks, Atmos. Chem. Phys., 9, 3075-3093, doi:10.5194/acp-9-3075-2009, 2009.

Stull, R. B.: An introduction to boundary layer meteorology, Kluwer Academic Publishers, 666pp.,1988.

Stutz, J., Alicke, B. r., Ackermann, R., Geyer, A., White, A., and Williams, E.: Vertical profiles of NO_3, N_2O_5, O_3, and NO_x in the nocturnal boundary layer: 1. Observations during the Texas air quality study 2000, J. Geophys. Res., 109, doi:10.1029/2003JD004209, 2004.

Thornton, J. A., Braban, C. F., and Abbatt, J. P. D.: N_2O_5 hydrolysis on sub-micron organic aerosols: The effect of relative humidity, particle phase, and particle size, Phys. Chem. Chem. Phys., 5, 4593-4603, 2003.

Thornton, J. A., and Abbatt, J. P. D.: N_2O_5 reaction on submicron sea salt aerosol: kinetics, products, and the effect of surface active organics, The Journal of Physical Chemistry A, 109, 10004-10012, doi:10.1021/jp054183t, 2005.

Thornton, J. A., Kercher, J. P., Riedel, T. P., Wagner, N. L., Cozic, J., Holloway, J. S., Dube, W. P., Wolfe, G. M., Quinn, P. K., Middlebrook, A. M., Alexander, B., and Brown, S. S.: A large atomic chlorine source inferred from mid-continental reactive nitrogen chemistry, Nature, 464, 271-274, 2009.

Toon, O. B.: Atmospheric science - how pollution suppresses rain, Science, 287, 1763, 2000.

Van Doren, J. M., Watson, L. R., Davidovits, P., Worsnop, D. R., Zahniser, M. S., and Kolb, C. E.: Uptake of dinitrogen pentoxide and nitric acid by aqueous sulfuric acid droplets, The Journal of Physical Chemistry, 95, 1684-1689, doi:10.1021/j100157a037, 1991.

Wesely, M. L., and Hicks, B. B.: A review of the current status of knowledge on dry deposition, Atmospheric Environment, 34, 2261-2282, doi:10.1016/j.atmosenv.2004.02.021, 2000.

Witte, H.J.: Airborne observations of cloud particles and infrared flux density (8-14um) in the Arctic, M.S. Thesis, Department of Atmospheric Science, University of Washington, 1968.

Wood, E. C., Bertram, T. H., Wooldridge, P. J., and Cohen, R. C.: Measurements of N_2O_5, NO_2, and O_3 east of the San Francisco bay, Atmospheric Chemistry and Physics, 5, 483-491, 2005.

Zhang, R., Leu, M., Taun, and Keyser, L. F.: Hydrolysis of N_2O_5 and $ClONO_2$ on the $H_2SO_4/HNO_3/H_2O$ ternary solutions under stratospheric conditions, Geophys. Res. Lett., 22, 1493-1496, 10.1029/95gl01177, 1995.

Zwally, H. J., Schutz, B., Abdalati, W., Abshire, J., Bentley, C., Brenner, A., Bufton, J., Dezio, J., Hancock, D., Harding, D., Herring, T., Minster, B., Quinn, K., Palm, S., Spinhirne, J., and Thomas, R.: ICESAT's laser measurements of polar ice, atmosphere, ocean, and land, Journal of Geodynamics, 34, 405-445, 2002.

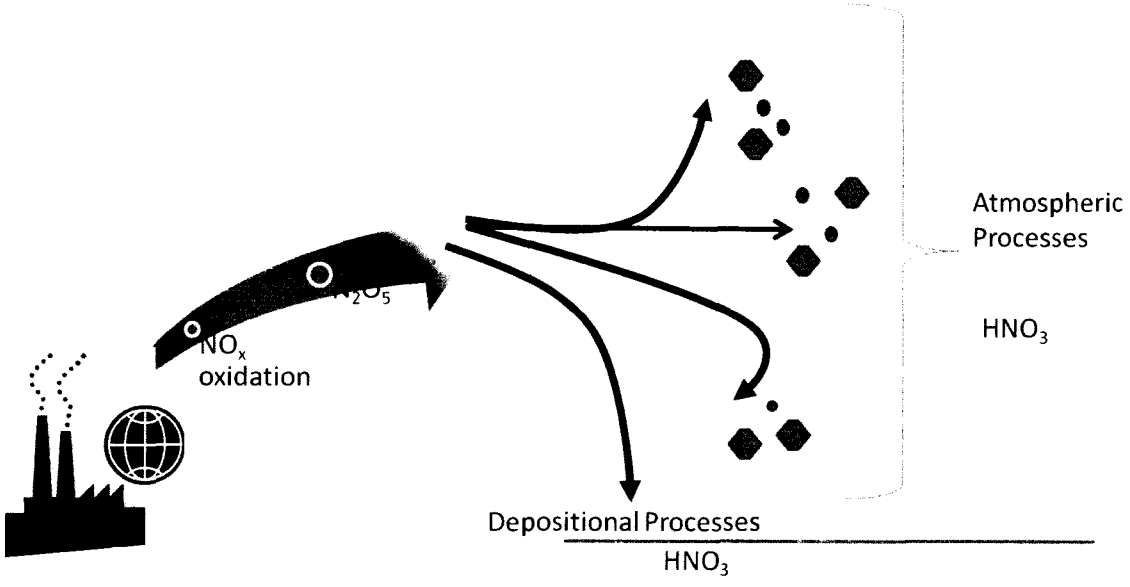

Figure 1.1. Schematic of two sub-processes for heterogeneous hydrolysis of N_2O_5. Reaction (R3) forming nitric acid, can be further partitioned into Reaction (R3a) depositional processes of N_2O_5 and Reaction (R3b) N_2O_5 reacting through atmospheric processes.

Chapter 2 Further insight into ice particles

Heterogeneous hydrolysis of N_2O_5 occurs on surfaces that catalyze the reaction to form nitric acid (R3). In the Arctic, our research group has correlated ice saturation conditions with increasing speed of reaction (R3) (Apodaca et al., 2008). However, we do not know if ice had actually nucleated when airmasses had achieved ice saturation, so we discuss the literature of ice nucleation, ice particle sizes, and number densities in the Arctic. Additionally ice particles can become relatively large, which means that their number density is reduced for a given availability of condensed water. Under these conditions, the distance from a N_2O_5 molecule to the nearest reactive ice surface may become large enough (microns) that diffusion limits the rate of N_2O_5 chemical loss. Therefore, we consider how diffusion may affect the ability of larger ice particles to act as a catalytic surface for Reaction (R3).

2.1 Past studies on ice particles

The formation of ice particles in the Arctic is a common occurrence. To consider the significance of N_2O_5 reacting with ice particles, we have to consider the size, shape, surface area and number density of the ice particles. As mentioned in the introduction several authors have measured ice particles in the Arctic. Kumai (1964) found ice particles sizes, in the polluted Fairbanks area, in the range of 2 to 30 microns in diameter, with an average diameter of 7 microns. The range in ice particle diameters is due to different types of particles categorized as ice fog, super-cooled fog and ice crystals.

Kumai (1964) examined ice from all three categories and found that the ice particles were spherical and hexagonal for ice fog and crystals respectively. Kumai (1964) concluded that the spherical shapes were due to the freezing of super-cooled water droplets and grew to become hexagonal crystals. The average size of 7 microns in diameter is similar to an earlier value reported by Thuman and Robinson (1954) of 13 microns in diameter. Benson (1965) measured ice fog in the Fairbanks area and found diameters of 5-10 microns, in the same range as previous authors. Gotaas and Benson (1965) separated the ice particles into two categories: ice fog and diamond dust. Girard et al. (2005) found an increased frequency of low level ice crystal events when acidic aerosol particles are present at the ALERT field site.

In addition to ground based studies, Witte (1968) conducted airborne observations of cloud particles in a remote Arctic region and reported ice particles with a modal radius of 9 microns (18 microns in diameter). Witte (1968) concluded that Arctic clouds were similar to cirrus clouds and contained high number densities, over 3 particles /cm^3 (3000 L^{-1}). Ohtake et al. (1982) reported ice crystals and diamond dust forming from open leads near Barrow, Alaska. Ohtake et al. (1982) found the ice crystals to be columnar in shape and larger at 30 to 300 microns in diameter. Curry et al. (1990) and Girard and Blanchet (2001) identified the two categories of ice particles: diamond dust formed during saturated with respect to ice air masses resulting in ice particles greater than 30 microns and ice fog resulting in ice particles less than 30 microns in diameter. Curry et al. (1990) noted that the low level ice particle concentrations are up to 1000 L^{-1}. Curry et al. (1990),

Girard and Blanchet (2001) and Zwalley (2002) noted the difficulty in measuring ice particles at night arise from darkness, varying humidity, water content and phase of the hydrometeor.

In an aircraft study by Brown et al. (2006), a reactive surface area of 1000 $\mu m^2/cm^3$ for sub-micron aerosol particles was found in the northeast US. There is some evidence in fog droplet measurements from a ship study done by Baynard et al. (2007), where surface areas were reported as high as $5x10^5$ $\mu m^2/cm^3$. Surface areas of ice particles also have been studied in large mid-latitude cirrus cloud studies for determining their effects on the Earth's radiative balance (CRYSTAL-FACE and NASA, MidCix SHEBA, FIRE, ARM and EMERALD-1) (Heymsfield et al., 2004; Curry et al., 2000; Ivanova et al., 2001; Garrett et al., 2003). All of the mid latitude cirrus cloud studies mentioned were focused on greater than 50 micron ice particle diameters.

2.2 Phase transitions in atmospheric particles

In addition to the size, shape and number density that can vary among observed ice particle events in the Arctic, there is evidence that the water phase is also a question. The phase transitions in aqueous atmospheric particles are known to be very important to the heterogeneous reactions on ice surfaces (Martin, 2000). The phase of lower tropospheric particles (water or ice) is still difficult to determine because super-cooled water droplets form at temperatures as low at -40°C (Witte, 1968; Curry et al., 1996; Curry et al., 1990; Girard and Blanchet 2001; Girard et al., 2005). The phase of the hydrometeor is an important variable for determining the available surface area and for the reactive uptake

coefficient of N_2O_5, γ. If the ice particle is liquid, the reactive surface of that particle will be different than if it is ice as discussed in the introduction (section 1.3). The reaction between N_2O_5 and ice surfaces has been studied under stratospheric conditions, but not extensively. There are several studies on polar stratospheric clouds (PSCs), clouds that form above 15 km in the polar atmosphere at very cold temperatures, and the ice surfaces reacting with N_2O_5 (Leu, 1988; Hanson and Ravishankara, 1991). Hanson and Ravishankara (1991) and Leu (1988) found a reactive uptake coefficient of N_2O_5 at very cold temperatures (180-220 K) of 0.024-0.03.

2.3 Diffusion limitations to reactions on ice surfaces

After our past field study investigation implicated ice surfaces as an important chemical loss mechanism of N_2O_5 (Apodaca et al., 2008), we focused on the feasibility of N_2O_5 reacting with ice particles surfaces. Under the cold temperatures and high humidity conditions experienced at our high latitude field site, it is reasonable that the additional catalytic surface area needed to account for the fast chemical loss rates of N_2O_5 is the formation of ice particles or hygroscopic growth of super-cooled water droplets at high relative humidity. However, we will have to theoretically predict the effect of these hydrometeor's on the N_2O_5 chemical loss rate. We account for all of the atmospheric processes (R3b) by calling the particles, ice particles, in the following discussion to understand the effect of varying particle size, number density and surface area on the lifetime of N_2O_5. In addition to the phase of the ice particle, there is a large range in reported ice particle sizes that needs to be considered in determining the mass transfer

limitations and terminal velocities of particles. The mass transfer limitation refers to the gas molecule of N_2O_5 reaching a few ice particles to be able to have the possibility of reacting. These limitations need to be addressed when considering the reaction of N_2O_5 on ice particle surfaces.

In the introduction we detail the use of Eq. (1.1) for calculating the reactive uptake coefficient of N_2O_5 on submicron aqueous aerosol particles. The use of Eq. (1.1) is valid when there are submicron range aerosol particles. In order to accommodate micron-size ice particles or larger, we have to consider mass transfer limitations of the gas molecule N_2O_5 colliding with an ice particle's surface. The relationship between the lifetime of a molecule and the chemical loss to micron-sized ice particles is complex and includes terms describing the diffusion, collision between the molecule and the particles surface and the phase of the particle. To calculate the lifetime of N_2O_5 (τ) with respect to ice particles, we use the following formula from Martinez et al. (2000),

$$\tau = \frac{1}{N}\left[\frac{1}{4\pi r D} + \frac{1}{\pi v D_p^{\,2}} + \frac{1-\gamma}{\gamma \pi v D_p^{\,2}}\right]. \qquad (2.1)$$

In Eq. (2.1) the variables and units are listed as the following:

N = particles/ m^3

D= Molecular diffusion constant (10^{-5} m^2/s for N_2O_5)

v = molecular velocity (236.4 m/s for N_2O_5)

D_p = particle diameter (m)

γ = uptake coefficient of N_2O_5

In Fig. 2.1, we use Eq. (2.1) with a constant surface area of the ice particles of 1000 $\mu m^2/cm^3$ and varied the reactive uptake coefficient, γ, from 0.01, 0.03 to 0.1 to calculate the predicted lifetime of N_2O_5 as a function of particle size at these three values of surface reactivity. In the limit of smaller, submicron, particles, Fig 2.1 shows that the lifetime plateaus and is inversely related to the reactive uptake coefficient of N_2O_5, γ. That result is in agreement with Eq. (1.1), because Eq. (1.1) is only valid for submicron aerosol particles, where diffusion limitation is not important.

For micron-sized and larger particles, diffusion limitations begin to slow the effective rate of gas-surface collisions and the lifetime increases with increasing particle size. The reason for this increase is that at a fixed aerosol particle surface area density (1000 $\mu m^2/cm^3$ in this case), larger particles must be present at a lower number density and therefore, the distance to diffuse to a particle surface becomes larger. As the inter-particle spacing exceeds a few microns, diffusion and not γ begins to control the effective lifetime of N_2O_5. This effect is seen in Fig. 2.1 by the convergence of the curves having different values of γ for 100 micron or larger particles. Based upon these results, we find that around 10 micron particles are the transitional region where both diffusion limitation and surface reactivity (γ) combine to control the lifetime of N_2O_5. It is unfortunate that the literature reviewed earlier in this chapter indicates that ice particle sizes are on the order of 10 micron diameters.

In Fig. 2.2, we use Eq. (2.1) with a constant $\gamma = 0.03$, based on Hanson and Ravishankara's (1991) surface reactivity of $\gamma = 0.024$ for pure ice and plot curves with various values of the surface area density versus the particle size. Presuming that the particles may have a diameter of 10 microns, and using our field observed ice-saturated N_2O_5 lifetime of 6 minutes (Apodaca et al., 2008), we would need around 3,000 $\mu m^2/cm^3$ of aerosol particle surface area density to obtain the observed lifetimes of N_2O_5.

If we assume that the ice particles are nearly spherical, then we can convert between the surface area density and the particle number density given an assumed particle diameter using,

$$SA = N\pi D_p^2 \ . \qquad (2.2)$$

In Eq. (2.2), the ice particle surface area density, *SA,* in $\mu m^2/cm^3$ is equal to the number of particles/cm^3 (N) multiplied by π and the ice particle diameter squared (D_p^2). For the ice particle size applicable to N_2O_5 chemistry of approximately 10 microns in diameter and the resulting 3000 $\mu m^2/cm^3$ in surface area density from Fig. 2.2, Using a surface area density of 3000 $\mu m^2/cm^3$ from Fig. 2.2 , we require 10,000 particles L^{-1} (10 particles/cm^3). However, Curry et al. (1990) reported that the maximum ice particle concentration that they observed was 4000 L^{-1}. While it is possible that our situation had significantly more particles present than Curry's flights measured, it seems that diffusion limitations are very significant if the reaction of N_2O_5 is actually occurring on suspended ice surfaces.

From these considerations of ice particle size, ice particle abundance, possible supercooling of droplets, and diffusion limitations, we find that although it still seems feasible that suspended ice particles could be providing the reactive surface area for N_2O_5 heterogeneous hydrolysis, the number density of these particles should be towards the high side of typically observed ice particle densities, the size should be towards the small size of typically observed ice fogs, and possibly the reactive uptake coefficient should be relatively large ($\gamma \approx 0.1$). Toon (2000) showed that in a polluted cloud, the presence of more condensation nuclei (the pollution) causes increased number density of droplets and reduced particle size. Possibly the Fairbanks pollution plume causes the same effect to increase the feasibility of suspended ice particles being the major reactive site for N_2O_5 heterogeneous hydrolysis.

References:

Apodaca, R. L., Huff, D. M., and Simpson, W. R.: The role of ice in N_2O_5 heterogeneous hydrolysis at high latitudes, Atmos. Chem. Phys., 8, 7451-7463, 2008.

Benson, C.S.: Ice Fog: Low temperature air pollution. Geophys. Inst. Rept. UAG R-173, Univ. of Alaska, 14-17 (DDC No. AD631553), 1965.

Baynard, T., Lovejoy, E. R., Pettersson, A., Brown, S. S., Lack,D., Osthoff, H., Massoli, P., Ciciora, S., Dubé, W. P., and Ravishankara,A. R.: Design and application of a pulsed cavity ringdown aerosol extinction spectrometer for field measurements, Aerosol Sci. Technol., 41, 447–462, 2007.

Benson, C. S.: Ice fog. Weather, 25, 11–18,1970.

Brown, S. S., Ryerson, T. B., Wollny, A. G., Brock, C. A., Peltier, R., Sullivan, A. P., Weber, R. J., Dubé, W. P., Trainer, M., Meagher, J. F., Fehsenfeld, F. C., and Ravishankara, A. R.: Variability in nocturnal nitrogen oxide processing and its role in regional air quality, Science, 5757, 67-70, doi: 10.1126/science.1120120, 2006.

Curry, J., Meyer, F., Radke, L., Brock, C., & Ebert, E.: Occurence and Characteristics of Lower Tropospheric Ice Crystals in the Arctic. International Journal of Climatology , 749-764, 1990.

Curry, J. A., Randall, D., and Rossow, W. B.: Overview of arctic cloud and radiation characteristics, J. Climate, 9, 1731-1764, 1996.

Garrett, T. J., H. Gerber, D. G. Baumgardner, C. H. Twohy, D. G. Baumgardner, and E. M. Weinstock Small, highly reflective ice crystals in low-latitude cirrus Geophys. Res. Lett., 30, doi:10.1029/2003GL018153, 2003.

Girard, E., and J.P. Blanchet: Microphysical Parameterization of Arctic Diamond Dust, Ice Fog, and Thin Stratus for Climate Models. J. Atmos. Sci., 58, 1181–1198, 2001.

Girard, E.; Blanchet, Jean-Pierre; Dubois, Yves: Effects of arctic sulphuric acid aerosol particles on wintertime low-level atmospheric ice crystals, Alert Nunavut. Atmospheric Research, 131-148, 2005.

Gotaas, Y., & Benson, C. S.: The effect of Suspended Ice Crystals on Radiative Cooling. Journal of Applied Meteorology , 446-453, 1965.

Hanson, D. R., and Ravishankara, A. R.: The reaction probabilities of $ClONO_2$ and N_2O_5 on 40 to 75% sulfuric acid solutions, J. Geophys. Res., 96, doi: 10.1029/91jd01750, 1991.

Heymsfield, A. J., C. G. Schmitt, A. Bansemer, D. Baumgardner, E. M. Weinstock, J. T. Smith, and D. Sayres ; Effective ice particle densities for cold anvil cirrus Geophys. Res. Lett., 31, doi:10.1029/2003GL018311, 2004.

Ivanova,D. , David L. Mitchell, W. Patrick Arnott and Michael Poello: A GCM parameterization for bimodal size spectra and ice mass removal rates in mid-latitude cirrus clouds, Atmospheric Research 59– 60,89– 113,2001.

Kumai, M.: A Study of Ice Fog and Ice-Fog Nuclei in Fairbanks, AK., Cold Regions Research and Engineering Laboratory Report, Part 1, 1964.

Leu, M.T.: Heterogeneous reactions of N_2O_5 with H_2O and HCl on ice surfaces: Implications for Antarctic ozone depletion, Geophys. Res. Lett., 15, 10.1029/GL015i008p00851, 1988.

Martin, S. T. : Phase Transitions of Aqueous Atmospheric Particles. Chemical Reviews 100(9): 3403, 2000.

Martinez, M., Perner, D., Hackenthal, E., Kulzer, S., and Schutz, L.: NO_3 at Helgoland during the Nordex campaign in October 1996, Journal of Geophysical Research 105, 22,685-622,695, 2000.

Ohtake, T., K. Jayaweera, and K.I. Sakurai: Observation of Ice Crystal Formation in Lower Arctic Atmosphere. J. Atmos. Sci., 39, 2898–2904,1982.

Thuman,W.C. and Robinson,E.: Study of Alaskan ice-fog particles, Stanford Research Institute, 1954.

Toon, O. B., : Science,Vol. 287. no. 5459, pp. 1763 – 1765,doi: 10.1126/science.287.5459.1763, March, 2000.

Witte, H.J.: Airborne observations of cloud particles and infrared flux density (8-14um) in the Arctic, M.S. Thesis, Department of Atmospheric Science, University of Washington, 1968.

Zwally, H. J., Schutz, B., Abdalati, W., Abshire, J., Bentley, C., Brenner, A., Bufton, J., Dezio, J., Hancock, D., Harding, D., Herring, T., Minster, B., Quinn, K., Palm, S., Spinhirne, J., and Thomas, R.: ICESAT's laser measurements of polar ice, atmosphere, ocean, and land, Journal of Geodynamics, 34, 405-445, 2002.

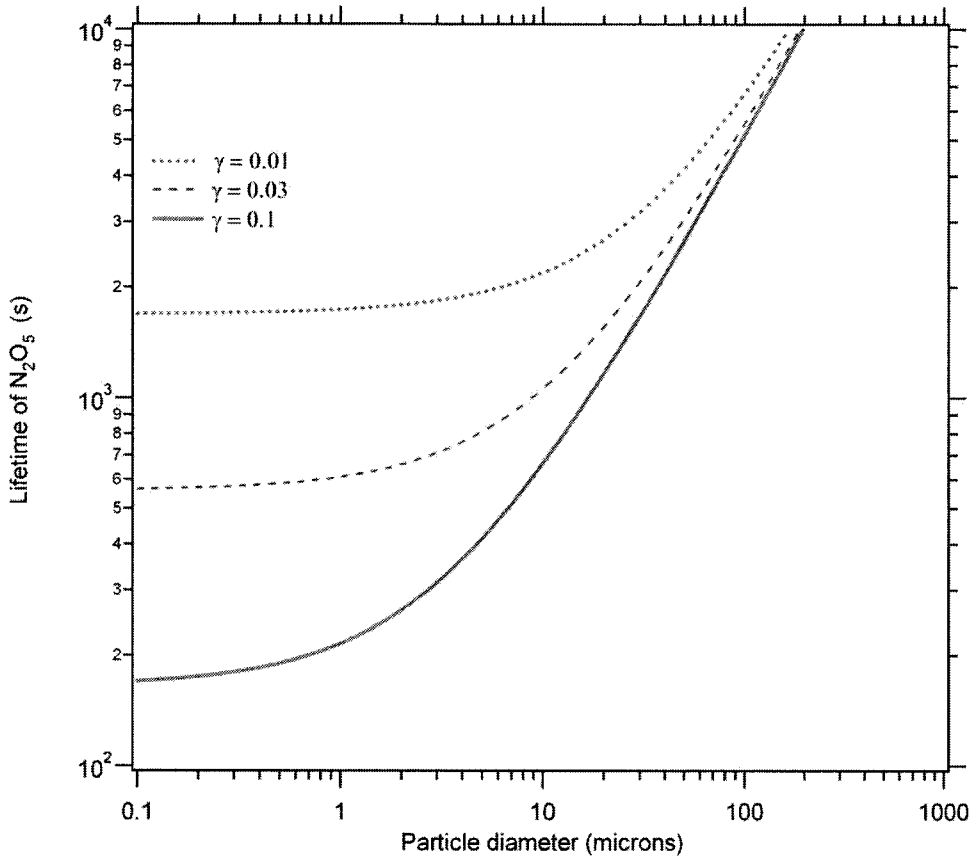

Figure 2.1. Plot of the lifetimes of N_2O_5 as a function of particle size. The surface area is constant at 1000 $\mu m^2/cm^3$. The dotted trace, dashed trace and solid line represents lifetime of N_2O_5 with γ values of 0.01, 0.03 and 0.1 respectively.

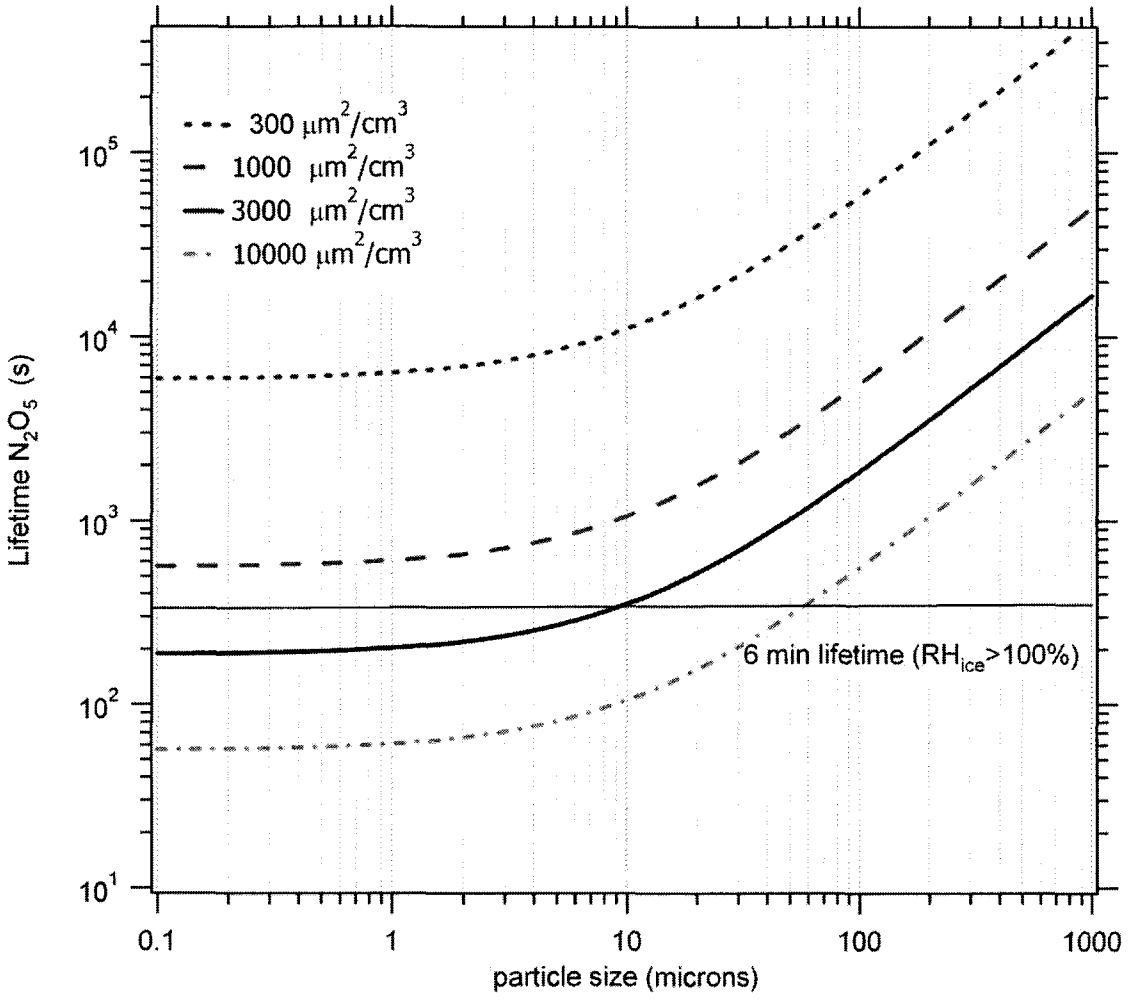

Figure 2.2. Plot of the lifetimes of N_2O_5 as a function of particle size. The value of γ is at a constant value of 0.03 . The dotted, dashed, solid and dot-dashed lines represent the following surface areas respectivly, 300, 1000, 3000, 10,000 $\mu m^2/cm^3$.

Chapter 3 Experimental design for fall 2009 field study

We measured the flux and deposition velocity of N_2O_5 in a fall 2009 field study in Fairbanks, Alaska. The field study was designed to use meteorological techniques to determine a N_2O_5 deposition velocity. The field study considered the effect of distance and wind direction from downtown Fairbanks, footprint of the upwind measurement area, and interference from local pollution sources on the N_2O_5 deposition velocity measurements.

The aerodynamic method relies on the Monin-Obukov (M-O) theory to measure fluxes, and the M-O theory requires that flux be measured in a nearly neutral atmosphere. A neutral atmosphere is defined by stability parameters such as the Richardson number (see Chapter 5) equal to zero, where buoyancy is negligible and winds are generally high. The flux is inferred from the differences in chemical mixing ratios of gases, temperatures and wind speeds at two heights (Oke, 1987).

To measure the N_2O_5 flux, we have to observe the boundary layer conditions in the atmosphere. An atmospheric flux is affected by dynamic processes in the boundary layer and turbulent contact with the ground. Understanding the impacts of upwind conditions and site characteristics on the meteorological measurements is important to measure the flux correctly. The undistributed flat field upwind distance from the measurement tower is called the fetch. We will characterize the fetch and examine several ways to consider whether we have an adequate fetch for our field study to measure a flux. Then, we will describe the location, wind direction, relationship to downtown Fairbanks and topography

characteristics. Lastly, we will discuss our tower placement at the site and sampling techniques.

3.1 Characterizing the fetch and affect on the measurement height

The placement of a flux measurement tower must allow for adequate fetch distance of a minimum of 100 meters per meter of the measurement height of the tower (Businger et al., 1971). The fetch distance is said to be farther in the case of stable atmospheric conditions and more than 100 times the maximum height of the measurement tower (Horst and Weil, 1994; Horst, 1999). Stable conditions that are commonly found in the Arctic are the most difficult to measure a flux. Strong inversions have the low wind speeds and cold temperatures near the surface and warmer temperatures above. However, Munro and Oke, (1975) found contradicting evidence that a fetch distance of 100 meters per meter height is too long and recommended closer to 30 meters per meter of profile height measurement. To account for the most common Arctic conditions, a cold stable atmosphere, we have chosen at least 100 meters per maximum profile height.

Table 3.1 details the two possible options for our measurement tower equipment, instruments and fetch requirements for each configuration. The disadvantage of having a maximum measurement height of 4 meters is the 100:1 fetch to height rule. The advantage to using 4 meter and 1 meter measurement heights is a larger possible gradient could be measured. The lower required fetch for the 2 meter maximum measurement height was the deciding factor. The smaller possible gradient measurements can be validated by the use of high frequency meteorological data obtained from two additional

sonic anemometers placed at the same measurements heights (two anemometers can validate the gradient meteorological data at any two heights). The actual heights are 2.38 meter and 0.98 meter. The measureable vertical gradients will be smaller using a 1.4 m difference in height, instead of a 3 meter gradient and the highest measurement height of 2.38 meter. The maximum height of 2.38 meters should have a constant flux layer about 10 times the maximum measurement height or a height of 23.8 meters. The surface layer is commonly considered the "constant-flux" layer and the lower 10% of the boundary layer (Arya, 2001).

We estimated the required fetch distance for a 2.38 meter measurement height and for comparison a 4 meter height using the following relationship between height and surface roughness as proposed in Horst and Weil (1994) as Z_m/Z_0. This ratio is the normalized measurement height, where Z_m is the maximum measurement height in meters and Z_0 is the roughness length in meters. The roughness length (Z_0) indicates the roughness of the surface and effect on neutral stability (Stull, 1988).

The ratio of Z_m/Z_o , using 2.38 m and 0.005 roughness length for snow from Stull (1988) is 476. Using these values and method described in Horst and Weil (1994), we would need 1,000 meters of required fetch to calculate a flux under the most stable atmospheric conditions. The required fetch using a 4 m maximum height and the most stable conditions is 3,000 meters. The probability of observing a stable atmosphere requiring a longer than 100:1 fetch-to-height ratio is high so we chose a height of 2.38

meters to decrease the fetch required at our site. According to Horst and Weil (1994), both height scenarios would still be measuring 90% of the flux.

Schuepp et al. (1990) uses the cumulative normalized flux relationship between the maximum fetch and measurement height to understand the percentage of flux measured. Using an analytical technique to examine flux requirements, Schuepp et al. (1990) reports that at a fetch of 1,000 meters and a measurement height of 5 meters, 95% of the surface flux will be measured.

3.2 Controlling features of the field site

After determining appropriate measurement heights, we have to determine the potential effect of our field site location only having a fetch distance of 400 meters. The chosen field site is located 20 miles downwind from downtown Fairbanks on a flat agricultural farm. Figure 3.1 shows the actual field site. The white line represents a distance of 400 meters from the measurement towers to the start of a spruce forest. The spruce forest is considered a disturbance in the flat terrain of the field and therefore 400 meters is the maximum fetch available at this site.

The maximum wind speeds at the field site are 3.5-4 m/s in every direction including the main wind direction of 45 degrees. An adequate fetch distance at 2.38 meter measurement height is 238 meters according to the 100:1 fetch to height ratio. For the most stable atmospheric conditions, we would need 1000 meters, according to the Horst and Weil (1994) method using a Richardson stability number of 0.25, the most stable.

However, we filter the data so that 0.12 is the threshold for stable atmospheric conditions (Chapter 5 details the Richardson number), reducing the required fetch distance.

Figure 3.3 shows that the field site is surrounded by a ridge to the NW, the Tanana River to the South and Fairbanks to the NE. A topographical view of the field site and surrounding area are shown on a contour map in Fig. 3.4. We need to know the surrounding area's topography so the effects of the topography on the meteorological air flow to the field site can be examined. The topographical structure of the area, as seen in the Fig. 3.4, creates a drainage flow guided by a U-shaped ridge that forms a bowl around the field site. Mildly polluted air originating in Fairbanks is carried from the northeast direction by a down-slope drainage flow towards the field site. The elevation profile of the upwind distance from the measurement towers is important, because if the terrain is hilly then extra correction factors have to be added to the flux data to account for turbulence resulting from the slope of the field (Turnipseed et al, 2003).

3.3 Designing the measurement towers

We analyzed the field site and meteorological components needed to successfully measure the snowpack deposition of N_2O_5 at high latitudes and decided that the field was appropriate for this experiment. Then we designed two measurement towers and an instrument hut to run the field experiment. We decided to run power 200 meters over a local driveway and out into the field, while still allowing for 400 meter undisturbed distance to the upwind forest edge. We pulled an insulated hut into the field to house the instruments and run the gas sampling inlet for N_2O_5, NO, NO_2 and ozone from the hut.

Figure 3.6 shows the hut's position and the field prior to a larger snow fall that provided an undisturbed snow surface on the field during our measurement period. The exact height of all of the instruments on both the gas sampling and the meteorological tower are depicted to scale in Fig. 3.7.

The measurement towers were located 3 meters upwind from the instrument hut. The meteorological tower (B) held two RM Young cup anemometers and wind vanes (model 03001-5) to measure wind speeds and directions and two temperature sensors (RM Young 41342) at the same heights as the moveable gas inlet sampling heights (within a few cm for vertical alignment). The data from these instruments were recorded as 1 minute averages on a Campbell Scientific CR10x data logger. The meteorological measurement tower (B) also had two sonic anemometers (RM Young model 84000) logging 10 Hz data on a separate data logger (Chaparral Physics). Both the sonic and cup anemometers were aligned to true north using a Garmin Venture GPS. The meteorological tower and sampling inlet both faced into the main wind direction of 45 degrees. Tower (A) consisted of a moveable gas sampling inlet that ran from the instrument hut. The gas sampling inlet faced into the wind and slightly at an angle to prevent larger particles from getting into the inlet. The Teflon inlet was 3/8" inner diameter and sampled the chemical gases: N_2O_5, NO_2, NO and O_3. The inlet was moved up and down to sample at the same two heights (2.38 m and 0.98 m) as the meteorological instruments. A long chain driven by a stepper motor allowed the inlet to move to an exact position. The inlet was moved every 120 seconds to match the

measurement cycle on the cavity ring down instrument that analyzed the sampled air for the mixing ratio of N_2O_5. Cavity ring down spectroscopy is the technique used to measure N_2O_5 in the portable instrument that was designed in our lab and used in previous field experiments (Simpson, 2003; Ayers et al., 2005). NO_x and O_3 were measured by the following standard instruments: Thermo Environmental 42c and Dasibi 1008 RS and logged at 6 second data rate. All computers that logged data from four different sources were time synced prior to the start of the field study and verified daily. The complete synchronization of the instrumentation, placement and field location allowed us to measure a gradient between the two heights of N_2O_5 and calculate the deposition velocity of N_2O_5.

References:

Arya, S. P.: Introduction to micrometeorology, second ed., Academic press, 420 pp., 2001.

Ayers, J. D., Apodaca, R. L., Simpson, W. R., and Baer, D. S.: Off-axis cavity ringdown spectroscopy: Application to atmospheric nitrate radical detection, Appl. Optics., 44, 7239-7242, 2005.

Businger, J. A., Wyngaard, J. C., Izumi, Y., and Bradley, E. F.: Flux-profile relationships in the atmospheric surface layer, Journal of the Atmospheric Sciences, 28, 181-189, 1971.

Horst, T. W., and Weil, J. C.: How far is far enough: The fetch requirements for micrometeorological measurement of surface fluxes, Journal of Atmospheric and Oceanic Technology, 11, 1018-1025, 1994.

Horst, T. W.: The footprint for estimation of atmosphere-surface exchange fluxes by profile techniques, Boundary-Layer Meteorology, 90, 171-188, 1999.

Munro, D. S., and Oke, T. R.: Aerodynamic boundary-layer adjustment over a crop in neutral stability, Boundary-Layer Meteorology, 9, 53-61, 1975.

Oke, T. R.: Boundary layer climates, 2nd ed., Methuen, London, 435 pp., 1987.

Schuepp, P. H., Leclerc, M. Y., MacPherson, J. I., and Desjardins, R. L.: Footprint prediction of scalar fluxes from analytical solutions of the diffusion equation, Boundary-Layer Meteorology, 50, 18, 1990.

Simpson, W. R.: Continuous wave cavity ring-down spectroscopy applied to in-situ detection of dinitrogen pentoxide (N_2O_5). Rev. Sci. Inst, 74, 3442-3452, 2003.

Stull, R. B.: An introduction to boundary layer meteorology, Kluwer Academic Publishers, 666 pp., 1988.

Turnipseed A.A., Anderson D.E., Blanken P.D., Baugh W.M, Monson R.K. : Airflows and turbulent flux measurements in mountainous terrain Part 1.Canopy and local effects. Agricultural and Forest Meteorology 119:1-2. 1-21, 2003.

Table 3.1. Profile height comparison

Heights	Advantage	Disadvantage
4 and 1 meter	Less critical inlet placement (larger gradients could be measurement with less error) 3 meter height gradient	Larger fetch distance (400 meters minimum)
2 and 0.5 meter	Smaller fetch distance (200 meters minimum) Easier to be the same atmospheric layer under stable inverted conditions	Need accurate instruments, sonic anemometers for small gradients Critical inlet placement (smaller gradients could have greater error) 1.5 meter gradient

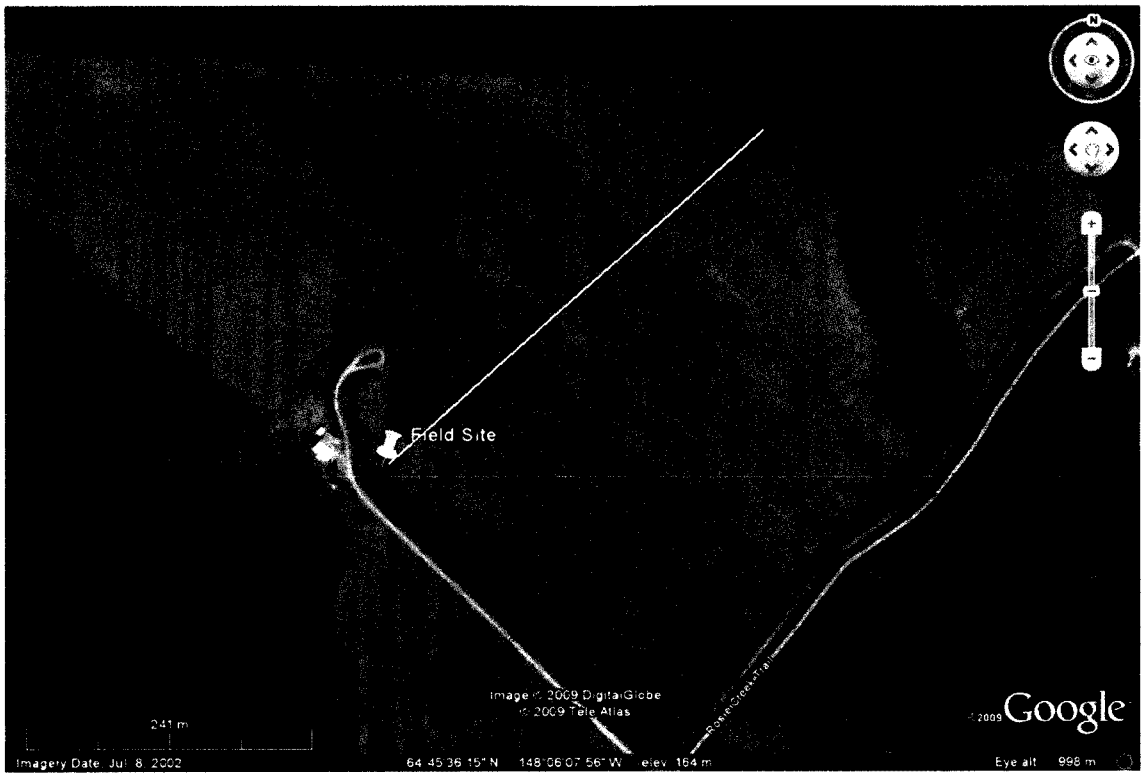

Figure 3.1. A Google image of the field study site. The field site is 20 km SW of Fairbanks. The location of the measurement instruments is represented by the yellow pin and labeled Field Site. The white line indicates the length of the field (400 m) in the main wind direction (45^0). The due North wind direction, not including declination, is given by the N in the top right hand corner (Google Inc., 2009).

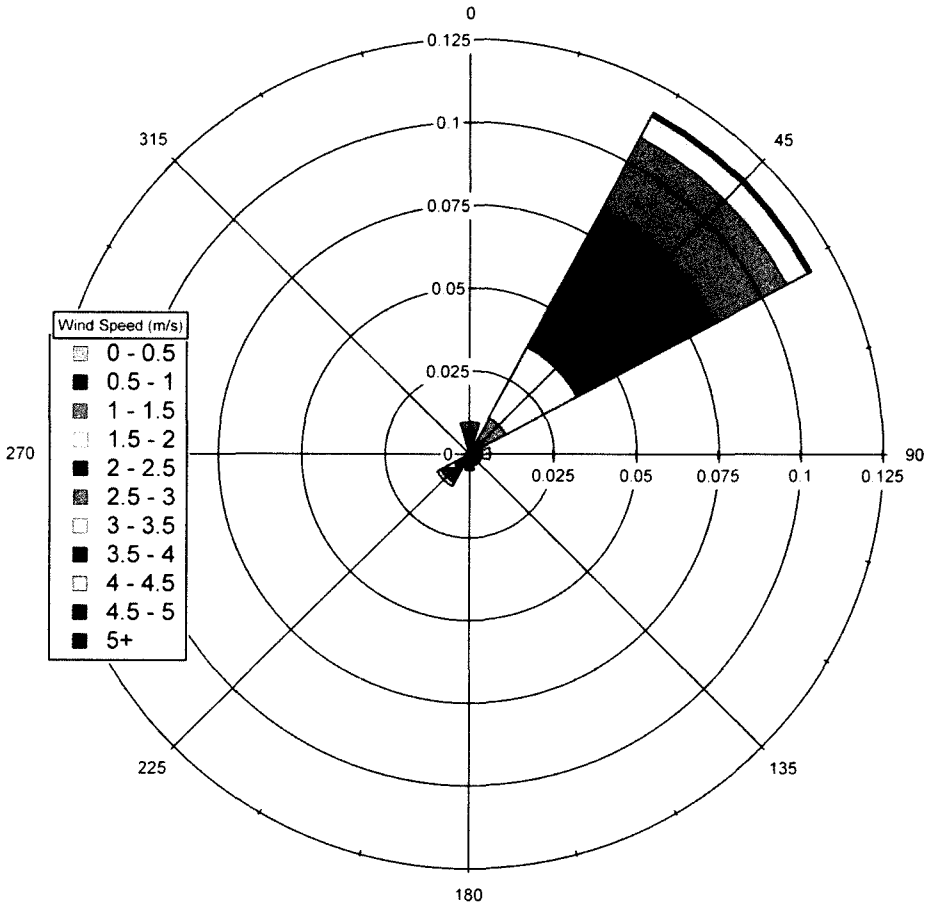

Figure 3.2. A wind plot representing the measured wind speed in m/s. The bins are 0.5 m/s and colored for each wind direction (in degrees) at the field site.

Figure 3.3. A Google map of the location of the field site with proximity to Fairbanks. The site is shown as approximately 20 km SW of downtown Fairbanks and labeled with a yellow pin. The site coordinates are 64.75929° North, 148.10618° West and 161 meters above mean sea level (Google, Inc., 2009)

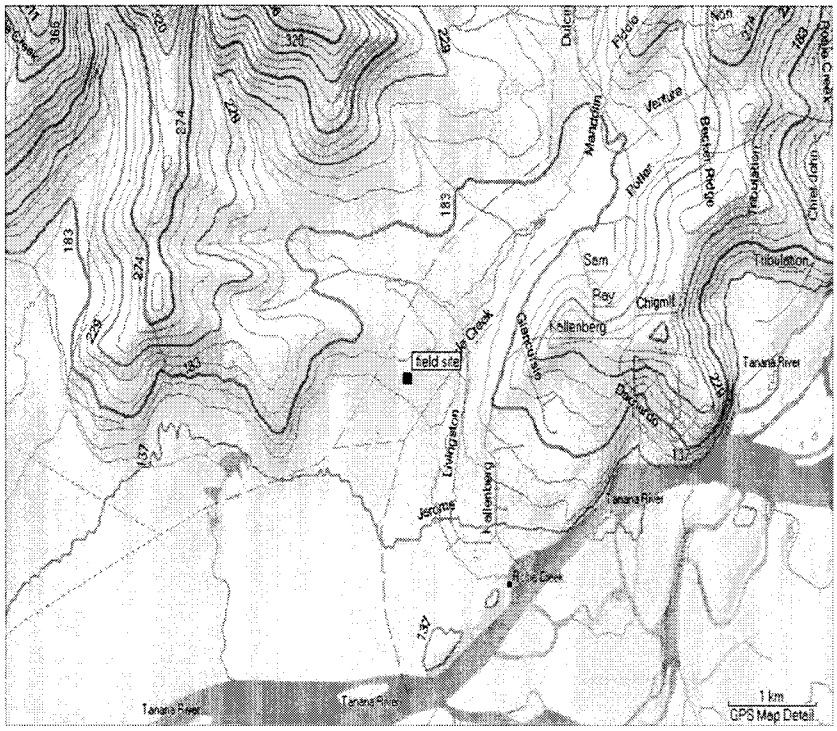

Figure 3.4. A topological contour plot using Garmin software. Contour lines are in meters of the fall 2009 field study site and surrounding area. The black square is the field site.

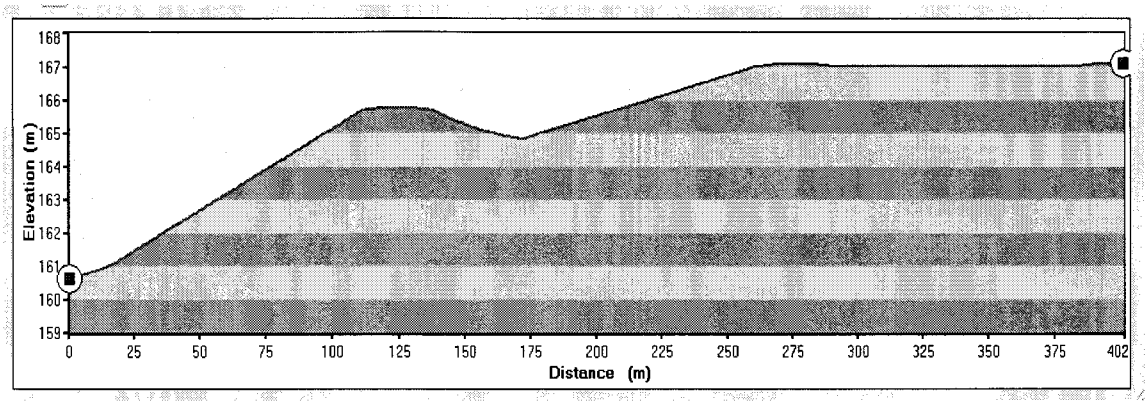

Figure 3.5. An elevation profile from the contour plot. The upwind distance from the measurement towers and heading in the main wind direction of 45 degrees until it reaches edge of the field at 400 meters.

Figure 3.6. Placement of the instrument hut. The view range of the picture is approximately 0-90 degrees.

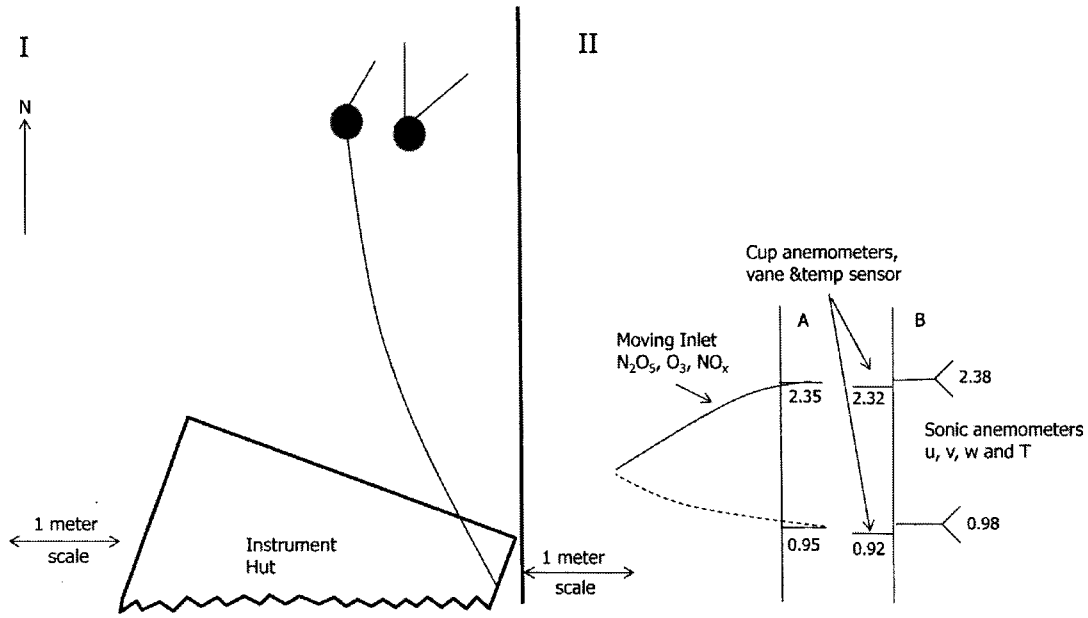

Figure 3.7. A to-scale depiction of the field site. I) The top down view and orientation of the two measurement towers and instrument hut. II) Detail plan view of the moving inlet tower (A) and the meteorological tower (B).

Chapter 4 Methods for measuring N_2O_5

This chapter focuses on measuring N_2O_5 in the field and under conditions appropriate for calculating a steady state lifetime of N_2O_5. The first section details measuring N_2O_5 in the field and the second section details using the steady state approximation to determine the lifetime of N_2O_5.

4.1 Measuring N_2O_5 in the field

We fielded a deployable instrument based on the CRDS (cavity ring-down spectroscopy) technique that measures N_2O_5 mixing ratios down to a few pptv. We have used this CRDS instrument during past field studies (Ayers and Simpson, 2006; Apodaca et al., 2008) . The CRDS instrument uses a high-flow Teflon inlet with a 9.4 mm inner diameter (3/8") and flow rate of 100 slpm to sample ambient air. The inlet is 10 meters long and has a gas residence time of 0.4 seconds. Using this configuration, the N_2O_5 inlet transmission was measured to be 76% through flow changing studies. The N_2O_5 loss on the inlet and instrumental surfaces were taken into account in the analysis. The sampled air leaves the sampling inlet and enters a 100°C heated instrument inlet where the N_2O_5 fully dissociates into NO_3 and NO_2. Next, the air flow enters at the 85°C heated measurement cell where NO_3 is measured by cavity ring down spectroscopy at 662 nm. The CRDS measures the optical loss in the cell, the time for the light to fully exist the cell with present absorbers (NO_3), by measuring a ring down during the measurement cycle and subtracting from a base line ring down during the titrant cycle. The chemical zero, which creates the reference for the base line ring down time, is formed by adding to

the airflow, NO which reacts quickly with NO_3. The result is an optical loss that is converted into a concentration using the following formula:

$$[NO_3] = 1/c\sigma[1/\tau - 1/t_0]. \qquad (4.1)$$

In this equation c is the speed of light in m/s, σ is absorption cross section in cm^2/molecule and τ is ring down time in the cavity (Simpson, 2003; Ayers et al., 2005). The data is post-processed and the ambient mixing ratios of N_2O_5 are corrected by the transmission as has been done in our past field studies (Ayers and Simpson, 2006 ; Apodaca et al., 2008).

4.2 Calculating the steady state lifetime of N_2O_5

Applying the steady state equation requires knowledge of the sources and sinks involved in the chemistry of N_2O_5. The following reactions are involved in the chemistry of N_2O_5 and used to calculate the steady state lifetime.

$$NO_2 + O_3 \rightarrow NO_3 + O_2 \qquad (R1)$$

$$NO_2 + NO_3 \rightarrow N_2O_5 \qquad (R2a)$$

$$NO_2 + NO_3 \leftarrow N_2O_5 \qquad (R2b)$$

$$N_2O_5 + H_2O \xrightarrow{\text{Surface}} 2HNO_3 \qquad (R3)$$

The cold temperatures at the field site allow us to assume rapid conversion of NO_3 to N_2O_5. The thermal dissociation of N_2O_5 (R2b) is slower than the heterogeneous

hydrolysis of N_2O_5 (R3) (Apodaca et al., 2008). This results in the following expression for the change in N_2O_5 with time:

$$d[N_2O_5]/dt = k_1[NO_2][O_3] - k_3[N_2O_5]. \quad (4.2)$$

If we assume N_2O_5 is at steady state, then we set Eq. (4.2) equal to zero and rearrange it to get the following formula for the steady state lifetime of N_2O_5. The lifetime of N_2O_5 is the inverse of its destruction rate:

$$\tau_{N_2O_5 ss} = \frac{1}{k_3} = \frac{[N_2O_5]}{k_1[NO_2][O_3]} . \quad (4.3)$$

As stated in chapter 1, the source rate of N_2O_5 is the rate coefficient for Reaction (R1), k_1, multiplied by the concentrations of NO_2 and ozone.

To indentify data where the steady state approximation is valid (Eq. 4.3), we have to consider the following reaction with NO:

$$NO_3 + NO \rightarrow 2\ NO_2. \quad (R4)$$

The nitrate radical (NO_3) can react rapidly with NO so to ensure that our N_2O_5 mixing ratio is not suppressed by this fast reaction, we eliminate all data where NO is greater than 1 ppbv. We also filter the data using the source rate; if the source rate is less than 10 pptv/hr. We only analyzed data when a pollution plume was present. In addition using chemical filters to remove data, we also removed data from when the sun was above the horizon to focus on nighttime reaction of N_2O_5. Additional meteorological filters were

applied depending on the atmospheric stability, wind speed and wind direction (detailed in Chapter 6).

References:

Apodaca, R. L., Huff, D. M., and Simpson, W. R.: The role of ice in N_2O_5 heterogeneous hydrolysis at high latitudes, Atmos. Chem. Phys., 8, 7451-7463, doi:10.5194/acp- 8-7451-2008, 2008.

Ayers, J. D., Apodaca, R. L., Simpson, W. R., and Baer, D. S.: Off-axis cavity ringdown spectroscopy: Application to atmospheric nitrate radical detection, Appl. Optics., 44, 7239-7242, 2005.

Ayers, J. D., and Simpson, W. R.: Measurements of N_2O_5 near Fairbanks, Alaska, J. Geophys. Res., 111, D14309, doi:10.1029/2006JD007070, 2006.

Simpson, W. R.: Continuous wave cavity ring-down spectroscopy applied to in situ detection of dinitrogen pentoxide (N_2O_5), Rev.Sci. Instrum., 3443–3452, doi:10.1063/1.1578705, 2003.

Chapter 5 Analysis using the aerodynamic gradient method

We use the aerodynamic gradient method to calculate a chemical flux of N_2O_5 and wind speed, wind direction and temperature data to understand the associated micrometeorological conditions. In this Chapter, we review the theory behind the aerodynamic gradient method and how we applied this method to our data to arrive at a deposition velocity of N_2O_5.

5.1 Monin-Obukhov similarity theory

To measure the deposition velocity, we use the aerodynamic gradient method. The atmosphere needs to be neutral, or near neutral stability, so that moderately turbulent flow over the snowpack is occurring in the nocturnal boundary layer. Neutral stability is defined by an air parcel motion where advection or dampening is not occurring. The aerodynamic method relies on the Monin-Obukhov similarity theory, which states that momentum and heat fluxes are constant with height under neutral atmospheric conditions. Using four independent variables, the height above the surface, surface drag, heat flux and buoyancy, we can quantify an unknown flux (Arya, 2001).

Under neutral atmospheric conditions, the logarithmic wind profile equation is as follows:

$$\bar{u}_z = \frac{u_*}{k} \ln \frac{z}{z_0}. \qquad (5.1)$$

In Eq. (5.1), z is the atmospheric height (m) above the surface, u_* is the friction velocity

in m/s, $\bar{u}_z$ is the wind speed in m/s, k is the Von Karman constant at a value of 0.4, and z_0 is the surface roughness in m. The Monin-Obukhov theory assumes neutral stability of the atmosphere, constancy of flux with height and similarity of all transfer coefficients for momentum (K_m), heat (K_Q), and gas ($K_{N_2O_5}$) (Oke, 1987; Arya, 2001; Monteith and Unsworth, 1990). Therefore, under neutral conditions we set the momentum flux equal to the unknown N_2O_5 flux and solve for the unknown flux as shown in Oke (1987):

$$\tau = \rho u_*^2 = \frac{K_m \partial(\rho u)}{\partial z} = -\frac{K_{N_2O_5} \partial(C_{N_2O_5})}{\partial z}. \qquad (5.2)$$

In Eq. 5.2, the momentum flux is τ, density of air is ρ and $C_{N_2O_5}$ is the mixing ratio of N_2O_5 in pptv. Rearranging Eq. 5.2, the transfer coefficient for momentum and N_2O_5 cancel out and the N_2O_5 chemical flux equation becomes (Oke, 1987):

$$F_{N_2O_5} = \frac{\Delta\bar{u}\Delta\overline{C_{N_2O_5}}}{\left[\ln(z_1/z_2)\right]^2}(\Phi_M\Phi_{N_2O_5})^{-1}. \qquad (5.3)$$

In Eq. 5.3, the flux of N_2O_5 is determined by the wind speed, $\Delta\bar{u}$ in m/s, and the N_2O_5 mixing ratio ($C_{N_2O_5}$) in pptv difference between the two heights in meters as z_2 and z_1. The differences are divided by the natural logarithm of the ratio of the two heights, z_1 and z_2. The last term is the generalized stability factor, $(\Phi_M\Phi_{N_2O_5})^{-1}$ which corrects the flux in a near neutral atmosphere so the logarithm of the wind speed is linear, as in a neutral atmosphere, and follows Eq. (5.1). Details of the generalized atmospheric stability parameterized by the Richardson number, R_i, are detailed below.

5.2 Gradient Richardson number (R_i)

One selection criterion for using the aerodynamic gradient method to measure a flux is the stability of the atmosphere. We use wind speed and temperature gradients to estimate atmospheric conditions near the surface and classify the atmosphere as: unstable, stable and neutral (Monteith and Unsworth, 1990). The Richardson number is an important parameter used to characterize the stability of the atmosphere and the degree of turbulence. The Richardson number is undefined above 0.25, because the turbulence decays and the atmosphere is very stable. The Richardson number is undefined less than -1 because the atmosphere is dominated by free convection (Monteith and Unsworth, 1990; Stull, 1988). The critical Richardson number is 0.25 and at this point the turbulent exchange is completely dissipated. Though the critical Richardson number value of 0.25 is still debated and is only an approximation to limit of turbulent exchange, some turbulent exchange as high as a Richardson number equal 1 can occur (Pardyjak et al., 2002). The dimensionless Richardson number relates the vertical gradients of wind and temperature by taking the ratio of the buoyancy to shear stress using the following equation (Oke, 1987):

$$R_i = \frac{g}{\overline{T}} \frac{\left(\frac{\Delta \overline{T}}{\Delta z}\right)}{\left(\frac{\Delta \overline{u}}{\Delta z}\right)^2} . \qquad (5.4)$$

The wind speed gradient in m/s/m is $\frac{\Delta \bar{u}}{\Delta z}$, the temperature gradient in °C/m is $\frac{\Delta \bar{T}}{\Delta z}$, and g is the gravitational constant.

5.3 Generalized stability function

When the Richardson number is zero, the atmosphere is defined as neutral. Since the atmosphere is dynamic and constantly changing, a completely neutral atmosphere is rare. We can use the Richardson number to define a range of near neutral conditions and can correct the flux of N_2O_5 using the generalized stability function, $(\Phi_M \Phi_{N_2O_5})^{-1}$ so that the logarithmic wind profile Eq. (5.1) is still valid. The flux of N_2O_5, $F_{N_2O_5}$ is applicable under a larger window of a near neutral atmosphere by using the generalized stability function.

Outside of the gradient Richardson number range of -1 to 0.25, the generalized stability function needs to corrected by greater than a factor of 8 for very stable (> 0.25) or very unstable (> -1) conditions and we cannot correct the flux to account for near neutral atmospheric conditions. Therefore, we used two different generalized stability functions, Eq. (5.5) for stable conditions and Eq. (5.6) for unstable conditions (Oke, 1987):

The dimensionless generalized stability functions are as follows:

$$(\Phi_M \Phi_{N_2O_5})^{-1} = (1 - 5R_i)^2 \qquad (R_i > 0) \qquad (5.5)$$

and

$$(\Phi_M \Phi_{N_2O_5})^{-1} = (1-16R_i)^{\frac{3}{4}} \qquad (R_i < 0). \qquad (5.6)$$

There are different value ranges and powers of the generalized stability factor formula $(\Phi_M \Phi_{N_2O_5})^{-1}$ used to correct the flux by extending the flux equation beyond a neutral atmospheric conditions (Oke, 1987; Monteith and Unsworth, 1990; Arya, 2001). We used the formulas and suggested R_i range from Oke (1987) in Eq. (5.5 and 5.6).

In addition to applying different correction factors, we narrow the range of acceptable atmospheric stability by using very small Richardson number range of 0.12 to -0.1 and allow the N_2O_5 flux data to be within the limits of our available fetch (Chapter 3).

5.4 Flux divergence

In addition to the flux only being applicable under conditions of neutral stability, the aerodynamic gradient approach only applies when there is a "constant flux layer" and no divergence of fluxes. A flux divergence for N_2O_5 occurs when there are other competing chemical reactions that are taking place between the two measurements levels. Chemical reactions can affect the flux measurements and the time scales of these reactions need to be addressed. (Kramm et al., 1991; Kristensen and Fitzjarrald, 1984). In the case of N_2O_5, we are measuring at night and we have to consider the reactions that would affect the mixing ratio of N_2O_5.

The main reaction that can compete for NO_3 with the formation of N_2O_5 (R 3) is:

$NO + NO_3 \rightarrow 2\ NO_2$ (R 4)

The rate constant for this reaction is very fast at 2.9 x 10^{-11} cm^3 $molecule^{-1}$ s^{-1} at 298 K. However, Reaction (R4) is filtered from the data set by elimination all data points that have a NO mixing ratio > 1 ppbv. Therefore, no points influenced by flux divergence, are used in this analysis.

5.5 Deposition velocity

We use a two-point profile to measure the gradients in wind speed, temperature and N_2O_5 to calculate a flux using Eq. (5.3). If the N_2O_5 flux is negative, a high mixing ratio of N_2O_5 at a higher level than near the Earth's surface, the N_2O_5 flux is directed downward toward the snowpack. Therefore the deposition velocity of N_2O_5 has a negative sign in the following Eq. (5.7) and a positive deposition velocity is being directed toward the snowpack. We divide the flux by the average mixing ratio of N_2O_5 to obtain the deposition velocity in the following equation:

$$v_{dep} = -\frac{F_{N_2O_5}}{\overline{C}_{N_2O_5}} = -k^2 \frac{\overline{\Delta u \Delta C_{N_2O_5}}}{\overline{[\ln(z_1/z_2)]^2}\,\overline{C}_{N_2O_5}} (\Phi_M \Phi_{N_2O_5})^{-1}. \qquad (5.7)$$

In Eq. (5.7), $\Delta\bar{u}$ is the change in the average wind speed in m/s, $\overline{\Delta C_{N_2O_5}}$ is the difference of 30 minute average periods of mixing ratio of N_2O_5 in pptv, $\overline{C_{N_2O_5}}$ is the average N_2O_5 mixing ratio, k is the Von Karman constant 0.4. The value of the deposition velocity is independent of the mixing ratio of N_2O_5 and therefore a more accurate measurement of snowpack deposition.

5.6 Operational approach to data analysis for deposition velocity

To use Eq. (5.3) for calculating a flux we first measured the N_2O_5 mixing ratio in pptv at two different heights, 2.35 meters and 0.95 meters. Initially the N_2O_5 data is collected at 0.5 Hz, processed to remove the instrument's zero cycle and then averaged over 6 seconds. Figure 5.1 displays 6 second averaged data for one of the selected nights, 5 Nov 2009. The mixing ratio of N_2O_5 is higher at the upper measurement height and lower near the ground. This gradient sign indicates a downward directed flux, which is represented by a negative flux of N_2O_5. The upper and lower level mixing ratios of N_2O_5 were then averaged to half hour data points, and differenced to calculate a flux.

Figure 5.2 also shows a slightly positive or directed upward flux of N_2O_5 and this is during a period with a very low difference in the mixing ratios of N_2O_5 between the two measurement heights. This data was used with the average wind speed difference for the two heights on the 5 Nov, 2009 was 0.45 m/s. The gradient in wind speed and N_2O_5 were then used to calculate the flux of N_2O_5 using Eq. (5.3). The maximum downward directed flux of N_2O_5 on 5 Nov, 2009 is -0.3 pptv m/s for flux calculated using Eq. (5.3), corrected by the generalized stability (Fig. 5.2). The average flux for the 5 Nov, 2009 is -0.12 pptv m/s. Note that the largest correction factors applied to the flux occur when the atmosphere is the farthest from neutral, but still in the acceptable Richardson number (R_i) range of -0.1 to 0.12.

The flux of N_2O_5 also depends on the gradients in NO_2 and ozone. These two molecules are important for measuring the gradient in N_2O_5, because they are both involved in the N_2O_5 formation (R1-R3). In Figure 5.3, the high and low measurements

for NO_2 and ozone were averaged over a half hour period. The high and low measurement heights show negligible differences in the mixing ratios of NO_2 and ozone. The average difference in NO_2 mixing ratios between the two measurement heights varied by less than 2.6 +/- 3% and the ozone varied by 1 +/- 2%.

References:

Arya, S. P.: Introduction to micrometeorology, second ed., Academic press, 420 pp., 2001.

Kristensen, L., and Fitzjarrald, D. R.: The effect of line averaging on scalar flux measurements with a sonic anemometer near the surface, Journal of Atmospheric and Oceanic Technology, 1, 138-146, 1984.

Kramm, G., Müller, H., Fowler, D., Höfken, K. D., Meixner, F. X., and Schaller, E.: A modified profile method for determining the vertical fluxes of NO, NO_2, ozone, and HNO_3 in the atmospheric surface layer, Journal of Atmospheric Chemistry, 13, 265-288, 10.1007/bf00058135, 1991.

Oke, T. R.: Boundary layer climates, 2nd ed., Methuen, London, 435 pp., 1987.

Monteith, J. L., and Unsworth, M. H.: Principles of environmental physics, second ed., 1990.

Pardyjak, E. R., Monti, P., and Fernando, H. J. S.: Flux Richardson number measurements in stable atmospheric shear flows, Journal of Fluid Mechanics, 459, 307-316, doi:10.1017/S0022112002008406, 2002.

Stull, R. B.: An introduction to boundary layer meteorology, Kluwer Academic Publishers, 666 pp., 1988.

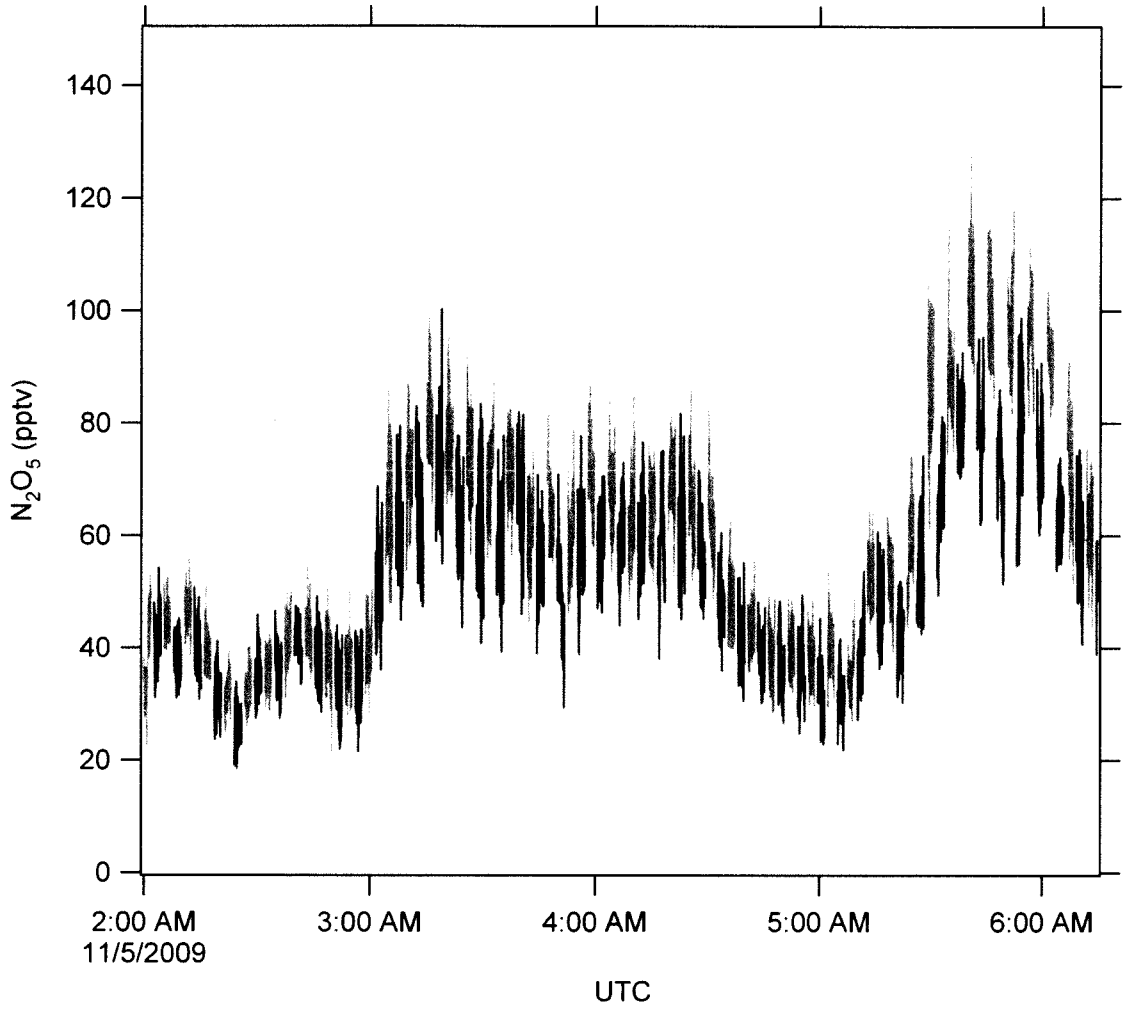

Figure 5.1. Time series of N_2O_5 mixing ratio in pptv on 5 Nov, 2009. The data points are 6 second averages with the 40 second zero (NO titrant) cycle removed and the 80 second measurement cycle present. The blue trace is for the upper measurement tower height and the red trace is for the lower height.

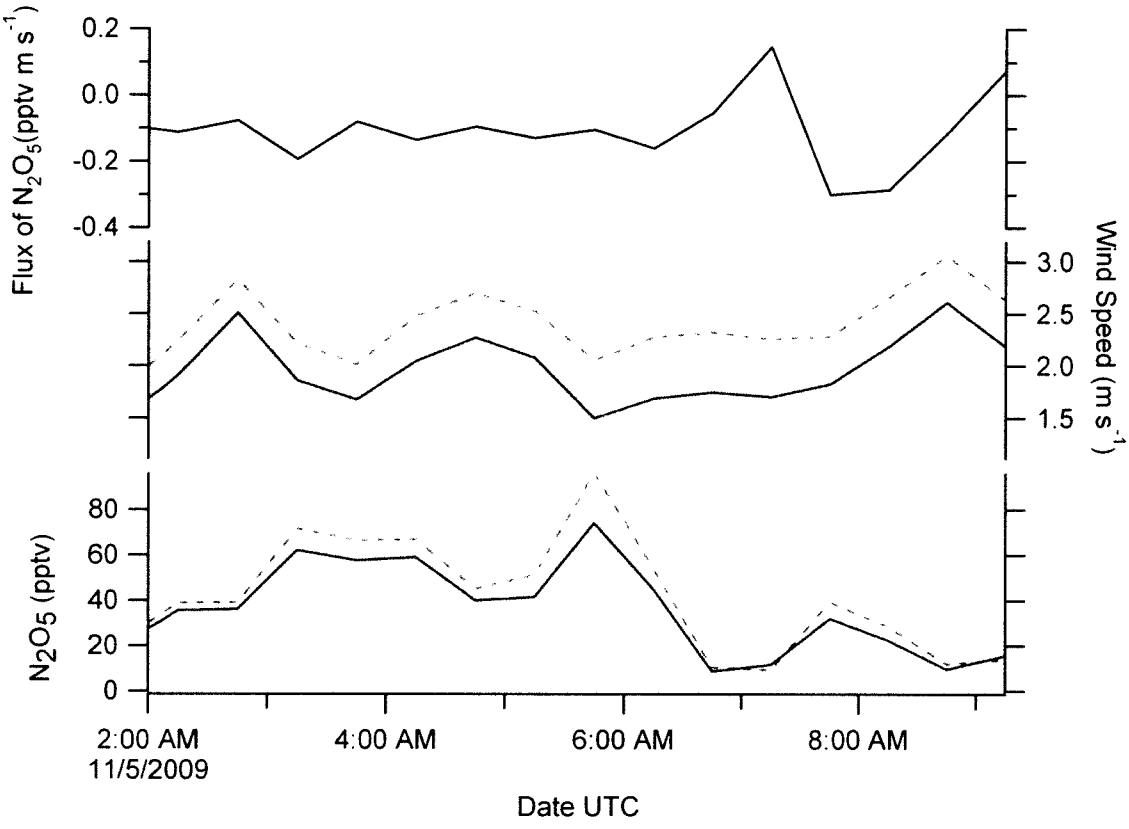

Figure 5.2. Times series of the flux of N_2O_5. The flux is averaged over a half hour with the generalized stability as the black solid line. Wind speed in m s^{-1} and the mixing ratio of N_2O_5 in pptv are shown as the higher measurement height represented by the blue dotted line and lower measurement height as the red solid line.

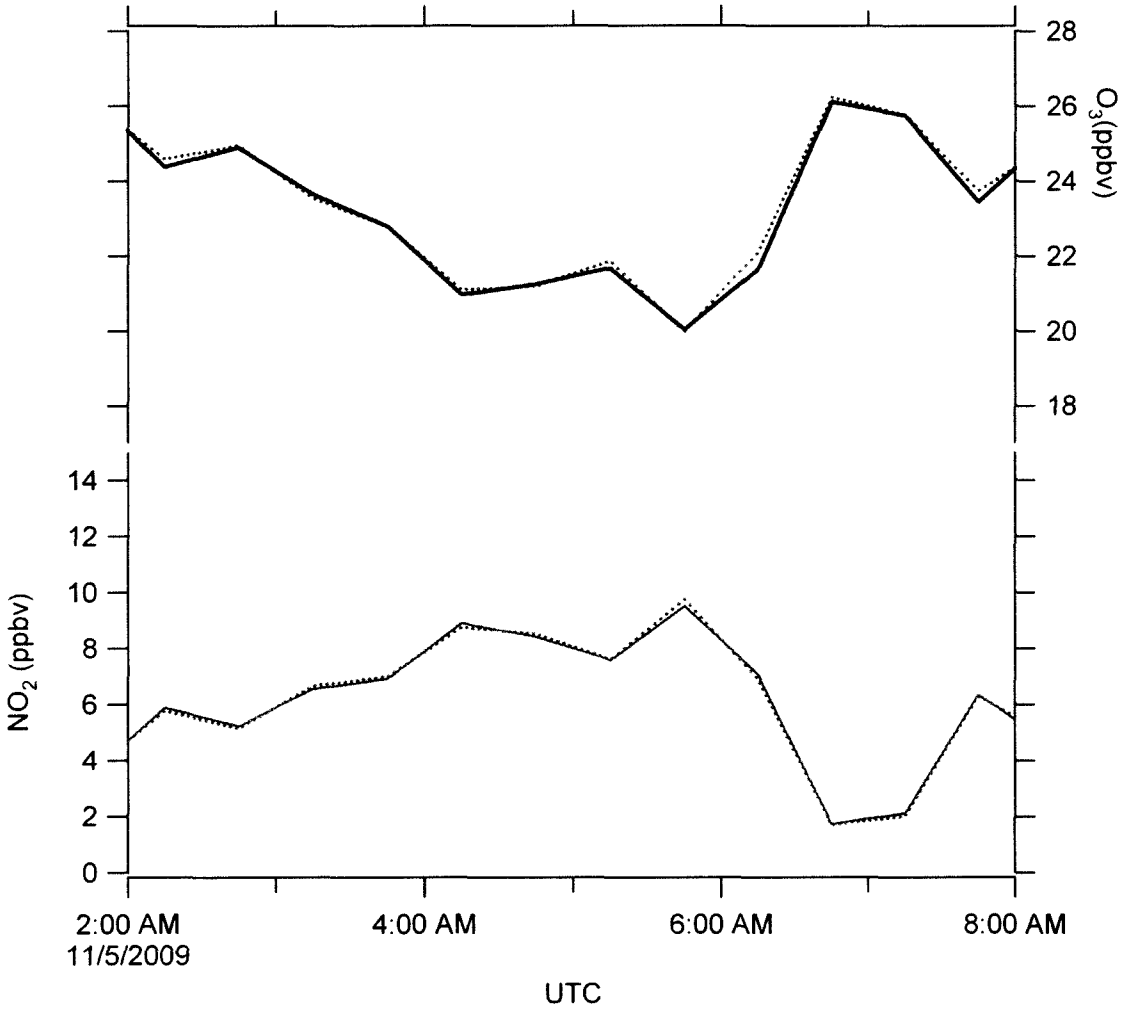

Figure 5.3. Difference of NO_2 and O_3 mixing ratios in ppbv. The mixing ratios are averaged over a half hour with the higher measurement height as the blue dotted line and the lower measurement height as the red solid line.

Chapter 6 Deposition of dinitrogen pentoxide, N_2O_5, to the snowpack at high latitudes[1]

Dinitrogen pentoxide, N_2O_5, is an important nighttime intermediate in oxidation of NO_x that is hydrolyzed on surfaces. We conducted a field campaign in Fairbanks, Alaska during November, 2009 to measure the flux (and deposition velocity) of N_2O_5 depositing to snowpack using the aerodynamic gradient method. The deposition velocity of N_2O_5 under Arctic winter conditions was found to be 0.59 +/- 0.47 cm/s, which is the first measurement of this parameter to our knowledge. Based on the measured deposition velocity, we compared the chemical loss rate of N_2O_5 via snowpack deposition to the total steady state loss rate and found that deposition to snowpack is a significant fraction of the total chemical removal of N_2O_5 measured within a few meters of the ground surface.

6.1 Introduction

High-latitude nighttime nitrogen oxide chemistry is dominated by the oxidation of NO_2 by ozone to form nitrate radical, NO_3 (R1). NO_3 and NO_2 combine to form N_2O_5,

[1] Huff, D.M., Joyce, P.J., Fochosatto, G.J., and Simpson, W.R. Deposition of dinitrogen pentoxide, N_2O_5, to the snowpack at high latitudes. (submitted to Atmospheric Chemistry and Physics Discussions (ACPD), 22 Sept 2010)

(R2) in a temperature dependent equilibrium that is favored under cold and dark conditions that exist in winter at high latitudes.

The major chemical loss process for N_2O_5 is heterogeneous hydrolysis (R3). The following reactions are the nighttime pathway for N_2O_5 chemical removal.

$$NO_2 + O_3 \rightarrow NO_3 + O_2 \qquad \text{(R1)}$$

$$NO_2 + NO_3 \leftrightarrows N_2O_5 \qquad \text{(R2)}$$

$$N_2O_5 + H_2O \xrightarrow{\text{Surface}} 2HNO_3 \qquad \text{(R3)}$$

The production of nitric acid (R3) contributes to acid rain, adds fixed nitrogen to the ecosystem, and removes NO_x. Acid rain is known to have many damaging effects on the environment. The effects of nitrification have been documented in mid latitudes (Andersen and Hovmand, 1995; Bytnerowicz et al., 1998; Fenn et al., 2003), and removal of NO_x affects the possibility of downwind ozone production.

The heterogeneous reaction of N_2O_5 (R3) is an important reaction for NO_x loss. In a modeling study, Dentener and Crutzen (1993) found that during the winter 80% of high latitude NO_x is lost by Reaction (R3), which is the dominant dark pathway to nitric acid. Since the Dentener and Crutzen (1993) modeling study, many laboratory experiments have been completed investigating N_2O_5 heterogeneous hydrolysis and the dependence on aerosol particle chemical composition (Mozurkewich and Calvert, 1988; Kirchner et al., 1990; Hanson and Ravishankara, 1991a; Van Doren et al,. 1991). The N_2O_5 uptake coefficient, or surface reaction probability, γ, describes the probability of chemical

reaction of N_2O_5 on an aerosol surface. In more recent models, different parameterizations of γ have been used that identify the dependence on aerosol composition and temperature (Riemer et al., 2003; Evans and Jacob, 2005). Bertram and Thornton (2009) parameterized N_2O_5 based on γ's dependence on $H_2O(l)$, Cl^- and NO_3^- for organic and inorganic mixed aerosol particles.

There have been several field measurements of N_2O_5 at mid-latitudes (Brown et al. , 2001; Matsumoto et al., 2005; Wood et al., 2005; Brown et al., 2006; Bertram et al., 2009). Brown et al. (2006) was the first field study to show a dependence on aerosol particle composition in a large aircraft field study over the Eastern US. Brown et al. (2006) related N_2O_5 chemistry to sulfate aerosol particle content and observed faster uptake of N_2O_5 to the aerosol particles when the aerosol particles had high sulfate content. Most recently, mid-latitude field studies found N_2O_5 in both coastal (Roberts et al., 2008) and inland (Thornton et al., 2009) regions reacts with chloride and forms nitryl chloride. Nitryl chloride is a photolabile nighttime reservoir that can produce reactive chlorine radicals when photolysed at sunrise (Thornton et al., 2009). Bertram et al. (2009) employed a new technique measuring the uptake coefficient of N_2O_5 on ambient aerosol particles directly by using chemical ionization mass spectroscopy (CIMS) to measure reactive loss of N_2O_5 when added to a flow tube reactor containing ambient aerosol particles.

Our research group has previously performed high latitude field studies and have reported aerosol surfaces densities were insufficient to account for all of the chemical loss of N_2O_5 at high latitudes (Ayers and Simpson, 2006; Apodaca et al., 2008). We

implicated other reactive surfaces for N_2O_5 chemical loss, such as ice, either on atmospheric particles or in the snowpack. Ayers and Simpson (2006) measured N_2O_5 on the top of a building, 30 meters above the local topography and found higher mixing ratios aloft, which is consistent with some of the N_2O_5 removal being by deposition to Earth's snow-covered surface. Calculated lifetimes aloft ranged from minutes to several hours. Higher N_2O_5 mixing ratios further from Earth's surface is in agreement with others who have studied the vertical profile of N_2O_5 (Brown et al., 2003; Geyer and Stutz, 2004; Stutz et al., 2004; Brown et al., 2007a; Brown et al., 2007b). Apodaca et al. (2008) observed the mixing ratios of N_2O_5 to be much lower and the average lifetime was 6 minutes under nighttime high relative humidity conditions, which is common in the wintertime Arctic near the surface. In these past studies, there was not a sufficient amount of meteorological data recorded to separate snowpack deposition from reaction on particles.

Here, we report upon a field campaign quantifying the heterogeneous hydrolysis loss of N_2O_5 by snowpack deposition. The deposition velocity of N_2O_5 helps to improve process-based models aimed at understanding the vertical profile of N_2O_5 at high latitudes and the fate of NO_x via the nighttime chemical pathway. Measuring a flux during nighttime in the Arctic is difficult due to extreme atmospheric stability. In a very stable atmosphere the vertical mixing is hindered and turbulence is sporadic and upper layers may become decoupled from the ground (Anderson and Neff, 2008). The experimental design to measure a flux required sufficient instrumentation and calculations to have an adequate fetch and neutral atmospheric conditions appropriate to

satisfy the Monin-Obukhov similarity theory. Although the deposition velocity of N_2O_5 has not been measured, its value is thought to be similar to that of nitric acid (Cadle et al. 1985; Lovett, 1994; Wesely and Hicks, 2000). Sommariva et al. (2009) conducted a large scale modeling study on marine boundary layer deposition and used a value for N_2O_5 of 1 cm/s based on Brown et al. (2004) reported deposition velocity of nitric acid.

In this study, we measure the N_2O_5 deposition flux using the aerodynamic gradient method. From the flux we can calculate the deposition velocity of N_2O_5. In addition to deposition of N_2O_5 to the surface, N_2O_5 is also lost by reaction on atmospheric particles. Therefore, we can divide Reaction (R3) into two sub-processes.

$N_2O_5 + H_2O \rightarrow 2HNO_3$ (snowpack deposition) (R3a)

$N_2O_5 + H_2O \rightarrow 2HNO_3$ (reaction on particles) (R3b)

The measured deposition velocity of N_2O_5 is combined with atmospheric assumptions to estimate the effective snowpack deposition rate k_{3a} (R3a). We also measured the total chemical removal rate of N_2O_5 via a steady-state analysis, which determines the sum of the loss rates k_{3a} and k_{3b}. Therefore, the relative role of the two sub-processes, snowpack deposition and atmospheric reactions, is determined. We conclude by discussing implications of these results for the deposition of nitric acid, NO_x losses, and N_2O_5 vertical profiles at high latitudes.

6.2 Experimental design

The field site for the study was located in a snow-covered agricultural field 20 km southwest of the city of Fairbanks (the site coordinates are 64.75929° North, 148.10618° West, 161 meters above mean sea level). An insulated hut on skis housed the instruments at this remote field site. The field study operated continuously from 5 Nov 2009 until 18 Nov, 2009. Mildly polluted air originating from Fairbanks is carried from the northeast direction by a down-slope drainage flow towards the field site. The local drainage flow is guided by a U-shaped ridge that forms a bowl around the field site as seen in the contour map in Fig. 1A.

Using the contour lines in Fig. 1A, we can estimate the slope of the field site. The bowl loses 6 meters of elevation in 400 meters of fetch, a change of 1.5% or a 0.8° slope. The fetch is a uniform flat upwind distance from the measurement towers. Oke (1987) estimates that the fetch should be at least 100 times the maximum measurement height, which, in our case, is 2.4 meters, indicating a 240 meter fetch is required. Our site satisfies the minimum requirement with a 400 meter fetch. Under the common nighttime cold and stable air flow in the Arctic, we recognize the possibility of needing longer fetch. Therefore, we considered other methods as described in Horst and Weil (1994) to calculate the adequacy of the fetch and are discussed in Huff (2010).

6.3 Methods

6.3.1 Chemical measurements

A field portable instrument using the cavity ring down spectroscopy (CRDS) was developed in our laboratory to measure N_2O_5 at remote sites (Simpson, 2003; Ayers et al., 2005). We have used this CRDS instrument during past field studies (Ayers and Simpson, 2006; Apodaca et al., 2008) and the major modification we made for the present field study was adding a 10 meter Teflon inlet. The 3/8" (9.5 mm) inner diameter PFA Teflon inlet was configured with a 100 slpm bypass flow to minimize the contact time of the sampled air with the inlet. The total residence time in the fast-flow inlet is 0.4 seconds. Flow-changing studies were carried out to determine inlet loss of N_2O_5 on the tubing resulting in a transmission of 76%. The transmission of N_2O_5 on the inlet and instrumental surfaces were taken into account in the analysis resulting in corrected ambient mixing ratios, as has been done in past studies (Ayers and Simpson, 2006; Apodaca et al., 2008). In addition to the N_2O_5 instrument, the same high-flow inlet provided air to ancillary instruments that measure NO_x (Thermo Environmental 42c) and ozone (Dasibi 1008 RS). The intake of the inlet was held on the chemical measurement tower and moved between two heights to quantify gradients in each chemical species being measured (Fig. 2, Part II).

6.3.2 Steady state analysis of N_2O_5 measurements

We use the steady state approximation to calculate a lifetime of N_2O_5 from the mixing ratio of N_2O_5 divided by the source rate of N_2O_5 (Apodaca et al., 2008),

$$\tau_{N_2O_5 ss} = \frac{[N_2O_5]}{k_1[NO_2][O_3]} \quad (6.1)$$

The source rate of N_2O_5 is the rate coefficient for Reaction (R1), k_1, multiplied by the mixing ratios of NO_2 and ozone. We assume we achieve steady state rapidly (Apodaca et al., 2008), although this assumption is discussed later. The steady-state lifetime of N_2O_5 is used to determine the total heterogeneous hydrolysis rate of N_2O_5, the sum of Reactions (R3a) and (R3b).

6.3.3 Near surface gradient measurements

Figure 2 shows the field configuration of the chemical inlet and meteorological measurement towers designed for near-surface gradient measurements. Two separate towers, one with a moving inlet for chemical measurements and one for meteorological measurements, were used so the vibration of the moving inlet did not affect the meteorological measurements. The measurement towers were located 2 meters upwind from the instrument-housing insulated hut.

The moveable-inlet tower alternated position between "up" and "down" heights, 2.35 meters and 0.95 meters, respectively. The moveable inlet sampled the gases, N_2O_5, NO_x and ozone, at the two levels. The up/down state of the inlet was recorded in data files and used in post-processing to calculate gradients in each chemical. The moveable inlet was mounted on a separate tower horizontally displaced 0.5 meters from the meteorological tower.

The meteorological tower supported both slow- and fast-response instrumentation. The slow-response system consisted of two RM Young cup anemometer and wind vanes to measure wind speed and direction (model 03001-5) and two temperature sensors (RM Young 41342) at the same heights as the moveable inlet (within a few cm, as noted on Fig. 2) and logged as one minute averages on a Campbell Scientific CR10x data logger. The meteorological tower and sampling inlet both faced into the prevailing wind direction at approximately the same length from the towers (within a few cm) so they were horizontally aligned.

The meteorological measurement tower also supported two sonic anemometers (RM Young model 84000) producing 10 Hz data on a separate data logger (Chaparral Physics). The purpose of the sonic anemometers at the same height as the low frequency meteorological tower instruments is twofold. First, the redundant measurements verify the temperature, wind speed and direction data and gradients. Second, the high frequency data from the sonic anemometers allow validation of our flux measurements by calculating the heat flux by both the aerodynamic gradient method and eddy covariance. The details of the heat flux comparison by the aerodynamic and eddy covariance methods can be found in the supplemental material.

6.3.4 Aerodynamic gradient flux analysis

There are three main flux measurement techniques: the aerodynamic method, the Bowen ratio method, and the eddy covariance method (Oke, 1987; Monteith and Unsworth, 1990; Bocquet, 2007). The aerodynamic method uses a two (or more) point

profile system to measure the chemicals near surface gradient and anemometers to measure the wind speed and direction and gradients. Using the aerodynamic method, we rely on the Monin-Obukhov similarity theory to derive a flux equation for N_2O_5. The similarity theory states that under neutral atmospheric stability the surface layer is homogenous and the eddy diffusivity transfer coefficient of momentum, K_m, is equal to the gas's transfer coefficient, $K_{N_2O_5}$ (Oke, 1987; Monteith and Unsworth, 1990; Arya, 2001). The two transfer coefficients can be set equal and the unknown flux can be solved for using the aerodynamic approach found in Oke (1987). A negative flux of N_2O_5 results from a higher mixing ratio of N_2O_5 at the higher measurement level than near the surface, which is a downward-directed flux. To obtain the deposition velocity, we divide the opposite of the flux by the average mixing ratio of N_2O_5,

$$v_{dep} = -\frac{F_{N_2O_5}}{\overline{C_{N_2O_5}}} = -k^2 \frac{\dfrac{\Delta\bar{u}\Delta\overline{C_{N_2O_5}}}{\left[\ln(z_1/z_2)\right]^2}}{\overline{C_{N_2O_5}}} (\Phi_M \Phi_{N_2O_5})^{-1}. \qquad (6.2)$$

In this equation, $\Delta\bar{u}$ is the average difference in wind speed between the two heights, z_1 and z_2, $\Delta\overline{C_{N_2O_5}}$ is the average difference in mixing ratio of N_2O_5 between the two heights, k is the Von Karman constant, which equals 0.4. The generalized stability factor, $(\Phi_M \Phi_{N_2O_5})^{-1}$, allows us to correct the flux ($F_{N_2O_5}$) for atmospheric conditions that are near neutral (Oke, 1987). The generalized stability factor has different equations under different atmospheric stabilities and we used the generalized stability factors and R_i range found in Oke (1987) and these factors are the same as Monteith and Unsworth

(1990), but the R_i range application is different. The average N_2O_5 mixing ratio is $\overline{C_{N_2O_5}}$. The deposition velocity (v_{dep}) is independent of the amount of pollution (the amount of N_2O_5) and is therefore more useful for modeling of snowpack deposition. When the deposition velocity is positive, N_2O_5 is directed downward toward the surface.

The aerodynamic method for calculating the flux of N_2O_5, $F_{N_2O_5}$ only applies under a very narrow window of atmospheric stability under a nearly neutral atmosphere. A neutral atmosphere is defined by having negligible buoyancy effects. We can use the gradient Richardson number, R_i, to indentify appropriate atmospheric stability conditions and to correct the flux for a slightly stable or unstable atmosphere. The dimensionless Richardson number relates the vertical gradients of wind and temperature by taking the ratio of the buoyancy to shear stress, (Stull, 1988)

$$R_i = \frac{\frac{g}{\overline{T}}\left(\frac{\Delta\overline{T}}{\Delta z}\right)}{\left(\frac{\Delta\overline{u}}{\Delta z}\right)^2} . \qquad (6.3)$$

The linear approximation for Richardson number Eq. (6.3) is more accurate than the logarithmic approximation (Arya, 2001) under stable atmospheric conditions. Under nighttime Arctic conditions, we are more commonly under stable atmospheric conditions, so we used the linear approximation for the Richardson number. On the other hand, when the Richardson number is above 0.25, turbulence decays and the atmosphere is very stable, and laminar flow, once established, is stable. When the Richardson number is less than -1, the atmosphere is dominated by free convection (Monteith and Unsworth, 1990;

Stull, 1988).

Outside of the gradient Richardson index range -1 to 0.25, the general stability factors, $(\Phi_M \Phi_{N_2O_5})^{-1}$ are unusually large or small and cannot correct the flux to account for divergence from near neutral atmospheric conditions. As the Richardson number approaches 0.25, this is considered the critical Richardson number beyond which turbulent exchange is completely dissipated. Though the value of 0.25 is still debated and is only an approximation to limit of turbulent exchange, some turbulence exchange with a gradient Richardson number as high as 1 (Pardyjak et al., 2002). Although other authors (Monteith and Unsworth, 1990; Stull, 1988; Arya, 2001) propose slightly different limiting R_i values ranges and formulations for the general stability factors, we chose to use general stability factors and acceptable R_i ranges from Oke (1987). Two different general stability factor correction functions are used, one for positive R_i values, and one for negative R_i values. Because these general stability factors become large towards limits, we only analyzed data in the range $-0.1 < R_i < 0.12$. We used a narrow range of R_i values to ensure we not reaching our fetch limitations, and based on a method described in Horst and Weil (1994), we are measuring > 90% of the true flux.

6.4 Results

Chemical species (N_2O_5, NO_2, and O_3) were averaged over 30 minute intervals. Within each half-hour data-averaging period, there are 15 minutes of "up" and 15 minutes of "down" data. The two individual state averages were differenced and divided by the height difference to get the chemical gradients. Steady-state chemical lifetimes

were calculated using temperature-dependent formation kinetics. Wind speed and temperature differences were calculated from the two inter-calibrated instrument sets. The gradient Richardson number, R_i, was calculated to determine periods where the stability was appropriate for the calculation of fluxes.

First, a filter was applied for the wind direction and a solar flag for nighttime data to find appropriate nights for analysis. The data were then selected by calculating the Richardson number in Eq. (6.3) and using the narrow range of $0.12 > R_i > -0.1$. From the results of the gradient Richardson number calculation, wind direction, and instrument calibrations we focused our analysis on three nights of the campaign. The three nights were 5, 10 and 11 Nov, 2009. On these three nights the parameters were met for calculating a deposition velocity except for one half hour period on 5 Nov, 2009 where the Richardson number was 0.16, and was slightly out of range; however, this point was included in the analysis for completeness.

In Fig. 6.3, all three nights had neutral to near neutral atmospheric conditions. The temperature averages on the 5, 10, and 11 Nov 2009 were -4°, -18°, -14°C, respectively. The highest temperature gradient was seen on 5 Nov with a 1°C difference in the two heights and a stable atmosphere. In this case, the upper level was warmer indicating an inversion, which is typical of cold, stable Arctic nights. Most of the data had small to no inversions, which was appropriate of measuring a flux. The average wind speeds were 2.3, 2.7 and 2.5 m/s, respectively. The difference in wind speeds and the difference in N_2O_5 mixing ratios were used to calculate the flux, the numerator in the deposition velocity Eq. (6.2). Figure 6.4 shows a histogram of the measurements of the deposition

velocity. More than 90% of the deposition velocities are positive or directed downward toward the snowpack. The average deposition velocity is 0.59+/-0.47 cm/s.

In addition to measuring chemical gradients and comparing the gradient data to the meteorology, we also used chemical measurements to calculate the steady state lifetime of N_2O_5 using Eq. (6.1). The steady state lifetime represents total chemical loss of N_2O_5, including snowpack deposition and atmospheric reactions. The time series of the average NO_2, O_3, source rate, N_2O_5 and steady state lifetime of N_2O_5 are displayed in Fig. 6.5. The mixing ratio of NO_2 in ppbv ranges from a few ppbv to 20 ppbv at night. Although we found large differences in N_2O_5 between heights (15% on average and up to 50%), the difference between NO_2 and ozone between the heights was small. The average difference in NO_2 between the two measurement heights varied by less than 2.6 +/- 3% and the ozone varied by 1 +/- 2%. Because the gradients in all chemicals other than N_2O_5 were small, Fig. 6.5 shows half-hour averages independent of the up/down state of the sampler.

The average steady state lifetime of N_2O_5 is 6 minutes. The transport timescale of polluted air to reach the site from Fairbanks given an average measured speed of 2.3 m/s and 20 km distance and assuming direct transport is around 2 hours. The transport timescale is longer than the maximum calculated lifetime of N_2O_5 of 10 minutes, reinforcing the picture that the steady-state approximation is decent in this application.

6.5 Discussion

6.5.1 Deposition velocity of N_2O_5

Deposition velocities are parameters used to model the effects of nitrogen oxides on the environment. There are many studies using micrometeorology methods to measure trace gas dry deposition velocities (Lovett, 1994; Wesely and Hicks, 2000; Watt et al., 2004; Muller et al., 2009). Deposition velocities above a snow pack have been measured for ozone and our summarized in, Helmig et al. (2007) and Wesley and Hicks (2000). Arctic studies of the deposition velocities to snow pack have been measured for ozone and found to be less than or equal to 0.01 cm/s (Helmig et al., 2009). Wesely and Hicks (2000) summarized NO and NO_2 deposition velocities and found they are generally negligible. There are several studies quantifying the emission of NO_x from the snowpack and though NO_x emission from the snowpack can be significant, it is driven by photochemistry (Honrath et al., 2002; Jones et al., 2001), which is not relevant in the present nocturnal study. Jones et al. (2001) studied NO_x emission form the Arctic snowpack by measuring NO_2 at two different heights and found a diurnal cycling of NO_x with deposition velocities near zero at night. To our knowledge, there are no reported deposition velocities for N_2O_5. A positive deposition velocity means N_2O_5 is reacting to other species on snowpack surfaces. At high latitude in winter, snow pack covers almost the entire ground surface. The snowpack deposition is a reactive loss of N_2O_5 and it is therefore important to quantify the deposition velocity for understanding the fate of nitrogen oxides in the high latitude environments.

Our measured downward directed deposition velocity of N_2O_5 to the snowpack is on the order of 1 cm/s and is in the same range as previously reported values for nitric acid over snow (0.5- 1.4 cm/s) (Cadle et al., 1985). In Fig. 6.4, the average deposition velocity for all three focus nights is 0.59 +/-0.47 cm/s.

6.5.2 Comparisons of N_2O_5 chemical removal rates

To compare the atmospheric N_2O_5 chemical removal rate arising from snowpack deposition to the total steady state chemical removal rate, we need to estimate an effective deposition layer height. The profile of the N_2O_5 deposition flux through the boundary layer is unknown, but decays to zero at the boundary layer height by the definition that the boundary layer is the region influenced by surface chemical processes. Because the flux decreases with height, the effective layer height, z_{eff}, over which N_2O_5 is deposited, is less than the boundary layer height under moderately stable conditions. The profile of the momentum flux is represented by the shear stress equation for a moderately stable boundary layer and decays toward zero as a power law, as shown in Arya (2001). The local scaling law that applies to the power law in Arya (2001) was originally proposed by Nieuwstadt (1984) showing that local friction velocity parameters and temperature scales are similar to the Monin-Obukhov similarity theory parameters under slightly stable boundary layer conditions. The vertical profile of the N_2O_5 deposition flux has the same shape as the momentum flux profile based the Monin-Obukov similarity theory, which assumes that all the fluxes are the same in the surface layer, typically the lower 10% of the boundary layer (Oke, 1987; Monteith and

Unsworth,1990; Arya, 2001). Using this flux profile, we show in the supplemental material that z_{eff} is approximately 15 meters. The N_2O_5 chemical removal rate arising from snowpack deposition (R3a) is then given by

$$k_{3a} = \frac{v_{dep}}{z_{eff}}. \qquad (6.4)$$

For these three nights, the average chemical removal rate is 0.024 min^{-1} for snowpack deposition (k_{3a}). This chemical removal can be compared to the total removal rate that is estimated from the steady-state lifetime of N_2O_5 by

$$k_3 = 1/\tau_{N_2O_5 ss}. \qquad (6.5)$$

During these three nights, we find that the total chemical removal rate, k_3, of N_2O_5 is 0.18 min^{-1}.

From these results, we find that, on average, about 1/8 of the chemical removal of N_2O_5 arises from deposition of N_2O_5 to the surface. However, there are a number of reasons that this estimate of the fraction of N_2O_5 depositional loss might be larger. First, the calculation of the effective surface layer relies upon an unknown flux profile for N_2O_5 and similarity theory. Because boundary layer height is difficult to determine under stable Arctic conditions, (Anderson and Neff, 2008) an error in the estimation of z_{eff} from the boundary layer height would directly impact the fraction of chemical removal that is due to surface deposition. Second, although the fetch in our experiment satisfies the Oke (1987) criteria, other authors (Horst and Weil, 1994; Horst, 1999) indicate that during

stable atmospheric conditions, more fetch is required. If the fetch were not sufficient, then the gradient in N_2O_5 would have not fully developed at the point of measurement and the deposition velocity would be underestimated. A larger value of deposition velocity would increase the fraction of the chemical removal that is due to the surface deposition. Lastly, it is possible that the system does not completely achieve steady state, in which case the total chemical removal of N_2O_5 would be overestimated. The majority of these factors would raise the fraction of chemical removal that is due to deposition to the snowpack, possibly even making it the dominant process for air masses sampled within a few meters of the snowpack.

The other possible chemical removal of N_2O_5 is heterogeneous hydrolysis on aerosol particles. Apodaca et al. (2008) found that measured aerosol particle loadings along with reasonable assumptions for reactive uptake of N_2O_5 (γ_{N2O5}) were insufficiently fast to explain the total steady-state removal of N_2O_5 measured earlier at this same field site. Apodaca et al. (2008) also found chemical removal of N_2O_5 is faster in the presence of ice saturation conditions, which was interpreted as possibly due to reactions on ice particles in the atmosphere or reactions on the snowpack. Reactions on the snowpack would give the signature of increased chemical removal of N_2O_5 for ice-saturated airmasses because air that comes in contact with snowpack will become saturated with respect to ice by either sublimation of the snowpack ice or condensation of super-saturated water vapor onto the snowpack. Therefore, the current measurements, which indicate a significant role for snowpack deposition combined with the result that aerosol

processes are probably too slow to be a major sink of N_2O_5 and the correlation with ice saturation all appear to point to a significant role for deposition of N_2O_5 to snowpack as a major process for air sampled within meters of the snowpack surface. This finding in combination with the fact that the Arctic wintertime conditions are very often stable with hindered vertical mixing indicates that removal process of N_2O_5 even just tens of meters from the Earth's surface are likely to be quite different and probably significantly slower. If the chemical removal of N_2O_5 is significantly slower at higher altitudes, N_2O_5 may act as a reservoir and transport farther than would be indicated by ground-based studies alone. Aircraft, or possibly tethered balloon studies would be able to assess the question of the fate of N_2O_5 aloft and possible role for frozen or unfrozen aerosol particles in that atmospheric layer.

6.6 Conclusions

The average deposition velocity towards the snowpack surface of N_2O_5 is 0.59+/-0.47 cm/s. The calculation of this deposition velocity is dependent upon the fetch being sufficient for complete development of the near-surface gradient as well as general stability factor corrections, which may act to underestimate the actual deposition velocity. This deposition velocity parameter can be used in models to help understand the fate of NO_x pollution at high latitudes. The deposition velocities along with an assumed flux profile were used to approximate the chemical removal rate arising from deposition and to compare this rate to the total steady state chemical removal rate. In this comparison, we find that deposition to snowpack is responsible for 1/8 of the total removal, and also

that the actual fraction of N_2O_5 deposition to snowpack may be more than this estimate. Therefore, we conclude that deposition of N_2O_5 to the snowpack is a significant and possibly the dominant process for air sampled with a few meters above snowpack. Airmasses aloft may experience slower losses, which would lead to enhanced transport of N_2O_5 aloft as well as an important role for vertical mixing in the fate of N_2O_5 emitted at high latitudes.

References:

Anderson, P. S., and Neff, W. D.: Boundary layer physics over snow and ice, Atmospheric Chemistry and Physics, 8, 3563-3582, doi:10.5194/acp-8-3563-2008, 2008.

Andersen, H. V., and Hovmand, M. F.: Ammonia and nitric acid dry deposition and throughfall, Water, Air, & Soil Pollution, 85, 2211-2216, doi:10.1007/BF01186162, 1995.

Apodaca, R. L., Huff, D. M., and Simpson, W. R.: The role of ice in N_2O_5 heterogeneous hydrolysis at high latitudes, Atmos. Chem. Phys., 8, 7451-7463, doi:10.5194/acp-8-7451-2008, 2008.

Arya, S. P.: Introduction to micrometeorology, second ed., Academic press, 420 pp., 2001.

Ayers, J. D., Apodaca, R. L., Simpson, W. R., and Baer, D. S.: Off-axis cavity ringdown spectroscopy: Application to atmospheric nitrate radical detection, Appl. Optics., 44, 7239-7242, 2005.

Ayers, J. D., and Simpson, W. R.: Measurements of N_2O_5 near Fairbanks, Alaska, J. Geophys. Res., 111, D14309, doi:10.1029/2006JD007070, 2006.

Bertram, T. H., Thornton, J. A., Riedel, T. P., Middlebrook, A. M., Bahreini, R., Bates, T. S., Quinn, P. K., and Coffman, D. J.: Direct observations of N_2O_5 reactivity on ambient aerosol particles, Geophysical Research Letters, 36, L19803, doi: 10.1029/2009gl040248, 2009.

Bertram, T. H., and Thornton, J. A.: Toward a general parameterization of N_2O_5 reactivity on aqueous particles: The competing effects of particle liquid water, nitrate and chloride, Atmospheric Chemistry and Physics, 9, 8351-8363, doi:10.5194/acp-9-8351-2009, 2009.

Bocquet, F.: Surface layer ozone dynamics and air-snow interactions at summit, Greenland spring and summer ozone exchange velocity and snowpack ozone: The complex interactions, Ph.D., Department of Atmospheric and Oceanic Sciences, University of Colorado, 197 pp., 2007.

Brown, S. S., Stark, H., Ciciora, S. J., and Ravishankara, A. R.: In-situ measurement of atmospheric NO_3 and N_2O_5 via cavity ring-down spectroscopy, Geophys. Res. Lett., 28, 3227, doi:10.1029/2001GL013303, 2001.

Brown, S. S., Stark, H., Ryerson, T. B., Williams, E. J., Nicks, D. K., Jr., Trainer, M., Fehsenfeld, F. C., and Ravishankara, A. R.: Nitrogen oxides in the nocturnal boundary layer: Simultaneous in situ measurements of NO_3, N_2O_5, NO_2, NO, and O_3, J. Geophys. Res., 108, 4299, doi: 10.1029/2002jd002917, 2003.

Brown, S. S., Dibb, J. E., Stark, H., Aldener, M., Vozella, M., Whitlow, S., Williams, E. J., Lerner, B. M., Jakoubek, R., Middlebrook, A. M., DeGouw, J. A., Warneke, C., Goldan, P. D., Kuster, W. C., Angevine, W. M., Sueper, D. T., Quinn, P. K., Bates, T. S., Meagher, J. F., Fehsenfeld, F. C., and Ravishankara, A. R.: Nighttime removal of NO_x in the summer marine boundary layer, Geophys. Res. Lett., 31, L07108, doi:10.1029/2004gl019412, 2004.

Brown, S. S., Ryerson, T. B., Wollny, A. G., Brock, C. A., Peltier, R., Sullivan, A. P., Weber, R. J., Dubé, W. P., Trainer, M., Meagher, J. F., Fehsenfeld, F. C., and Ravishankara, A. R.: Variability in nocturnal nitrogen oxide processing and its role in regional air quality, Science, 5757, 67-70, doi: 10.1126/science.1120120, 2006.

Brown, S. S., Dubé, W. P., Osthoff, H. D., Wolfe, D. E., Angevine, W. M., and Ravishankara, A. R.: High resolution vertical distributions of NO_3 and N_2O_5 through the nocturnal boundary layer, Atmos. Chem. Phys., 7, 139-149, doi:10.5194/acp-7-139-2007, 2007a.

Brown, S. S., Dubé, W. P., Osthoff, H. D., Stutz, J., Ryerson, T. B., Wollny, A. G., Brock, C. A., Warneke, C., de Gouw, J. A., Atlas, E., Neuman, J. A., Holloway, J. S., Lerner, B. M., Williams, E. J., Kuster, W. C., Goldan, P. D., Angevine, W. M., Trainer, M., Fehsenfeld, F. C., and Ravishankara, A. R.: Vertical profiles in NO_3 and N_2O_5 measured from an aircraft: Results from the NOAA P-3 and surface platforms during the New England air quality study 2004, J. Geophys. Res., 112, D22304, doi:10.1029/2007jd008883, 2007b.

Bytnerowicz, A., Percy, K., Riechers, G., Padgett, P., and Krywult, M.: Nitric acid vapor effects on forest trees -- deposition and cuticular changes, Chemosphere, 36, 697-7 02, doi:10.1016/S0045-6535(97)10110-2, 1998.

Cadle, S. H., Dasch, J. M., and Mulawa, P. A.: Atmospheric concentrations and the deposition velocity to snow of nitric acid, sulfur dioxide and various particulate species, Atmospheric Environment, 19, 1819-1827, doi:10.1016/0004-6981(85)90008-3, 1985.

Dentener, F. J., and Crutzen, P. J.: Reaction of N_2O_5 on tropospheric aerosol particles: Impact on the global distributions of NOx, O_3, and OH, J. Geophys. Res., 98, 7149-7163, doi: 10.1029/92jd02979, 1993.

Evans, M. J., and Jacob, D. J.: Impact of new laboratory studies of N_2O_5 hydrolysis on global model budgets of tropospheric nitrogen oxides, ozone and oh, Geophys. Res. Lett., 32, L09813, doi:10.1029/2005GL022469, 2005.

Fenn, M. E., Baron, J. S., Allen, E. B., Rueth, H. M., Nydick, K. R., Geiser, L., Bowman, W. D., Sickman, J. O., Meixner, T., Johnson, D. W., and Neitlich, P.: Ecological effects of nitrogen deposition in the western united states, BioScience, 53, 404-420, doi:10.1641/0006-3568(2003)053[0404:EEONDI]2.0.CO;2, 2003.

Geyer, A., and Stutz, J.: Vertical profiles of NO_3, N_2O_5, O_3, and NO_x in the nocturnal boundary layer: 2. Model studies on the altitude dependence of composition and chemistry, J. Geophys. Res., 109, D12307, doi: 10.1029/2003jd004211, 2004.

Hanson, D. R., and Ravishankara, A. R.: The reaction probabilities of $ClONO_2$ and N_2O_5 on 40 to 75% sulfuric acid solutions, J. Geophys. Res., 96, doi: 10.1029/91jd01750, 1991a.

Hanson, D. R., and Ravishankara, A. R.: The reaction probabilities of $ClONO_2$ and N_2O_5 on polar stratospheric cloud materials, J. Geophys. Res., 96, 5081-5090, 10.1029/90jd02613, 1991b.

Helmig, D., Ganzeveld, L., Butler, T., and Oltmans, S.: The role of ozone atmosphere-snow gas exchange on polar, boundary-layer tropospheric ozone - a review and sensitivity analysis, Atmos. Chem. Phys., 7, 15-30, doi: 10.5194/acp-7-15-2007, 2007.

Helmig, D., Cohen, L. D., Bocquet, F., Oltmans, S., Grachev, A., and Neff, W.: Spring and summertime diurnal surface ozone fluxes over the polar snow at summit, Greenland, Geophys. Res. Lett., 36, L08809, doi: 10.1029/2008gl036549, 2009.

Honrath, R. E., Lu, Y., Peterson, M. C., Dibb, J. E., Arsenault, M. A., Cullen, N. J., and Steffen, K.: Vertical fluxes of NOx, HONO, and HNO_3 above the snowpack at summit, Greenland, Atmospheric Environment, 36, 2629-2640, doi:10.1016/S1352-2310(02)00132-2, 2002.

Horst, T. W., and Weil, J. C.: How far is far enough: The fetch requirements for micrometeorological measurement of surface fluxes, Journal of Atmospheric and Oceanic Technology, 11, 1018-1025, 1994

Horst, T. W.: The footprint for estimation of atmosphere-surface exchange fluxes by profile techniques, Boundary-Layer Meteorology, 90, 171-188, doi: 10.1023/A:1001774726067,1999.

Huff, D. M.: The role of ice surfaces in affecting nighttime removal of nitrogen oxides in high latitude plumes Ph.D. thesis, University of Alaska Fairbanks,(in prep) 2010.

Jones, A. E., Weller, R., Anderson, P. S., Jacobi, H., W, Wolff, E. W., Schrems, O., and Miller, H.: Measurements of NOx emissions from the antarctic snowpack, Geophys. Res. Lett., 28, 1499-1502, doi:10.1029/2000gl011956, 2001.

Kirchner, W., Welter, F., Bongartz, A., Kames, J., Schweighoefer, S., and Schurath, U.: Trace gas exchange at the air/water interface: Measurements of mass accommodation coefficients, Journal of Atmospheric Chemistry, 10, 427-449, doi:10.1007/bf00115784, 1990.

Lovett, G. M.: Atmospheric deposition of nutrients and pollutants in North America: An ecological perspective, Ecological Applications, 4, 630-650, doi:10.2307/1941997, 1994.

Matsumoto, J., Imai, H., Kosugi, N., and Kajii, Y.: In situ measurement of N_2O_5 in the urban atmosphere by thermal decomposition/laser-induced fluorescence technique, Atmospheric Environment, 39, 6802-6811, doi:10.1016/j.atmosenv.2005.07.055, 2005.

Monteith, J. L., and Unsworth, M. H.: Principles of environmental physics, second ed., 291pp., Edward Arnold, 1990.

Mozurkewich, M., and Calvert, J. G.: Reaction probability of N_2O_5 on aqueous aerosol particles, J. Geophys. Res., 93, doi:10.1029/JD093iD12p15889, 1988.

Muller, J. B. A., Coyle, M., Fowler, D., Gallagher, M. W., Nemitz, E. G., and Percival, C. J.: Comparison of ozone fluxes over grassland by gradient and eddy covariance technique, Atmospheric Science Letters, 10, 164-169, 2009.

Nieuwstadt, F. T. M.: The turbulent structure of the stable, nocturnal boundary layer, Journal of the Atmospheric Sciences, 41, 2202-2216, doi:10.1175/1520-0469(1984)041<2202:TTSOTS>2.0.CO;2, 1984.

Oke, T. R.: Boundary layer climates, 2nd ed., Methuen, London, 435pp.,1987.

Pardyjak, E. R., Monti, P., and Fernando, H. J. S.: Flux richardson number measurements in stable atmospheric shear flows, Journal of Fluid Mechanics, 459, 307-316, doi:10.1017/S0022112002008406, 2002.

Riemer, N., Vogel, H., Vogel, B., Schell, B., Ackermann, I., Kessler, C., and Hass, H.: Impact of the heterogeneous hydrolysis of n2o5 on chemistry and nitrate aerosol formation in the lower troposphere under photosmog conditions, J. Geophys. Res., 108, doi:10.1029/2002jd002436, 2003.

Roberts, J. M., Osthoff, H. D., Brown, S. S., and Ravishankara, A. R.: N_2O_5 oxidizes chloride to Cl_2 in acidic atmospheric aerosol, Science, 321, 1059-, doi: 10.1126/science.1158777, 2008.

Simpson, W. R.: Continuous wave cavity ring-down spectroscopy applied to in-situ detection of dinitrogen pentoxide (N_2O_5). Rev. Sci. Inst, 74, 3442-3452, 2003.

Sommariva, R., Osthoff, H. D., Brown, S. S., Bates, T. S., Baynard, T., Coffman, D., de Gouw, J. A., Goldan, P. D., Kuster, W. C., Lerner, B. M., Stark, H., Warneke, C., Williams, E. J., Fehsenfeld, F. C., Ravishankara, A. R., and Trainer, M.: Radicals in the marine boundary layer during NEAQS 2004: a model study of day-time and night-time sources and sinks, Atmos. Chem. Phys., 9, 3075-3093, doi:10.5194/acp-9-3075-2009, 2009.

Stull, R. B.: An introduction to boundary layer meteorology, Kluwer Academic Publishers, 666pp.,1988.

Stutz, J., Alicke, B., Ackermann, R., Geyer, A., White, A., and Williams, E.: Vertical profiles of NO_3, N_2O_5, O_3, and NO_x in the nocturnal boundary layer: 1. Observations during the Texas air quality study 2000, J. Geophys. Res., 109, doi:10.1029/2003JD004209, 2004.

Thornton, J. A., Kercher, J. P., Riedel, T. P., Wagner, N. L., Cozic, J., Holloway, J. S., Dubé, W. P., Wolfe, G. M., Quinn, P. K., Middlebrook, A. M., Alexander, B., and Brown, S. S.: A large atomic chlorine source inferred from mid-continental reactive nitrogen chemistry, Nature, 464, 271-274, doi:10.1038/nature08905, 2009.

Van Doren, J. M., Watson, L. R., Davidovits, P., Worsnop, D. R., Zahniser, M. S., and Kolb, C. E.: Uptake of dinitrogen pentoxide and nitric acid by aqueous sulfuric acid droplets, The Journal of Physical Chemistry, 95, 1684-1689, doi:10.1021/j100157a037, 1991.

Watt, S. A., Wagner-Riddle, C., Edwards, G., and Vet, R. J.: Evaluating a flux-gradient approach for flux and deposition velocity of nitrogen dioxide over short-grass surfaces, Atmospheric Environment, 38, 2619-2626, doi:10.1016/j.atmosenv.2004.02.021, 2004.

Wesely, M. L., and Hicks, B. B.: A review of the current status of knowledge on dry deposition, Atmospheric Environment, 34, 2261-2282, doi:10.1016/j.atmosenv.2004.02.021, 2000.

Wood, E. C., Bertram, T. H., Wooldridge, P. J., and Cohen, R. C.: Measurements of N_2O_5, NO_2, and O_3 east of the San Francisco bay, Atmospheric Chemistry and Physics, 5, 483-491, doi:10.5194/acp-5-483-2005, 2005.

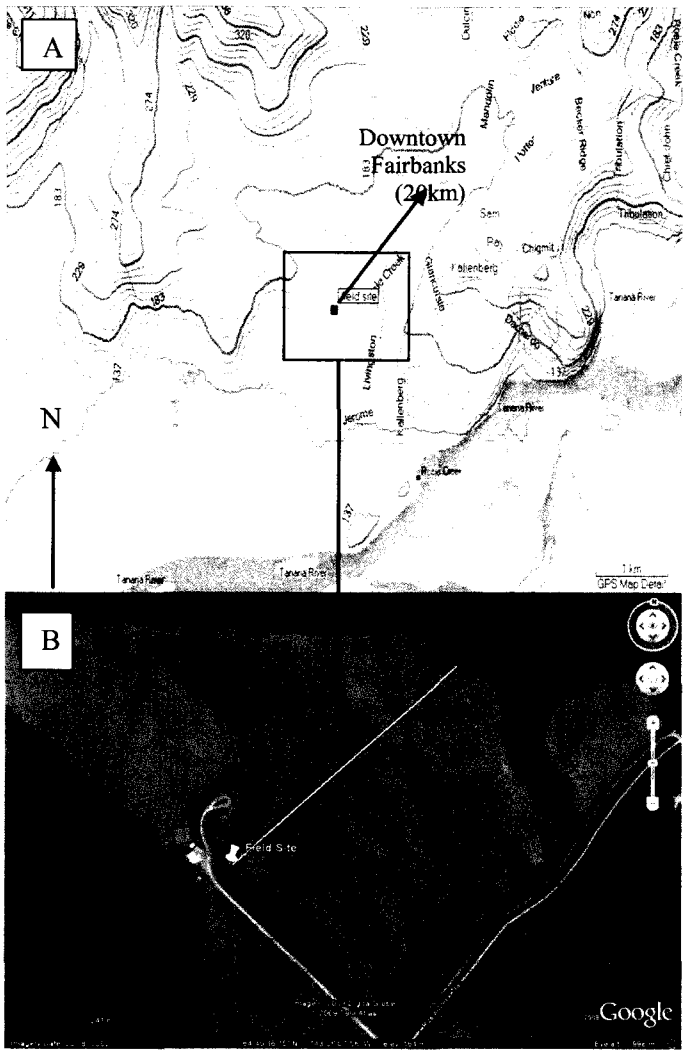

Figure 6.1. Field site location. A) contour map of field site with a black outline of the field site area. B) Expanded satellite image of the inside of the black box area on map A. The black arrows in map B represent the wind direction selection criteria. The white line is the dominant wind direction with a maximum distance to the trees of 400 meters (fetch). The yellow marker is location of field site. During the field campaign, the field was covered with snow.

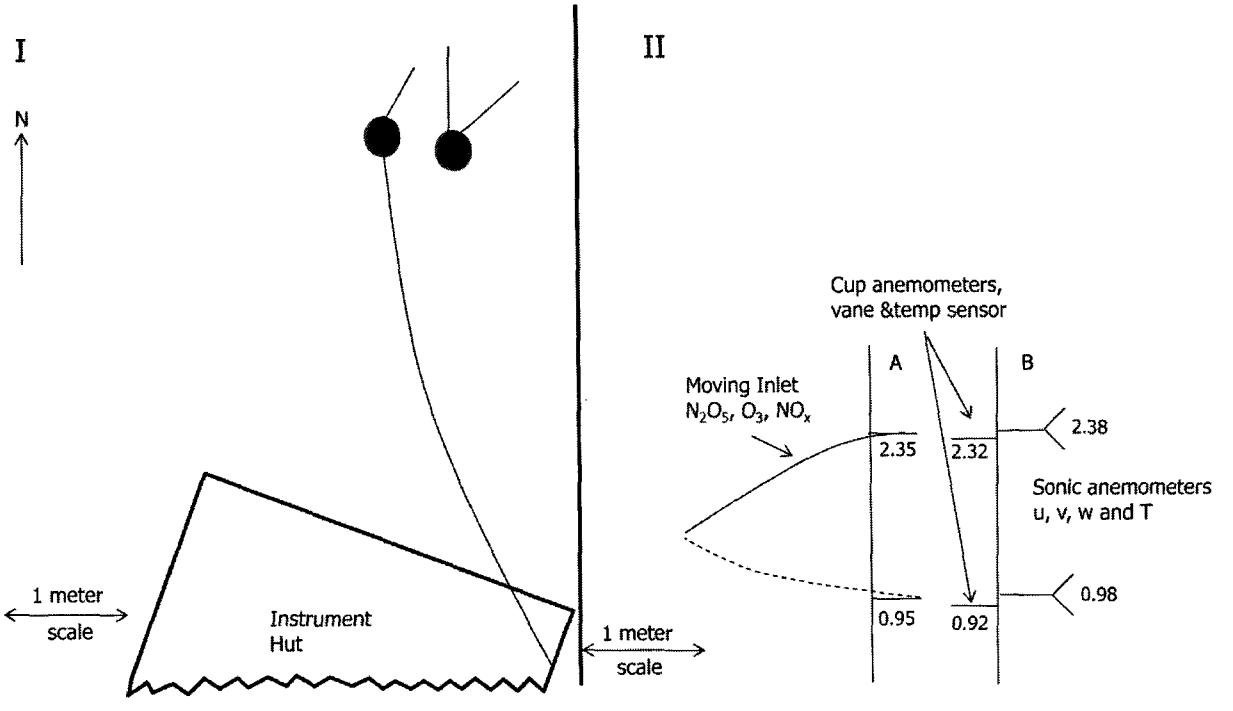

Figure 6.2. I The plan view and orientation of the two measurement towers. II. Elevation view of the moving inlet tower (A) and the meteorological tower (B). All distances are in meters.

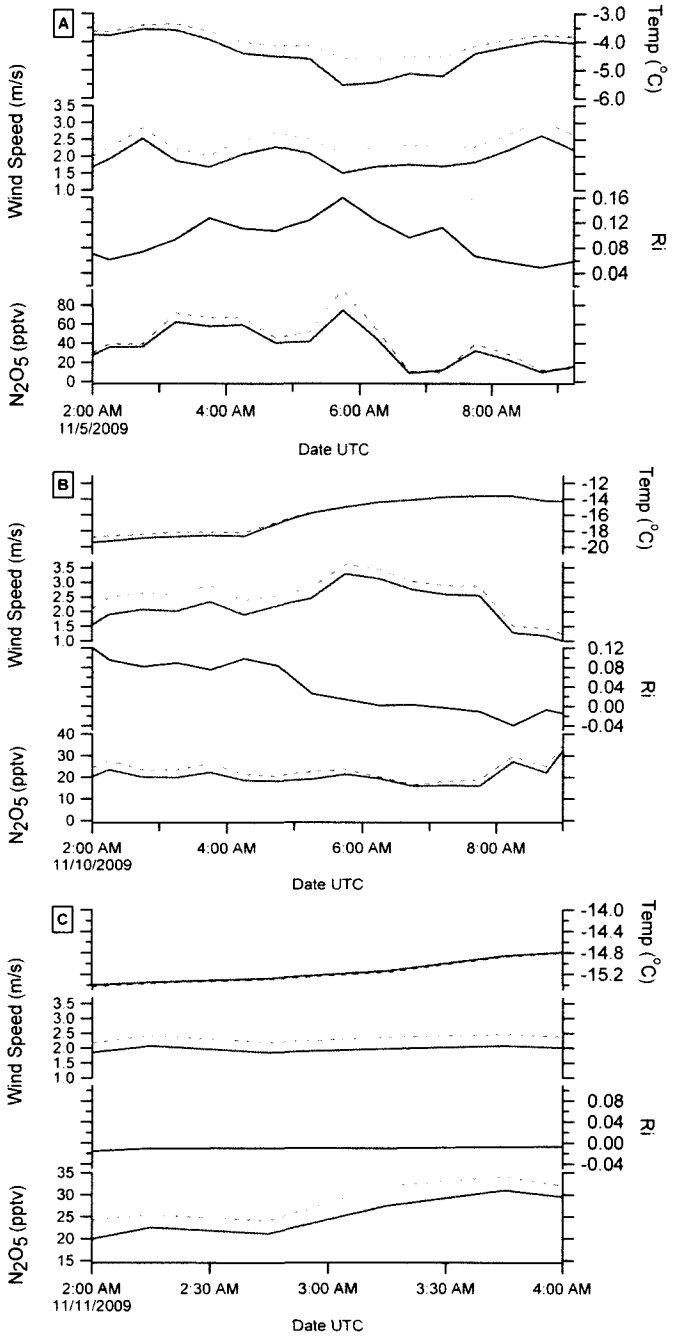

Figure 6.3. Time series of the Richardson number and components. Temperature (°C), wind speed (m/s), Richardson number and mixing ratio of N_2O_5 in pptv for A. 5 Nov 2009, B. 10 Nov 2009 and C. 11 Nov 2009 . The red solid trace is always the

lower height and the blue dashed trace is the higher measurement height. The black solid line, 3rd axis from the top is the Richardson number.

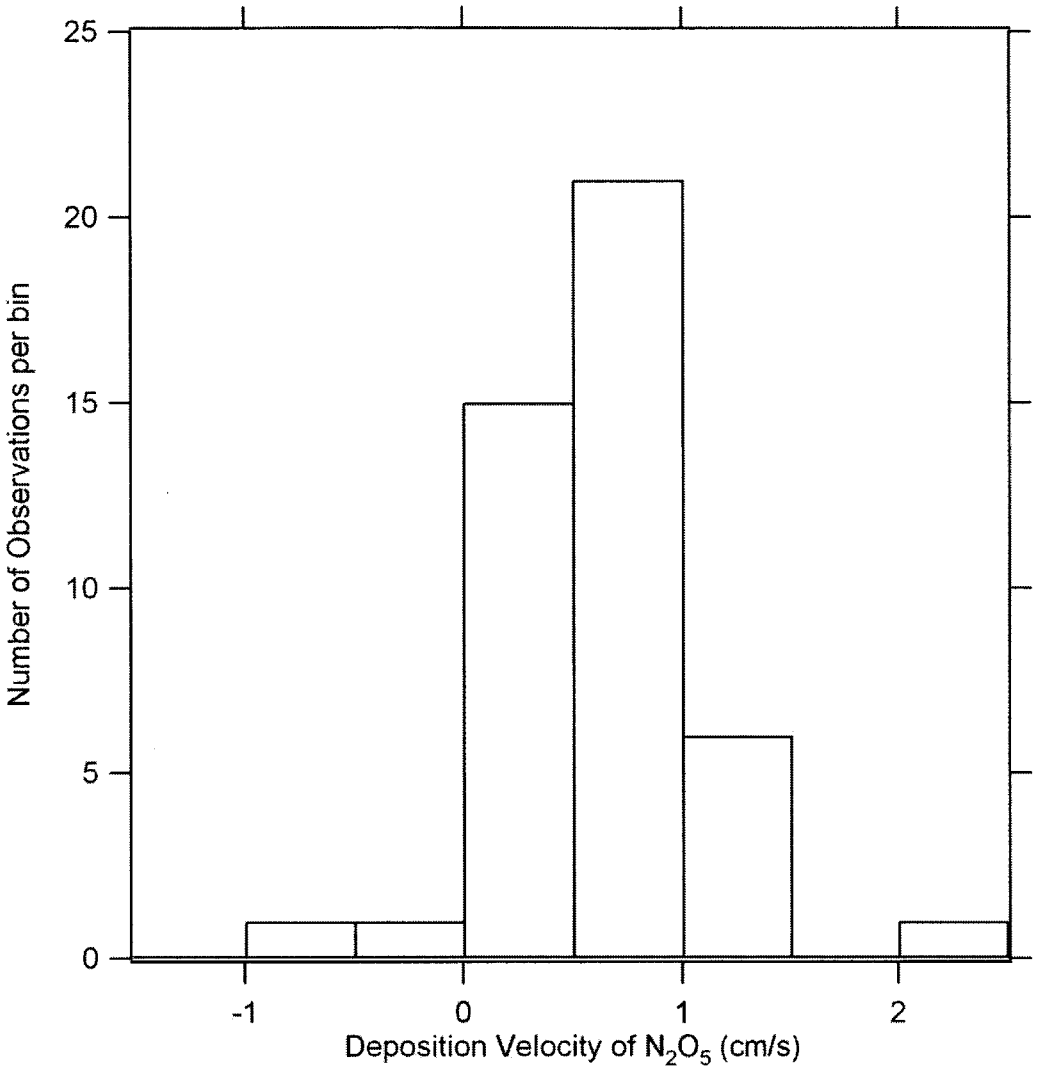

Figure 6.4. Histogram showing the distribution of deposition velocities of N_2O_5 on the selected data analysis nights 5, 10 and 11 Nov 2009.

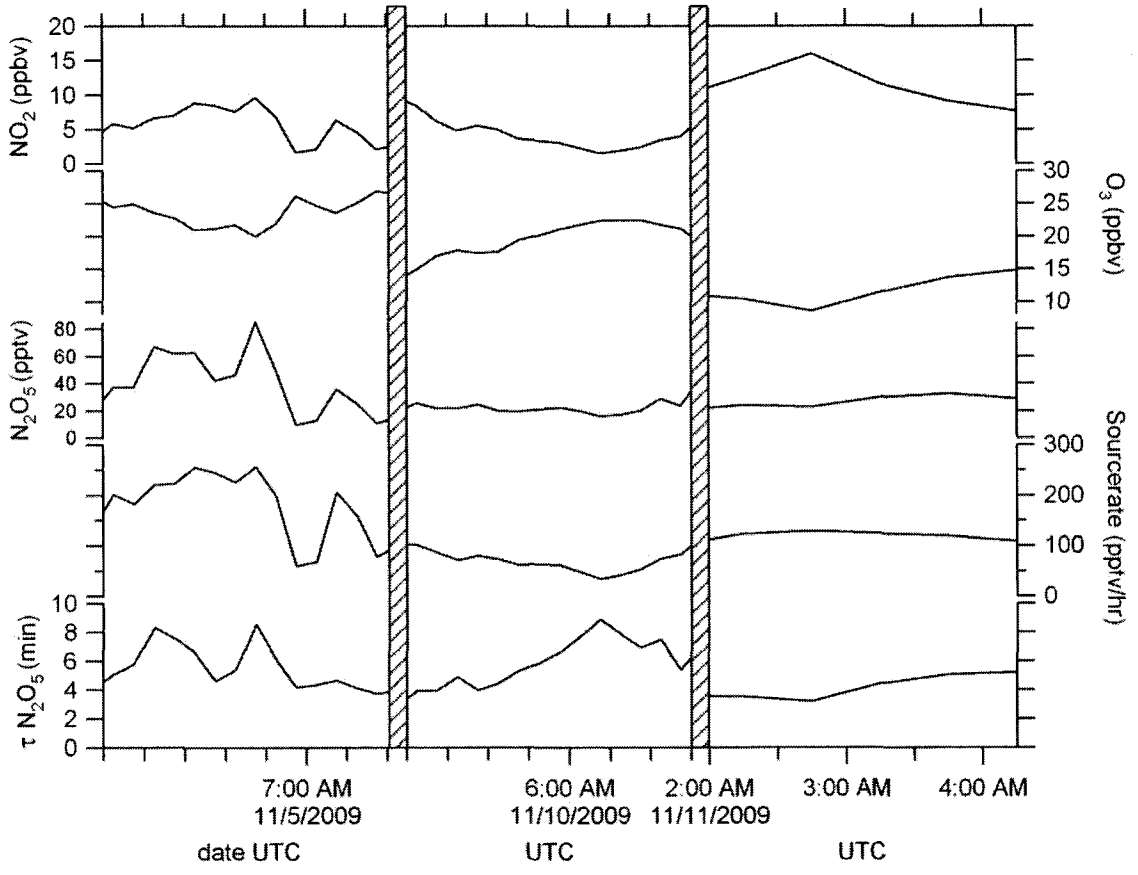

Figure 6.5. Times series of steady state lifetimes of N_2O_5 and chemical components. From top to bottom are the mixing ratios of NO_2 (ppbv), O_3 (ppbv) and N_2O_5 (pptv), source rate of N_2O_5 (pptv/hr) and the steady state lifetime of N_2O_5 as τN_2O_5 (min) on three nights 5, 10 and 11 Nov 2009.

Chapter 7 Comparison of the aerodynamic gradient to eddy covariance method[2]

The eddy covariance (EC) method is a more direct method to measure fluxes than the aerodynamic gradient method. However, measurements using the EC method require high-frequency (at least 10 Hz) observations of both air motion and the species interacting with the surface. Because our chemical instruments and inlet have a response time slower than 1 second, we cannot use the EC method to measure N_2O_5 deposition fluxes. However, the meteorological observations were sufficient to measure the sensible heat fluxes by both the aerodynamic gradient method and the EC method, allowing validation of the gradient method for that property. Similarly, we have used the EC measurements to calculate the friction velocity and stability parameter, z/L, to ensure the boundary layer parameter calculations.

7.1 Boundary layer characteristics

Because the aerodynamic method is applicable under very restricted stability conditions, it is necessary to ensure that little change in flux occurs across the observations heights.

---

[2] Expanded version of Supplemental material submitted to Atmospheric Chemistry and Physics Discussions as a part of "Huff, D.M., Joyce, P.J., Fochosatto, G.J., and Simpson, W.R. Deposition of dinitrogen pentoxide, N_2O_5, to the snowpack at high latitudes. (submitted to ACPD, 22 Sept 2010)"

In addition, the two measurement heights need to remain in the same atmospheric layer. These conditions are achieved if the highest measurement point remains below 10% of the boundary layer height (Oke, 1987; Monteith and Unsworth, 1990), therefore constraining the measurements in the "constant flux layer". Because the highest measurement height is 2.38 meters, this criterion requires boundary layer heights of more than 24 meters. There are slightly different percentages given for the estimate of the constant flux layer and Stull (1988) estimates the boundary layer to be the lowest 5%. In this case the criterion would be 48 meters minimum boundary layer height, or 20 times the highest measurement height. In addition to the percentage of the constant flux layer, there are several different parameterizations to define the boundary layer height. We have chosen the most applicable to our data, but note the difficulty in estimating a boundary layer height under stable Arctic conditions (Anderson and Neff, 2008).

The gradient boundary layer height, H_g, is given by (Arya, 2001)

$$H_g = 1.2u_*(fN)^{-0.5}. \qquad (7.1)$$

In this equation, u_* is the friction velocity, f is the Coriolis force, and N is the Brunt-Väisälä frequency, which is given by

$$N^2 = \frac{g}{\theta}\left[\frac{\Delta\theta}{\Delta z}\right]. \qquad (7.2)$$

In Equation (7.2), g is the gravitational constant, θ is the potential temperature, and z is the measurement heights. Figure 7.1 shows the gradient boundary layer height during

each night of the campaign during which we measured the deposition velocity. The gradient boundary layer height using Eq. (7.1) ranges from 15 meters to 150 meters for the three nights under study. The average gradient boundary layer height during the observation periods used to measure fluxes was 45 meters.

The friction velocity can be calculated using the gradient method by

$$u_* = k \frac{\Delta U}{\left[\ln(z_2/z_1)\right]} (\Phi_m)^{-1}. \qquad (7.3)$$

In Equation (7.3), Φ_m, is the stability correction factor for momentum and is unity, less than unity or greater than unity under neutral, unstable or stable conditions respectively. The variable U, is the wind speed, k the Von Karman constant, which has the value 0.4, and the z_i values are the measurement heights. Figure 7.2 shows the friction velocity for the three study nights that we calculated a deposition velocity. The average friction velocity using the gradient method was 0.13 +/- 0.02 m/s.

The calculation of the friction velocity, u_*, using eddy covariance, EC, observations is given by Stull (1988),

$$u_* = \left((u'w')^2 + (v'w')^2\right)^{(1/4)}. \qquad (7.4)$$

Where the primed variables are the turbulent components and the mean, is represented by a bar over the variable. For example, the vertical component of the wind, w, has its fluctuations and means defined by

$$w' = w - \overline{w}. \qquad (7.5)$$

All properties (*e.g.* vertical wind, w) are measured at 10 Hz, and the turbulent quantities are calculated based on the streamline coordinates rotation and mean subtraction by half-hour block with the corresponding de-trending of the signals. Similar separations of fluctuations exist for horizontal wind components, u and v, and temperature, T.

The Obukhov length, L, is given by

$$L = -\frac{u_*^3 \overline{\theta}}{kg(\overline{w'\theta'})}. \qquad (7.6)$$

The product $\overline{w'\theta'}$ is the covariance of the vertical wind velocity, w, and the potential temperature, θ. In Equation (7.6), the friction velocity is calculated from high frequency data using Eq. (7.4). In Fig. 7.2, the average friction velocity for the eddy covariance method was 0.09 +/- 0.05 m/s.

The eddy covariance derived stable boundary layer height, H, is (Arya, 2001)

$$H = d(u_* L / f)^{0.5}. \qquad (7.7)$$

In Eq. (7.7), d is a constant at 0.3, u_* is the friction velocity, f is the Coriolis force and L is the Obukhov length determined using Eq. (7.6). The third night 11 Nov, 2009 is marginally unstable and instead we use the following formula from Mahrt (2003),

$$H = 0.6(u_* / f). \qquad (7.8)$$

Equation (7.8) uses the friction velocity (u_*) divided by the Coriolis force (f). Zilintinkevich and Baklanov (2002) summarize several boundary layer height equations that are in the literature including Mahrt (2003).

In Fig. 7.1., the first two study nights, 5 and 10 Nov, 2009 are marginally stable nights and the boundary layer height cannot be determined using Eq. (7.1) because the Brunt-Väisälä frequency will be imaginary and instead we used Eq. (7.8). The red solid line with markers in Fig. 7.1 represents the results of using the gradient boundary layer Eq. (7.1). In Fig. 7.1 the eddy covariance method of calculating a boundary layer height (Eq. 7.7) is represented by the black solid line. Equation (7.7) was used to calculate the boundary layer height for the first two nights under neutral to slightly stable conditions with an average of 39 meters. In Fig. 7.1, on the third night the conditions were slightly unstable. Under these conditions, we calculated a negative L using the eddy covariance method so we used Eq. (7.8) to calculate the boundary height represented by the blue solid line. Using Eq. (7.8), we find an average of 38 meters for all three nights. When the Obukhov length is negative (11 Nov 2009) the estimate of boundary layer height is not reliant on the turbulence length scale (Arya, 2001). Calculating the boundary layer height shows that even under the most restricted conditions (i.e., $H_g \approx 24$ m) the sampling height (2.38 meters) remains within the constant flux layer a majority of the time.

The friction velocity can be used to filter data when the wind effect on the surface is too large and no measurable gradients will exist, approximately > 0.5 m/s or < 0.05 m/s, but the threshold is not agreed upon (Arya, 2001, Andreas et al., 2004). The threshold

varies with experimental instruments, such as cup or sonic anemometers and study site constraints. Andreas et al. (2004) found an upper limit of friction velocity for blowing snow particles at > 0.3 m/s. Bocquet (2007) used a minimum threshold of 0.05 m/s because cup anemometers were used. We used sonic anemometers for the EC method and did not have a threshold, because our maximum friction velocity was 0.28 m/s for study nights 5, 10 and 11 Nov, 2009.

Figure 7.3 correlates the stability parameter calculated by the eddy covariance and to the same parameter calculated by the aerodynamic gradient method and the agreement is reasonable with an $r^2 = 0.56$. Comparing the stability parameter by the eddy covariance method to the same parameter calculated by the aerodynamic gradient method, the results are similar to other authors Bocquet (2007).

The Obukhov length scale, L, is an important parameter that is also used in the stability parameter relationship (Arya, 2001) z/L. This relationship is used to characterize the atmospheric stability similar to the Richardson number (Eq. 6.3). The height, z, in meters is the sonic anemometer height and L, as mentioned earlier, is the Obukhov length in meters. The Obukhov length, L, can be negative or positive and corresponds to an unstable or stable atmosphere for the stability parameter z /L, similar to the Richardson number. When the covariance $\overline{w'\theta'}$ in the denominator of Eq. (7.6) is positive, then L is negative for an unstable atmosphere. When $\overline{w'\theta'}$ is negative the result a positive z/L stability parameter. To compare the stability parameters the Richardson number to z/L, the following corrections factors need to be used from Kaimal and Finnigan (1994):

$R_i = z/L$ (for unstable conditions $R_i < 0$) (7.9a)

$R_i = z/L\ (1+5\ (z/L))^{-1}$ (for stable conditions $R_i > 0$). (7.9b)

We compared our results for the Richardson number, which we used to define the acceptable range of $0.12 > R_i > -0.1$ for measuring a flux, to z/L using the sonic anemometer data.

7.2 Comparison of heat flux measured by eddy covariance and gradient method

To validate the use of the aerodynamic gradient method, we compared sensible heat fluxes measured by the aerodynamic gradient method to the eddy covariance method. The eddy covariance (EC) derived sensible heat flux, Q_{EC}, is (Arya, 2001)

$$Q_{EC} = \rho c_p \overline{w'T'}. \qquad (7.10)$$

In Equation (7.10), ρ is the air density, c_p is the heat capacity. Similar to Eq. (7.4) w' is the vertical turbulent component of the wind. The temperature, T' is a scalar quantity and also averaged to a half hour together $w'T'$ is the covariance of the vertical wind and temperature.

The aerodynamic gradient method can also be used to calculate the sensible heat flux, Q_{aero}, using an equation similar to Eq. (6.2) in the Chapter 6, (Arya, 2001)

$$Q_{aero} = -k^2 \rho c_p \frac{\Delta\bar{u}\Delta\bar{T}}{[\ln(z_2/z_1)]^2}(\Phi_M \Phi_h)^{-1} \qquad (7.11)$$

Note that the same generalized stability flux correction factors are used in Eq. (7.11) and Eq. (6.2) in the Chapter 6. We use the generalized stability correction factor equation from Oke (1987) for both gradient flux calculations. The use of these correction factors is critical in arriving at a good correlation between the two methods shown below, and thus it is important that we consistently use these validated factors in the calculation of N_2O_5 deposition velocity in the Chapter 6.

The heat fluxes are measured by the two different methods (Fig. 7.4) and are in good agreement with an $r^2 = 0.76$, importantly, the slope is within standard error of unity. The heat flux ranged from +8 to -70 W/m^2, with the average heat flux of -5.4 W/m^2. At the larger negative heat flux values, the atmosphere becomes increasingly stable, requiring a large stability correction factor. The effect of these large corrections is seen in the high scatter at negative heat flux values.

7.3 Estimation of the height of N_2O_5 snowpack deposition

In a stable boundary layer, the flux is a function of height, with a maximal value at the surface that decreases to zero at the top of the boundary layer. The shape of this flux profile is not known for N_2O_5, but by extension of the similarity theory, we expect that the shape of the deposition flux profile is similar to that of the momentum flux profile $\tau(z)$ Micrometeorological observations of the stable boundary layer typically found in the Arctic indicate that the momentum flux profile is described by a power law, (Arya, 2001)

$$\tau(z) = \rho u_*^2 (1 - z/H)^{\alpha_1} \quad . \qquad (7.12)$$

The exponent value, α_1, can change depending upon the development of the stable boundary layer (Arya, 2001), but is often assumed to be 1.75 (Lenschow et al., 1988; Smedman, 1991). If we assume the same power law dependence for the flux profile of N_2O_5, we find that the vertical dependence of the flux is

$$F_{N_2O_5}(z) = \left(F_{N_2O_5}\right)_{surf} (1 - z/H)^{\alpha_1} \quad . \qquad (7.13)$$

In this equation, the surface flux, which we have observed, is indicated by the "surf" subscript, and the flux is a function of height, z. We define the effective height for N_2O_5 deposition, z_{eff}, by the height of the box profile (constant flux with height through some effective height, z_{eff}) with the same integral as the power law flux profile, Eq. (7.13). The result is

$$z_{eff} = \frac{H}{1 + \alpha_1} \, . \qquad (7.14)$$

We use the average boundary layer height, $H = 43$ meters, and $\alpha_1 = 1.75$, to find that $z_{eff} =$ 15 meters.

References:

Anderson, P. S., and Neff, W. D.: Boundary layer physics over snow and ice, Atmospheric Chemistry and Physics, 8, 3563-3582, doi:10.5194/acp-8-3563-2008, 2008.

Andreas, E. L, Jordan,R.E. and Makshtas, A.P.: Simulations of snow, ice, and near-surface atmospheric processes on Ice Station Weddell. Journal of Hydrometeorology, 5, 611–624, 2004.

Arya, S. P.: Introduction to micrometeorology, second ed., Academic press, 420 pp., 2001.

Bocquet, F.: Surface layer ozone dynamics and air-snow interactions at summit, Greenland spring and summer ozone exchange velocity and snowpack ozone:The complex interactions, Ph.D., Department of Atmospheric and Oceanic Sciences, University of Colorado, 197 pp., 2007.

Kaimal, J. C., and Finnigan, J. J.: Atmospheric boundary layer flows: Their structure and measurement, Oxford University press, 1994.

Lenschow, D. H., Li, X. S., Zhu, C. J., and Stankov, B. B.: The stably stratified boundary layer over the great plains, Boundary-Layer Meteorology, 42, 95-121, 1988.

Mahrt, L., and Vickers, D.: Formulation of turbulent fluxes in the stable boundary layer, Journal of the Atmospheric Sciences, 60, 2538-2548, doi:10.1175/1520-0469(2003)060<2538:FOTFIT>2.0.CO;2, 2003.

Monteith, J. L., and Unsworth, M. H.: Principles of environmental physics, second ed., 291pp., Edward Arnold, 1990.

Oke, T. R.: Boundary layer climates, 2nd ed., Methuen, London, 435pp.,1987.

Smedman, A. S.: Some turbulence characteristics in stable atmospheric boundary layer flow, Journal of the Atmospheric Sciences, 48, 856-868, doi:10.1175/1520-0469(1991)048<0856:STCISA>2.0.CO;2, 1991.

Stull, R. B.: An introduction to boundary layer meteorology, Kluwer Academic Publishers, 666pp., 1988.

Zilitinkevich, S., and Baklanov, A.: Calculation of the height of the stable boundary layer in practical applications, Boundary-Layer Meteorology, 105, 389-409, doi:10.1023/a:1020376832738, 2002.

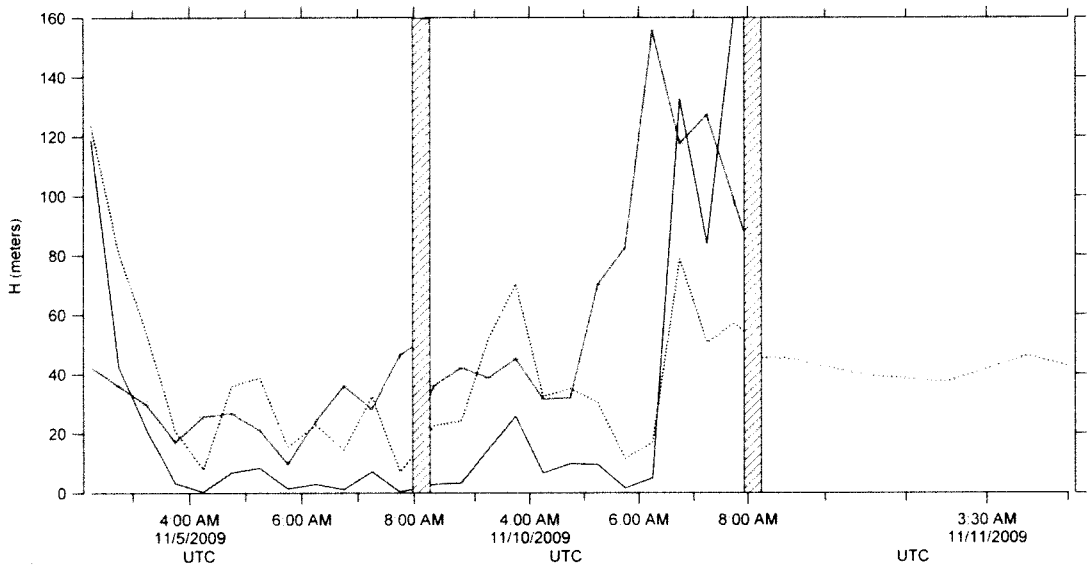

Figure 7.1. Boundary layer heights. Boundary layer is H in meters for 5 Nov 2009, 10 Nov 2009 and 11 Nov 2009. The red line and marker traces are always the boundary layer height (H_g) using the aerodynamic gradient method and Eq. (7.1). The black solid trace is eddy covariance method (H) using Eq. (7.7). The blue dotted line trace is the boundary layer height using the eddy covariance method and Eq. (7.8).

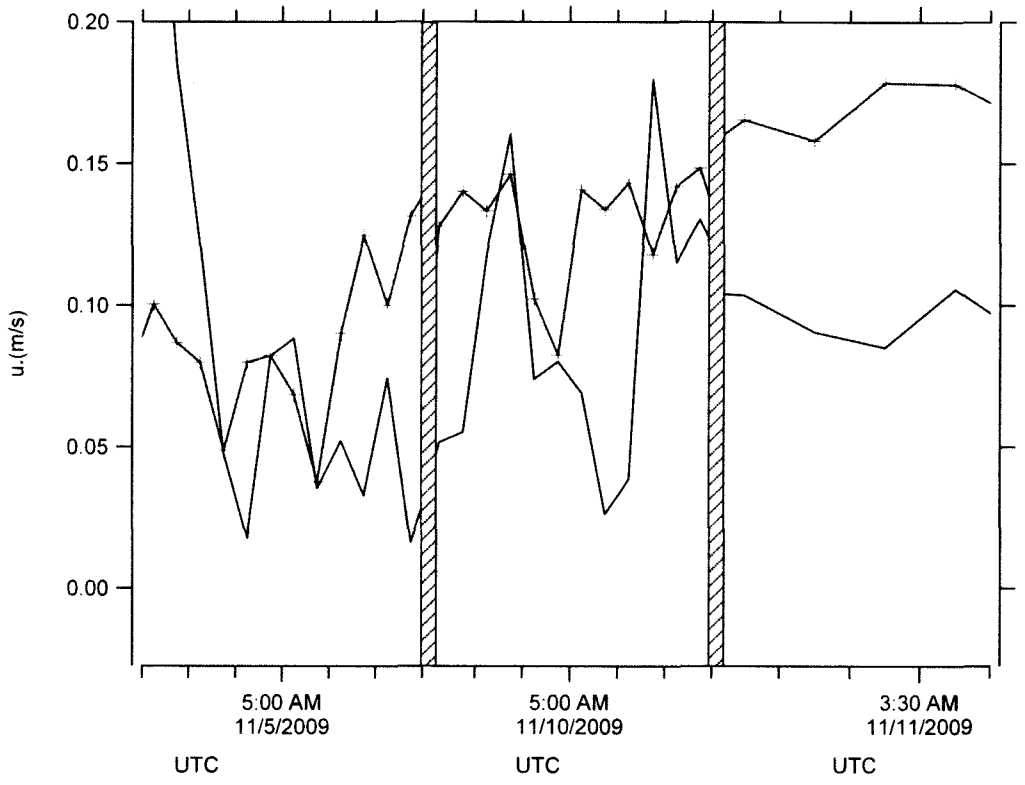

Figure 7.2. Time series of the friction velocity, u_* (m/s). The 3 selected nights are 5 Nov 2009, 10 Nov 2009 and 11 Nov 2009. The red line and marker trace is the aerodynamic gradient method of calculating the friction velocity, using Eq. (7.3) and the black solid trace is eddy covariance (EC) method to calculate the friction velocity using Eq. (7.4).

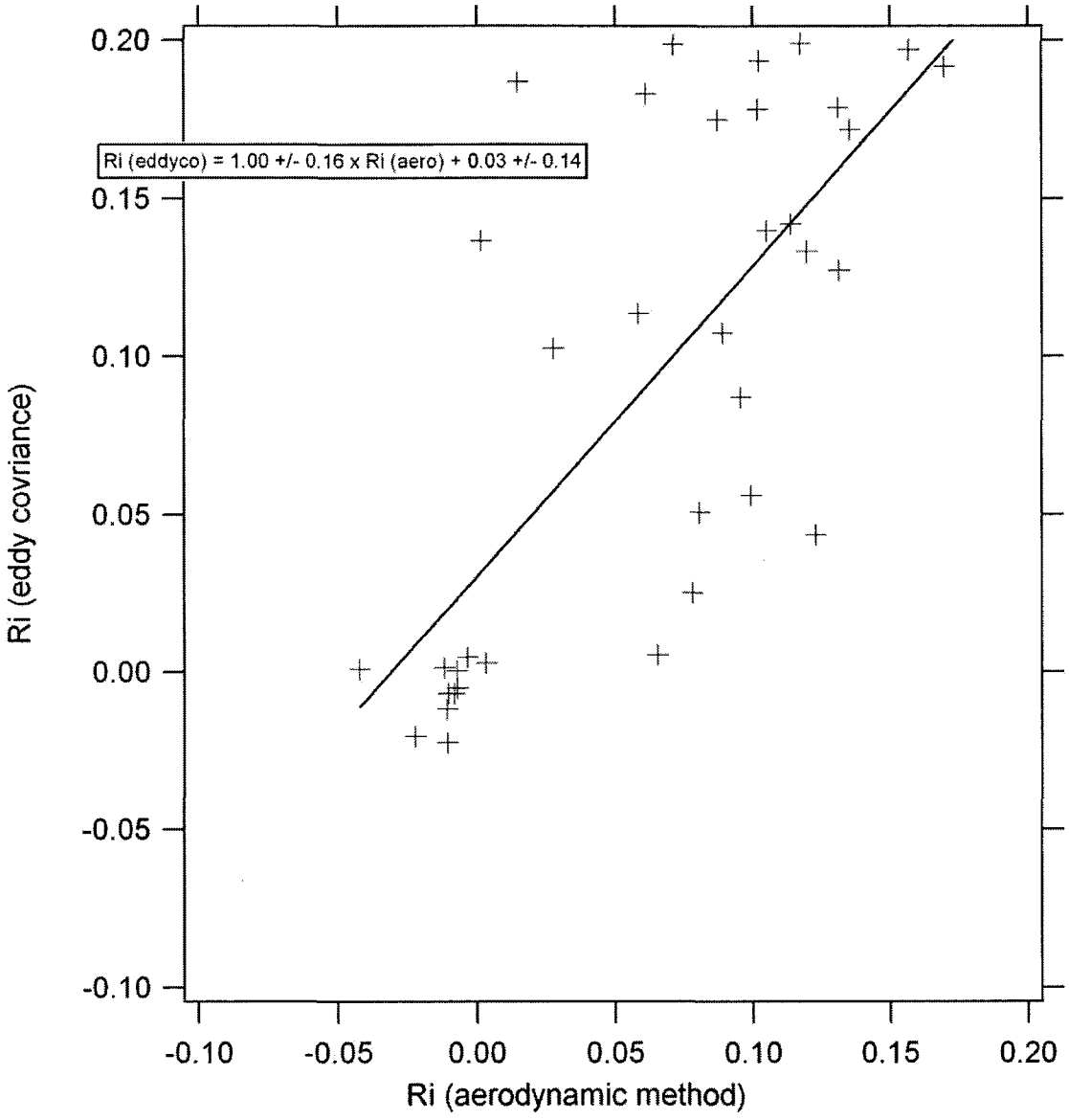

Figure 7.3. Comparison of the stability parameters. The stability parameter, the Richardson number, R_i calculated by the aerodynamic gradient method and by the eddy covariance method. R_i (eddy covariance) is calculated using the relationship z/L and Eq. (7.9a and 7.9b).

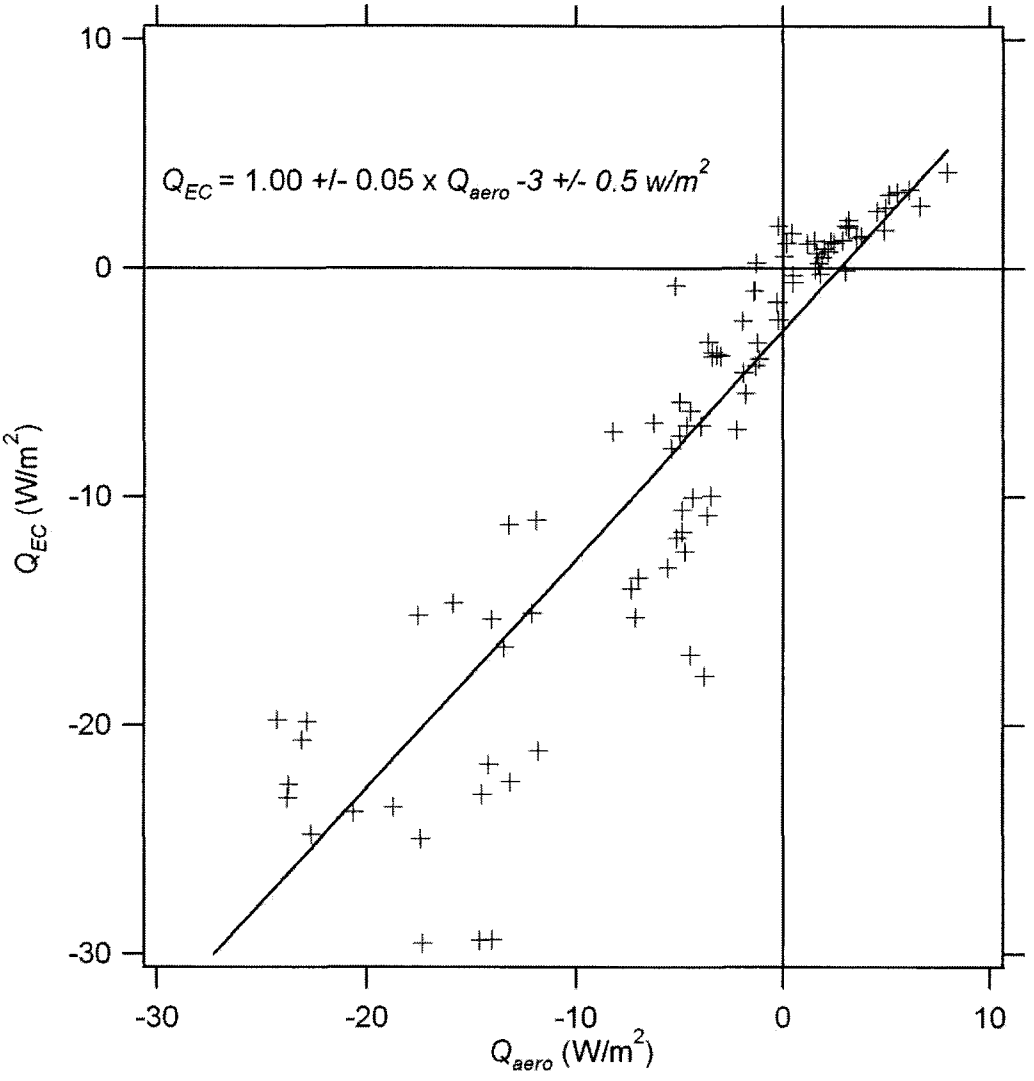

Figure 7.4. Comparison of the sensible heat fluxes. The eddy covariance method, Q_{EC}, versus sensible heat flux by the aerodynamic gradient method, Q_{aero}. The errors are reported as +/- 1 standard deviation.

Chapter 8 Measurements of N_2O_5 mixing ratios and lifetimes aloft at high latitudes[3]

The vertical profile of dinitrogen pentoxide, N_2O_5, is important for nighttime chemistry and implicates different loss mechanisms near the Earth's surface and aloft at high latitudes. We conducted a field campaign in Fairbanks, Alaska during March, 2010 on top of a building, at a height of 30 meters from the local topography to measure the chemical removal rate and steady state lifetime of N_2O_5 decoupled from the Earth's surface. The average steady state lifetime of N_2O_5 aloft was 44 minutes with a maximum lifetime greater than two hours. The transport distance from source to the field site is probably comparable to these inferred steady-state lifetimes, possibly invalidating the steady-state assumption and implying an even longer lifetime than the steady-state method calculates. The lifetimes of N_2O_5 are compared under different meteorological conditions that occurred during the sampling period and recent observations from our previous field studies performed near the Earth's surface. We found that the N_2O_5 mixing ratio increases with height and that the steady state lifetime of N_2O_5 are a factor of 5 longer aloft than near the Earth's surface at high latitudes during winter.

[3]Huff, D.M., Joyce P.L., Donohoue D.L., Simpson, W.R.: Measurements of N_2O_5 mixing ratio and lifetimes aloft at high latitudes, (In preparation for ACPD).

8.1 Introduction

The role of nocturnal nitrogen oxide chemistry in the removal of pollutants and formation of nitric acid is especially important at high latitudes where dark and cold conditions dominate during winter. The chemical family NO_x ($NO+NO_2$) is a combustion pollutant emitted by industry, home heating and automobiles. As this pollution ages, it forms the nitrate radical, NO_3, and dinitrogen pentoxide, N_2O_5. The nitrate radical is formed from the oxidation of NO_x at night, when the photochemical processes that degrade NO_3 are suppressed and the formation of N_2O_5 is favored (R1-R3).

$$NO_2 + O_3 \rightarrow NO_3 + O_2 \qquad \text{(R1)}$$

$$NO_2 + NO_3 \leftrightarrows N_2O_5 \qquad \text{(R2)}$$

$$N_2O_5 + H_2O \xrightarrow{\text{Surface}} 2HNO_3 \qquad \text{(R3)}$$

Reaction (R3) is the heterogeneous hydrolysis of N_2O_5, which requires a surface to catalyze the reaction to form nitric acid. The process of N_2O_5 reacting with a surface depends on the atmospheric processes aloft coupled with surface depositional processes. The atmospheric processes include interactions with aerosol particles, super cooled water droplets and ice particles that all may be present in some form in the atmosphere at high latitudes. The depositional processes include chemical loss of N_2O_5 due to deposition to the snowpack.

Several studies have measured the vertical profile of N_2O_5 and found that its mixing ratio increases with height (Brown et al., 2003; Stutz et al., 2004; Brown et al., 2007a;

Brown et al., 2007b). Brown et al. (2007b) conducted a field study on a 300 meter tower to get a high-resolution vertical profile of N_2O_5 mixing ratios near the Earth's surface up to 300 meters. Brown et al. (2007b) found three distinct layers: the surface layer (20 m or less), boundary layer (up to 150 m), and residual layer (>150 m). The mixing ratio of N_2O_5 increased with height through the boundary layer (150 m) and then stabilized at a constant mixing ratio. Brown et al. (2007a) found similar results during an aircraft study over the Northeast US. The aircraft measurements did not penetrate the boundary layer, but in situ N_2O_5 measurements were made simultaneously at the surface. Brown et al. (2007a) found higher mixing ratios aloft, as high as 1 ppbv of N_2O_5 (> 150 m), than near the surface. They also found much longer lifetimes of N_2O_5 aloft (> 150 m) implying that different chemical loss mechanisms occur near the surface. These findings imply that NO_x is a sink for ozone and a reservoir of NO_x aloft (Brown et al., 2007a). Stutz et al. (2004) was in agreement with these findings. They found calculated steady state N_2O_5 mixing ratios increased with height up and a maximum mixing ratio of 300 pptv aloft in a Texas air quality study (TEXAQS).

In addition to measuring the vertical profiles of N_2O_5, we can determine the efficiency of the reaction of gaseous N_2O_5 colliding with the surface of submicron particles by measuring the reactive uptake coefficient of N_2O_5, γ. The reactive uptake coefficient of N_2O_5 has been studied in the lab (Mozurkewich and Calvert, 1988; Kirchner et al., 1990; Hanson and Ravishankara, 1991; Van Doren et al., 1991; Hu and Abbatt, 1997) and at mid-latitudes in the field (Brown et al., 2006; Bertram and Thornton, 2009). These lab

and field experiments investigated N_2O_5 heterogeneous hydrolysis and the dependence of the rate of hydrolysis on aerosol chemical composition.

We have conducted several high latitude field studies that measured the mixing ratios and steady state lifetimes of N_2O_5 (Ayers and Simpson, 2006; Apodaca et al., 2008). We reported fast lifetimes on the order of 10 minutes near the Earth's surface and average N_2O_5 mixing ratios of 20-40 pptv near the surface and few hundred pptv aloft. In addition we measured the deposition velocity of N_2O_5 to be downward at 0.6 cm/s (Huff et al., 2010). This deposition velocity caused a significant loss of N_2O_5 near the Earth's surface. Snowpack deposition for N_2O_5 implies additional chemical loss mechanisms near the Earth's surface.

Modeling studies investigated the heterogeneous hydrolysis of N_2O_5. Dentener and Crutzen (1993) found that during the winter 80% of high latitude NO_x is lost by Reaction (R3), the dominant dark pathway to nitric acid. In addition, recent models have used different parameterizations of γ from laboratory and field studies to identify the dependence of N_2O_5 on aerosol composition and temperature (Riemer et al., 2003; Evans and Jacob, 2005). Bertram and Thornton (2009) parameterized N_2O_5 based on γ's dependence on $H_2O(l)$, Cl^- and NO_3^- for organic and inorganic mixed aerosol particles.

Due to additional chemical reactions of NO_x occurring during profile measurements, modeling been used to interpret the vertical profiles. Modeling vertical profiles of N_2O_5 (Geyer and Stutz, 2004) shows different possible loss mechanisms near the Earth's surface and aloft. Geyer and Stutz (2004) used dry deposition velocities near the Earth's

surface from HNO_3 and reactive uptake coefficients of N_2O_5 (γ) from the laboratory study by Hu and Abbatt (1997). Geyer and Stutz (2004) found that the model results followed experimental data showing different loss mechanisms for N_2O_5 at different altitudes.

The heterogeneous reaction of N_2O_5 (R3) is an important reaction for NO_x loss and needs to include the partitioning of different chemical loss mechanisms with increasing altitude. Here, we report on steady state lifetimes and mixing ratios of N_2O_5 aloft and compare these lifetimes to those obtained from snowpack deposition studies (Huff et al., 2010). Since the past measurements of N_2O_5 (Ayers et al., 2006) on the roof of the Geophysical Institute at the University of Alaska Fairbanks, in Fairbanks Alaska, we have added an improved inlet for sampling unobstructed air flow, meteorological data of wind speed, wind direction, temperature and a visibility monitor. We also compare different meteorological conditions and the visibility to surface area relationship to atmospheric particles. These particles may include ice particles and super-cooled water droplets in addition to aerosol particles, which may increase the surface area available for chemical loss of N_2O_5 at high latitudes.

8.2 Experimental

8.2.1 Instrumental and site descriptions

To measure the mixing ratio and steady state lifetime of N_2O_5 aloft, we chose a field study site on top of the Geophysical Institute's Elvey Building. Downtown Fairbanks is located approximately 6 km from the Geophysical Institute (Fig. 8.1). The roof top is 85 meters above the Tanana valley floor and 220 meters above sea level. However, our sampling location is on the Northwest (NW) side of the building and the topography is

sloping. The height of the Geophysical Institute's Elvey building is 30 meters high from local topography in the main sampling direction and the Tanana Valley floor 85 meters below is south of the building. The instruments were located on the NW corner of the building and the north-facing side of the roof is aligned at 90 degrees to the sampling inlet. The main flow inlet for sampling all chemical gases (N_2O_5, NO_x and O_3) was 10 meters long and attached securely at the NW corner edge of the building, 3 meters up and 1 meter out from the building housing the instruments. The sampling inlet direction and location minimized influences from the building, rooftop objects and surrounding buildings. The data was only analyzed when the wind direction was greater than 300 degrees and less than 30 degrees in true coordinates in order to minimize influence from the building's edge.

A field-portable instrument using cavity ring down spectroscopy (CRDS) was developed by our laboratory group to measure N_2O_5 at remote sites (Simpson, 2003; Ayers et al,. 2005). We have used this CRDS instrument during past field studies (Ayers and Simpson, 2006; Apodaca et al., 2008, Huff et al., 2010 [submitted]). In addition to the CRDS, instruments that measure NO_x (Thermo Environmental 42c) and ozone (Dasibi 1008 RS) were also sampled from the same inlet.

The pole that held the high flow sampling inlet had meteorological instruments including an RM Young cup anemometer and wind vane to measure wind speed and direction (model 03001-5), a temperature sensor (RM Young 41342) and a relative humidity and temperature sensor combined (HMP 45). These instruments were at the same height as the sampling inlet and logged one-minute averaged data on a Campbell

Scientific CR10x data logger. Located 10 meters east from the chemical and meteorological instruments was a visibility monitor (Vaisala FS11) that measured visibility and logged in 1 minute intervals. All instruments collected data continuously from 16-31 March, 2010.

8.2.2 Steady state assumptions

Given the close proximity to town the steady state analysis is complicated and the air parcel transport to the site becomes important. The site's meteorology is detailed in the discussion section. We used the steady state approximation to calculate a N_2O_5 lifetime from the N_2O_5 concentration divided by the N_2O_5 source rate (Apodaca et al., 2008),

$$\tau_{N_2O_5 ss} = \frac{[N_2O_5]}{k_1[NO_2][O_3]} . \qquad (8.1)$$

The N_2O_5 source rate is given by the rate coefficient for Reaction (R1), k_1, multiplied by the concentrations of NO_2 and ozone.

8.3 Results

The mixing ratios of the chemical species (N_2O_5, NO_2, and O_3) were averaged to 1 minute intervals. The N_2O_5 source rate was calculated using the denominator in Eq. (8.1) and the steady state lifetime was calculated using Eq. (8.1). The relative humidity, temperature, wind direction, and wind speed were averaged over 30 minute intervals.

The entire meteorological time series for the field study is displayed in Fig. 8.2. The relative humidity with respect to ice is only saturated (>100%) on one night, 16 March, 2010. The average temperature was 4.6°C with minimum temperature -15.2°C on 27 March, 2010. The wind direction was used to filter out the data from > 300 degrees and <

30 degrees. We then filtered out for wind speeds less than 1 m/s, the threshold of the cup anemometers. The source rate, mixing ratio and lifetime of N_2O_5 were averaged to one minute. A filter was applied with a minimum value of the source rate of 10 pptv/hr in order to filter out clean, unpolluted air masses in the steady state lifetime calculations. The N_2O_5 source rate threshold allows us not to analyze clean air episodes where negative steady state lifetimes of N_2O_5 would occur due to levels of N_2O_5 near the detection limit of 2 pptv. During the study we had a high synoptic pressure gradient form, which resulted in uncharacteristically high winds and unpolluted air flow into Fairbanks area from 21-26 March, 2010.

In Fig. 8.3 we compare the steady-state lifetimes of N_2O_5 on three nights with different meteorology in which all of our meteorological (wind speed and direction) and chemical (> 10 pptv/hr source rate) filters were applied. The first night, 16, March 2010 is characterized by high humidity with respect to ice (> 100%), colder temperatures and a NNW wind direction. The average steady state lifetime of N_2O_5 is 20 minutes. The second night, 20 March, 2010, has the same wind direction, temperatures, and low relative humidity of 48% and a steady state lifetime of 22 minutes. The third night, 27 March 2010, also has low relative humidity with respect to ice (47%), slightly warmer temperature average and similar wind direction (NNW) and an average lifetime of 90 minutes.

8.4 Discussion

8.4.1 Steady state lifetimes of N_2O_5 aloft

In order to compare the steady state lifetimes of N_2O_5 aloft, we need to make sure our steady state assumptions are valid and our transport time of the polluted air flow to our site is longer than the observed steady state lifetimes of N_2O_5. In Fig. 8.3 the source rate and mixing ratio of N_2O_5 are plotted on the same axis against time for the three study nights. On all three nights the source rate follows the mixing ratio of N_2O_5, suggesting that the N_2O_5 is at steady state. On the first two nights we have a steady state lifetime calculated using Eq. (8.1) of 22 minutes.

The transport time for the polluted air flow to reach the observation site is part of a drainage flow with complex characteristics. The straight line distance to downtown Fairbanks is 6 km and the average wind speed (Fig. 8.1) is 2.8 m/s during the field study. The air-flow traveling from downtown to the site if direct would be around 30 minutes and our steady state assumption would mostly likely be valid because the steady state lifetime of 20-22 minutes on 16th and 20st of March, 2010 is slightly shorter than the transport time. In addition, the source rate follows the mixing ratio of N_2O_5. The direct air flow regime, where downtown air is flowing towards the site (from the SE), only occurs when a high pressure gradient and high winds are present. On the other nights, a defined drainage flow originating from the Goldstream Valley and flowing towards the Tanana Valley is present. The drainage flow wind direction is typically from the NW. The drainage air-flow regime can be seen in Figure 8.2 during the nights when the wind speed changes direction coming from NW at night and increases in speed. This forms a

drainage flow originating from the concave shape of the surrounding hills and funnels down Goldstream Valley (Fig. 8.1). At this point, the synoptic wind flow in the Fairbanks area is opposite the drainage flow from the Goldstream valley. Under these conditions the synoptic winds are calm and temperature gradients form between the bottom of the Tanana valley to the top of Geophysical Institute's Elvey building. The Fairbanks area is known to have strong inversions where the air temperature at the surface is often 20°C cooler than air 100 meters aloft. For example, using the temperature at the Fairbanks International Airport located at the bottom of the Tanana Valley on night the 16 March, 2010 (UTC) the average surface temperature at night was -19°C and the average temperature on the roof was -12°C, a gradient of 7°C over 85 meters.

The air mass that flows from the drainage, presumably from the Goldstream Valley (Fig.8.1) and possibly including downtown, is polluted. This implicates that either the valley or the town is producing the observed pollution because Fairbanks is isolated and the next major town is 400 km to the south. The Goldstream Valley is approximately 10 km from the sampling site and the air transport time is approximately 1 hour at a wind speed of 2.8 m/s.

The topography and wind speed data crudely estimate that possible transport times of pollution from the north are on the order of an hour, indicating that inferred steady state lifetimes less than an hour may be accurate, while inferred lifetimes over an hour are probably underestimated. The timescale of air transport to the field site of 1 hour, coupled with Fig. 8.3 showing the source rate following the mixing ratio of N_2O_5 and the third night 27 March, 2010 with an average 90 minute steady state lifetime (maximum around

2 hours), may not be at steady state. The average steady state lifetime of N_2O_5 on 27 March, 2010 is directly following the high pressure synoptic gradient episode and high winds seen from 21-26 March, 2010. The longer lifetimes and higher mixing ratio of N_2O_5 could be from the low surface area of atmospheric particles to react with N_2O_5 due to the high winds bringing unpolluted air to Fairbanks on the previous nights. If the N_2O_5 is not allowed to build to steady levels then our steady state lifetime would be underestimated and increase the average steady state lifetime of N_2O_5.

If we compare these steady state lifetimes and the three night average of 44 minutes to the steady state lifetimes obtained near the surface of 6 minutes from our previous campaign, we see much longer lifetimes aloft than near the Earth's surface (Huff et al., 2010). The average lifetime aloft of 44 minutes is a factor of 5 longer than the lifetime of N_2O_5 near the Earth's surface and further enforces our findings that snowpack deposition is a major chemical loss process for N_2O_5 near the surface. In addition the mixing ratios of N_2O_5 on all three nights in Fig.8.3 reach a maximum of 400 pptv and are higher than mixing ratios of N_2O_5 with a maximum of 80 pptv found near the surface (Huff et al., 2010, Apodaca et al., 2008).

8.4.2 Ice particles and visibility

On the nights we have measured the steady state lifetimes of N_2O_5, we want to compare relative humidity with respect to ice and the saturation of the air mass. If the relative humidity with respect to ice is greater than 100%, the conditions are favorable for additional ice surface area in the form of ice particles to be present. If ice particle formation is favorable then we can use the visibility monitor data to relate visibility to

atmospheric particle surface area using Eq. (8.4). In Fig. 8.3, two nights have short lifetimes, 16 and 20 March, 2010 with an average steady state lifetime of N_2O_5 of 20 minutes. Interestingly, 16 March 2010 was the only night with >100% relative humidity with respect to ice, which would implicate the possibility of ice particle formation (Apodaca et al., 2008). The relative humidity was much lower (48%) on 20 March, 2010, but we still see a relatively short lifetime of 20 minutes. The first hypothesis that could explain these results are that the same lifetime under different relative humidity conditions on the two nights (100 and 48%) indicates that the atmospheric loss to ice particles is not occurring. Unfortunately, we only have one night with high relative humidity during the field study available for comparison. Secondly, the second night may not be at steady state and that the lifetimes could be longer, but would require the transport time to the site to be at least double under the present average wind speeds.

Another way to measure the effect of ice particle is by measuring an available surface area density. We used the inverse relationship of visibility to surface area. To use this relationship, we used a visibility monitor to measure the scattering and absorption of particles in the atmosphere. Measuring the extinction coefficient of these particles allows us to calculate a surface area density (Finlayson-Pitts and Pitts, 2000). The following set of equations is used:

$$V_{is} = 3.9 / b_{ext} \qquad (8.2)$$

$$b_{ext} = SA * Q_{ext} / 4 \approx SA / 2 . \qquad (8.3)$$

In Eq. (8.2), V_{is} is the visibility in meters and b_{ext} is equal to Eq. (8.3). In Eq. (8.3),

Q_{ext} = scattering plus absorption. It is unitless and approaches 2 as particle size increases. The variable *SA* is the surface area of the particle in $\mu m^2/cm^3$. Rearranging Eq. (8.3) and substituting it into Eq. (8.2), results in an equation that directly relates the visibility to an approximate surface area density;

$$V_{is} = 3.9/ (SA/2) = 7.8 / SA. \qquad (8.4)$$

A visibility of 10 miles (16 km) would correlate to approximately 800 $\mu m^2/cm^3$ of possible surface area for the N_2O_5 heterogeneous hydrolysis by atmospheric processes. The surface area density value for a non-spherical ice crystal is measured by the equivalent spheres method (Neshyba et al., 2003). The ice crystal's non-spherical shape correlates to an equivalent sphere of the volume of the ice crystal. We did have the lowest visibility on the shortest average N_2O_5 lifetime day 16 March, 2010 (Fig. 8.1) and highest 100% RH with respect to ice (Fig. 8.2) at 14 km. However the range of visibilities over the entire field study was 12 to 25 km and we did not have any extremely low or high visibility days with which to compare.

8.5 Conclusions

The average steady state lifetime of N_2O_5 was 44 minutes in March, in Fairbanks Alaska. The mixing ratios of N_2O_5 at this roof top site were a few hundred pptv aloft as compared to previous measurements near the Earth's surface in November, December and January where the typical mixing ratios are 40 pptv. In addition to increasing mixing ratios with height we also found that the lifetimes were longer aloft (44 minutes) compared to near surface measurements over a snowpack at high latitudes (6 min). A

longer lifetime aloft than near the Earth's surface reinforces the importance of snowpack deposition as a chemical loss mechanism for N_2O_5 near the surface and implies different chemical loss mechanisms of N_2O_5 at different altitudes.

References:

Apodaca, R. L., Huff, D. M., and Simpson, W. R.: The role of ice in N_2O_5 heterogeneous hydrolysis at high latitudes, Atmos. Chem. Phys., 8, 7451-7463, doi:10.5194/acp-8-7451-2008, 2008.

Ayers, J. D., Apodaca, R. L., Simpson, W. R., and Baer, D. S.: Off-axis cavity ringdown spectroscopy: Application to atmospheric nitrate radical detection, Appl. Optics., 44, 7239-7242, 2005.

Ayers, J. D., and Simpson, W. R.: Measurements of N_2O_5 near Fairbanks, Alaska, J. Geophys. Res., 111, D14309, doi:10.1029/2006JD007070, 2006.

Bertram, T. H., and Thornton, J. A.: Toward a general parameterization of N_2O_5 reactivity on aqueous particles: The competing effects of particle liquid water, nitrate and chloride, Atmospheric Chemistry and Physics, 9, 8351-8363, doi:10.5194/acp-9-8351-2009, 2009.

Brown, S. S., Stark, H., Ryerson, T. B., Williams, E. J., Nicks, D. K., Jr., Trainer, M., Fehsenfeld, F. C., and Ravishankara, A. R.: Nitrogen oxides in the nocturnal boundary layer: Simultaneous in situ measurements of NO_3, N_2O_5, NO_2, NO, and O_3, J. Geophys. Res., 108, 4299, doi:10.1029/2002jd002917, 2003.

Brown, S. S., Ryerson, T. B., Wollny, A. G., Brock, C. A., Peltier, R., Sullivan, A. P., Weber, R. J., Dubé, W. P., Trainer, M., Meagher, J. F., Fehsenfeld, F. C., and Ravishankara, A. R.: Variability in nocturnal nitrogen oxide processing and its role in regional air quality,Science,5757, 67-70, doi: 10.1126/science.1120120, 2006.

Brown, S. S.,Dubé, W. P.,Osthoff, H. D.,Wolfe, D. E.,Angevine, W. M.,and Ravishankara, A. R.: High resolution vertical distributions of NO_3 and N_2O_5 through the nocturnal boundary layer, Atmos. Chem. Phys., 7, 139-149, doi:10.5194/acp-7-139-2007, 2007a.

Brown, S. S., Dubé, W. P., Osthoff, H. D., Stutz, J., Ryerson, T. B., Wollny, A. G., Brock, C. A., Warneke, C., de Gouw, J. A., Atlas, E., Neuman, J. A., Holloway, J. S., Lerner, B. M., Williams, E. J., Kuster, W. C., Goldan, P. D., Angevine, W. M., Trainer, M., Fehsenfeld, F. C., and Ravishankara, A. R.: Vertical profiles in NO_3 and N_2O_5 measured from an aircraft: Results from the NOAA P-3 and surface platforms during the New England air quality study 2004, J. Geophys. Res., 112, D22304, doi:10.1029/2007jd008883, 2007b.

Dentener, F. J., and Crutzen, P. J.: Reaction of N_2O_5 on tropospheric aerosol particles: Impacts on the global distributions of NOx, O_3, and OH., J. Geophys. Res., 98, 7149-7163, 1993.

Evans, M. J., and Jacob, D. J.: Impact of new laboratory studies of N_2O_5 hydrolysis on global model budgets of tropospheric nitrogen oxides, ozone and OH, Geophys. Res. Lett., 32, L09813, doi:10.1029/2005GL022469, 2005.

Finlayson-Pitts, B. J., and Pitts, J. N.: Chemistry of the upper and lower atmosphere., 2000.

Geyer,A.,and Stutz, J.: Vertical profiles of NO_3, N_2O_5, O_3, and NOx in the nocturnal boundary layer: 2.Model studies on the altitude dependence of composition and chemistry, J. Geophys. Res., 109, D12307, doi:10.1029/2003jd004211,2004.

Hanson, D. R., and Ravishankara, A. R.: The reaction probabilities of $ClONO_2$ and N_2O_5 on 40 to 75% sulfuric acid solutions, J. Geophys. Res., 96, doi:10.1029/91jd01750,1991.

Hu, J. H., and Abbatt, J. P. D.: Reaction probabilities for N_2O_5 hydrolysis on sulfuric acid and ammonium sulfate aerosol particles at room temperature, The Journal of Physical Chemistry A,101, 871,1997.

Huff, D. M., Joyce, P. L., Fochesatto, G. J., and Simpson, W. R.: Deposition of dinitrogen pentoxide, N_2O_5, to the snowpack at high latitudes, Atmos. Chem. Phys. Discuss., 10, 25329- 25354, doi:10.5194/acpd-10-25329-2010,2010.

Kirchner, W., Welter, F., Bongartz, A., Kames, J., Schweighoefer, S., and Schurath, U.: Trace gas exchange at the air/water interface: Measurements of mass accommodation coefficients, Journal of Atmospheric Chemistry, 10, 427-449, doi:10.1007/bf00115784, 1990.

Mozurkewich, M., and Calvert, J. G.: Reaction probability of N_2O_5 on aqueous aerosol particles, J. Geophys. Res.,93, doi:10.1029/JD093iD12p15889,1988.

Neshyba, S. P., Grenfell, T. C., and Warren, S. G.: Representation of a nonspherical ice particle by a collection of independent spheres for scattering and absorption of radiation: 2. Hexagonal columns and plates, J. Geophys. Res., 108,doi: 10.1029/2002jd003302, 2003.

Riemer, N., Vogel, H., Vogel, B., Schell, B., Ackermann, I., Kessler, C., and Hass, H.: Impact of the heterogeneous hydrolysis of N_2O_5 on chemistry and nitrate aerosol

formation in the lower troposphere under photosmog conditions, J. Geophys. Res., 108,doi: 10.1029/2002jd002436, 2003.

Simpson, W. R.: Continuous wave cavity ring-down spectroscopy applied to in-situ detection of dinitrogen pentoxide (N_2O_5). Rev. Sci. Inst, 74, 3442-3452, 2003.

Stutz, J., Alicke, B., Ackermann, R., Geyer, A., White, A., and Williams, E.: Vertical profiles of NO_3, N_2O_5, O_3, and NO_x in the nocturnal boundary layer: 1. Observations during the Texas air quality study 2000, J. Geophys. Res., 109, doi:10.1029/2003JD004209, 2004.

Van Doren, J. M., Watson, L. R., Davidovits, P., Worsnop, D. R., Zahniser, M. S., and Kolb, C. E.: Uptake of dinitrogen pentoxide and nitric acid by aqueous sulfuric acid droplets, The Journal of Physical Chemistry, 95, 1684-1689, doi:10.1021/j100157a037, 1991.

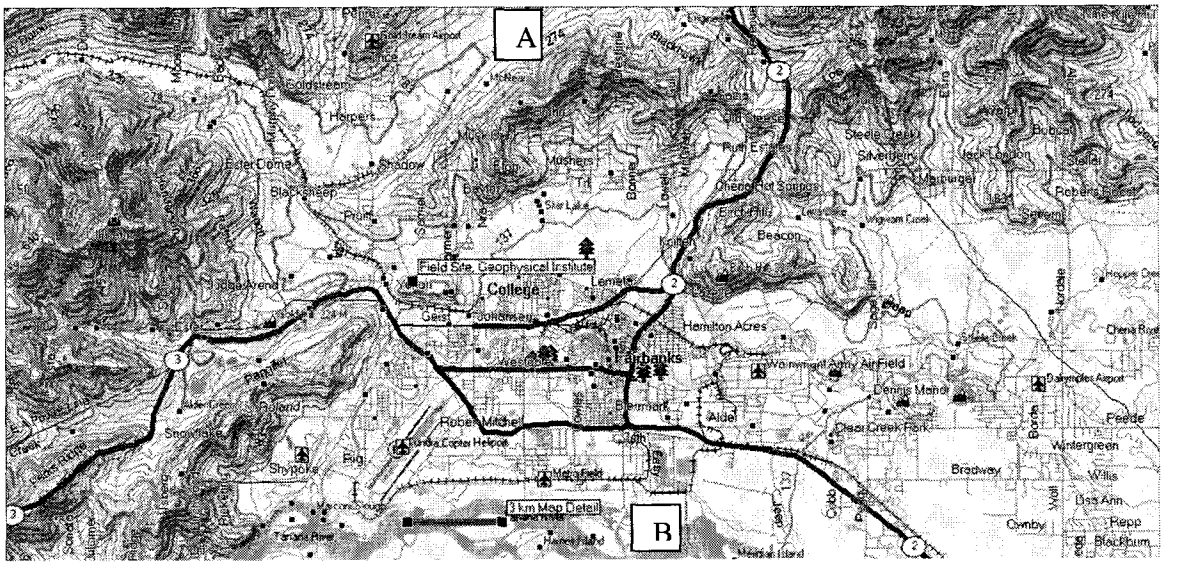

Figure 8.1. Contour plot and location of the Geophysical Institute building. With respect to downtown Fairbanks, Goldstream Valley (A) and the Tanana Valley (B). Downtown Fairbanks is located approximately 6 km and the Goldstream Valley (A) is approximately 10 km from the observation site at the Geophysical Institute.

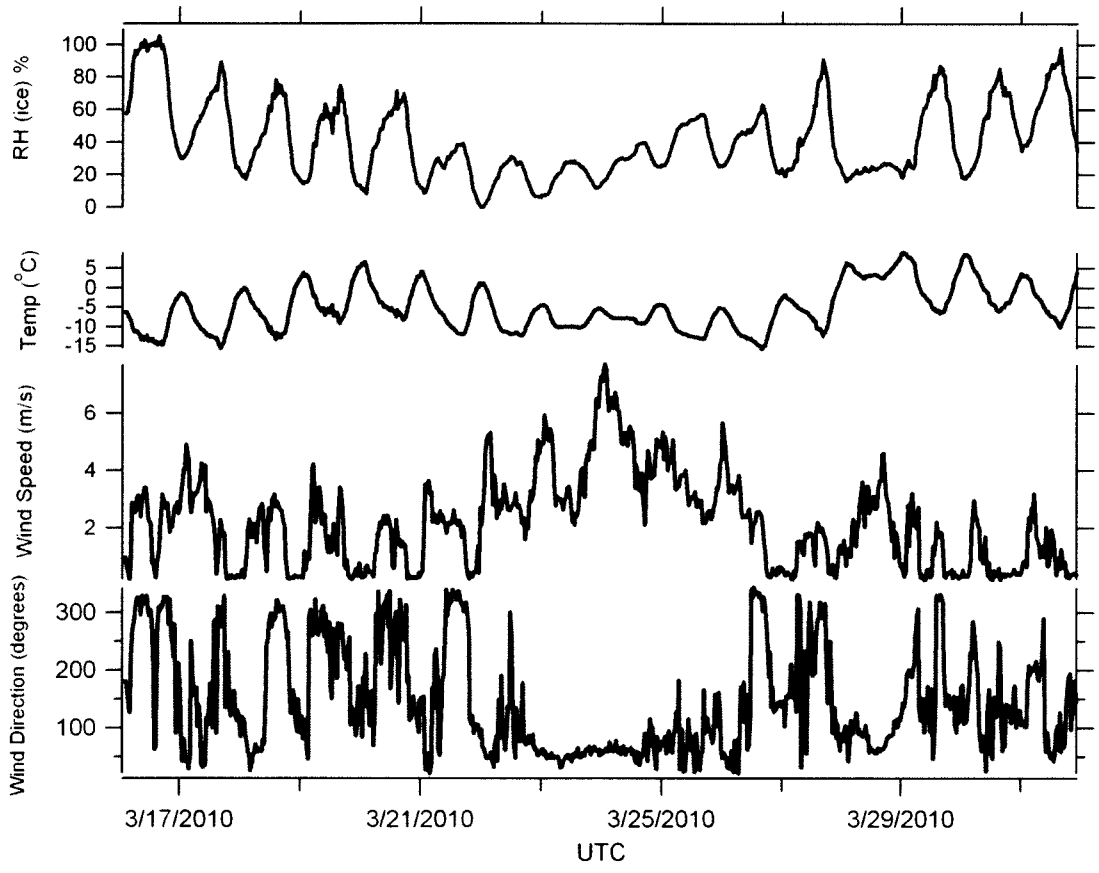

Figure 8.2. Time series of the meteorological data. The relative humidity (%), temperature (°C), and wind speed (m/s) and wind direction (degrees) are in half hour data points for 16-28, March 2010.

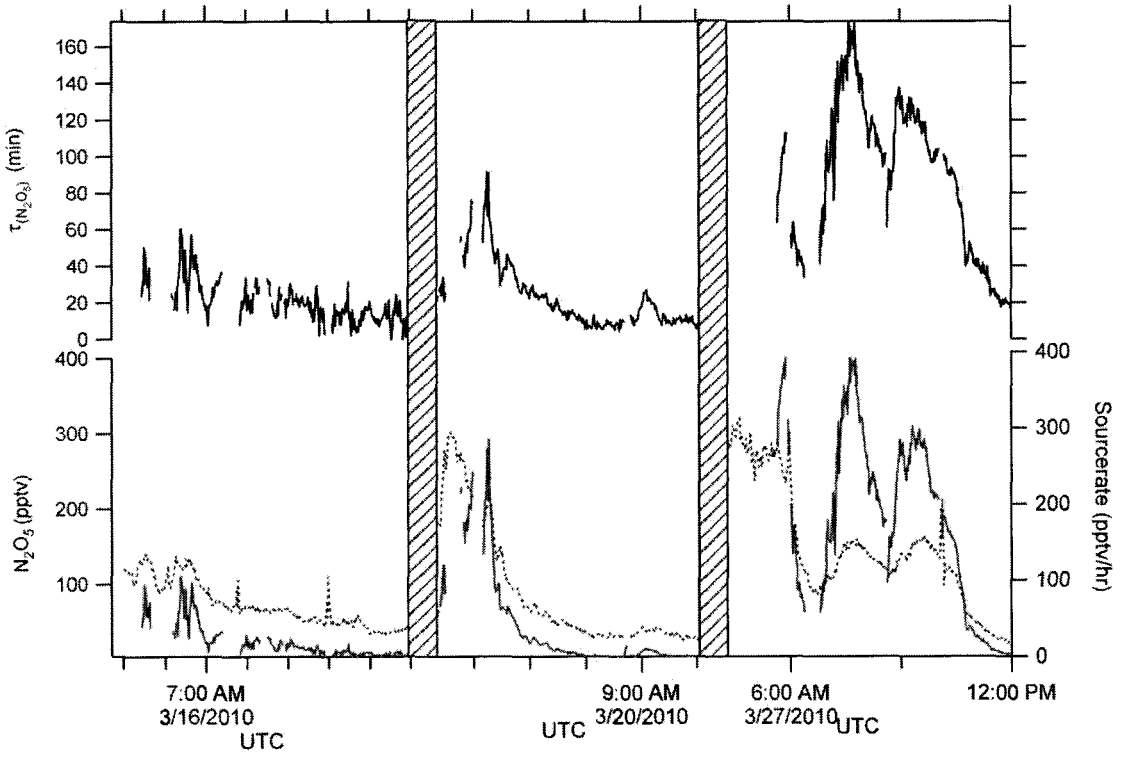

Figure 8.3. Time series of N_2O_5, mixing ratio, source rate and lifetimes. Comparison of the N_2O_5 mixing ratios in pptv (red solid trace), source rate (blue dotted trace) in pptv/hr and steady state lifetimes of N_2O_5 (black trace, top axis) in minutes on 16, 20 and 27 March, 2010.

Chapter 9 Conclusions and outlooks

We completed field studies investigating the chemical loss of N_2O_5 by snowpack deposition near the Earth's surface and the N_2O_5 lifetimes and mixing ratios aloft. We measured the average deposition velocity of N_2O_5 to 0.6 cm/s and downward directed toward the snowpack. The calculation of this deposition velocity is dependent upon near-surface meteorological conditions related to the stability of the atmosphere. The boundary layer conditions in the Arctic are very complex (Anderson and Neff, 2008) and include stable air with strong inversions. We limited our data to periods with neutral, and near neutral, stability conditions to minimize the complex structure that forms under very stable conditions. This limitation allowed the data to still satisfy the assumptions required by the aerodynamic gradient method we used to determine a flux and calculate the deposition velocity. The deposition velocity was then used to calculate the chemical removal rate due to snowpack deposition and compare it to the overall steady state removal rate for N_2O_5. We found that deposition to the snowpack is responsible for at least $1/8^{th}$ of the total N_2O_5 removal and likely even a higher fraction due to possible differences in the boundary layer height calculations. The overall steady state lifetime of N_2O_5 near the surface during the snowpack deposition field study was 6 minutes.

In addition to snowpack deposition we also measured the N_2O_5 mixing ratio and steady state lifetimes aloft. We found the N_2O_5 steady state lifetime aloft to be 44 minutes, which is much longer than the approximate 10 minute lifetime observed near the

surface (Apodaca et al., 2008; Huff et al., 2010). The mixing ratio of N_2O_5 also increased with height from less than 80 pptv near the Earth's surface to a few hundred pptv aloft (at a height of 30 meters). We did see a slight difference in visibility on high relative humidity days aloft that may have shortened the lifetime of N_2O_5 due to a higher surface area associated with the visibility-reducing particle availability to catalyze the heterogeneous hydrolysis of N_2O_5. However, the effect was small enough that we could not quantitatively see a correlation between surface area of atmospheric particles and steady state lifetimes of N_2O_5.

We have concluded from our experimental data near the surface and aloft that N_2O_5 mixing ratios and lifetimes increase with height. We have seen that near the surface snowpack deposition plays an important role in the overall heterogeneous hydrolysis of N_2O_5. In addition, we see short lifetimes near the surface ($\approx$10 minutes) and longer steady-state lifetimes aloft ($\approx$44 minutes).

Airmasses aloft may experience slower N_2O_5 chemical losses than near-surface airmasses, which would lead to enhanced transport of N_2O_5 aloft. Vertical mixing will play an important role in the fate of N_2O_5 emitted at high latitudes. A longer lifetime aloft than near the Earth's surface reinforces the importance of snowpack deposition as a chemical loss mechanism of N_2O_5 near the surface and implicates different chemical loss mechanisms of N_2O_5 at altitude. If the steady state lifetimes of N_2O_5 are underestimated due to validity of the steady state approximation from short transport times of the polluted plume then even further range transport of NO_x is possible. If the N_2O_5 lifetimes

are found to be on the order of the length of night, then this would implicate N_2O_5 as a NO_x reservoir and lead to a source of NO_x and ozone farther downwind of the original pollution plume.

To further characterize the vertical distribution of N_2O_5, we can use the deposition velocity parameter in models to help understand the fate of NO_x pollution at high latitudes. We can sample ambient air further aloft in aircraft studies to ensure that we are away from any turbulence around buildings and validate the measurements of the steady state lifetime of N_2O_5 by moving farther from the pollution sources. We can couple aircraft studies of N_2O_5 at high latitudes with modeling of the near surface conditions using the deposition velocity to characterize the different chemical loss mechanisms of N_2O_5. Currently, ongoing research in our lab is focusing on using our measured deposition velocity of N_2O_5 as a parameter in the one-dimensional (vertical) model MISTRA (Von Glasow, 2008). The main goal is to further quantify the partitioning of chemical loss of N_2O_5 aloft, using Bertram and Thornton's (2009) γ parameterization and the dry deposition velocity of N_2O_5 measured in our previous field study (Huff et al., 2010).

References:

Anderson, P. S., and Neff, W. D.: Boundary layer physics over snow and ice, Atmospheric Chemistry and Physics, 8, 3563-3582, doi:10.5194/acp-8-3563-2008, 2008.

Apodaca, R. L., Huff, D. M., and Simpson, W. R.: The role of ice in N_2O_5 heterogeneous hydrolysis at high latitudes, Atmos. Chem. Phys., 8, 7451-7463, doi:10.5194/acp-8-7451-2008, 2008.

Bertram, T. H., and Thornton, J. A.: Toward a general parameterization of N_2O_5 reactivity on aqueous particles: The competing effects of particle liquid water, nitrate and chloride, Atmospheric Chemistry and Physics, 9, 8351-8363, 2009.

Huff, D. M., Joyce, P. L., Fochesatto, G. J., and Simpson, W. R.: Deposition of dinitrogen pentoxide, N_2O_5, to the snowpack at high latitudes, Atmos. Chem. Phys. Discuss., 10, 25329- 25354, doi:10.5194/acpd-10-25329-2010,2010.

Von Glasow, R.: Atmospheric chemistry: Sun, sea and ozone destruction, Nature, 453, 1195-1196, 2008.